The strange quantum transition from the pseudogap metal to the Fermi liquid

Northeastern University
August 12, 2020

Subir Sachdev

PHYSICS
HARVARD

Talk online: sachdev.physics.harvard.edu

Yahui Zhang

Physical Review Research, **2**, 023172 (2020)

arXiv:2006.01140

Physical Review X
10, 021033 (2020)

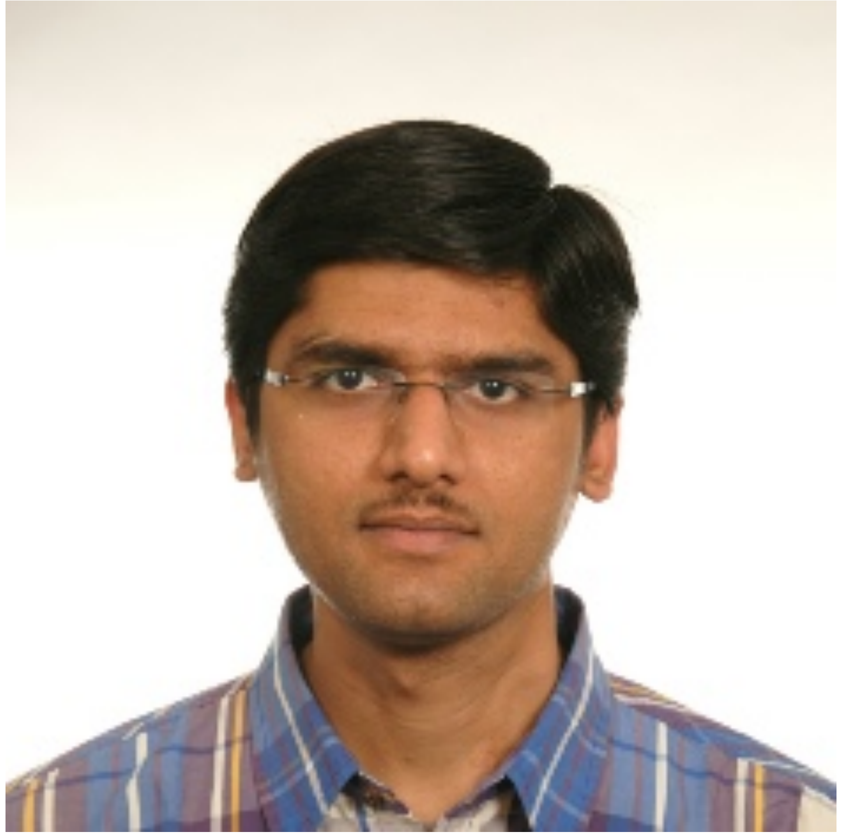

Darshan Joshi

Henry Shackleton

Chenyuan Li

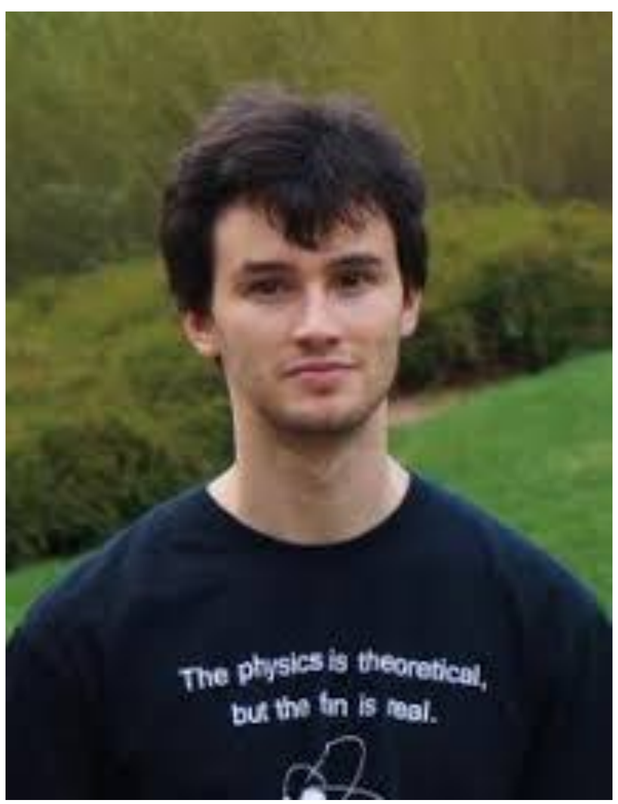

Grigory Tarnopolsky

Alexander Wietek

Antoine Georges

Haoyu Guo

Annals of Physics, **418**, 168202 (2020)

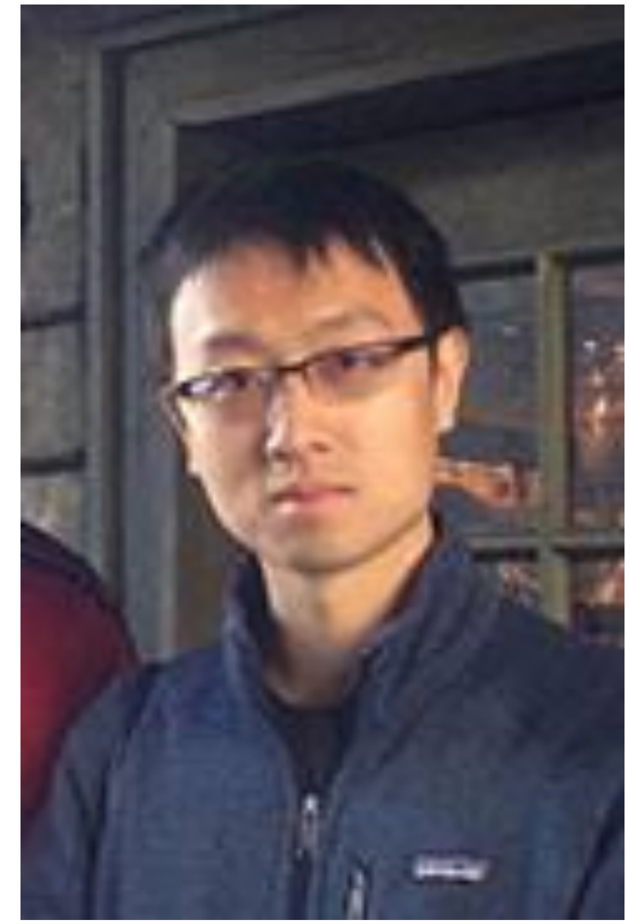

Yingfeu Gu

High temperature superconductors

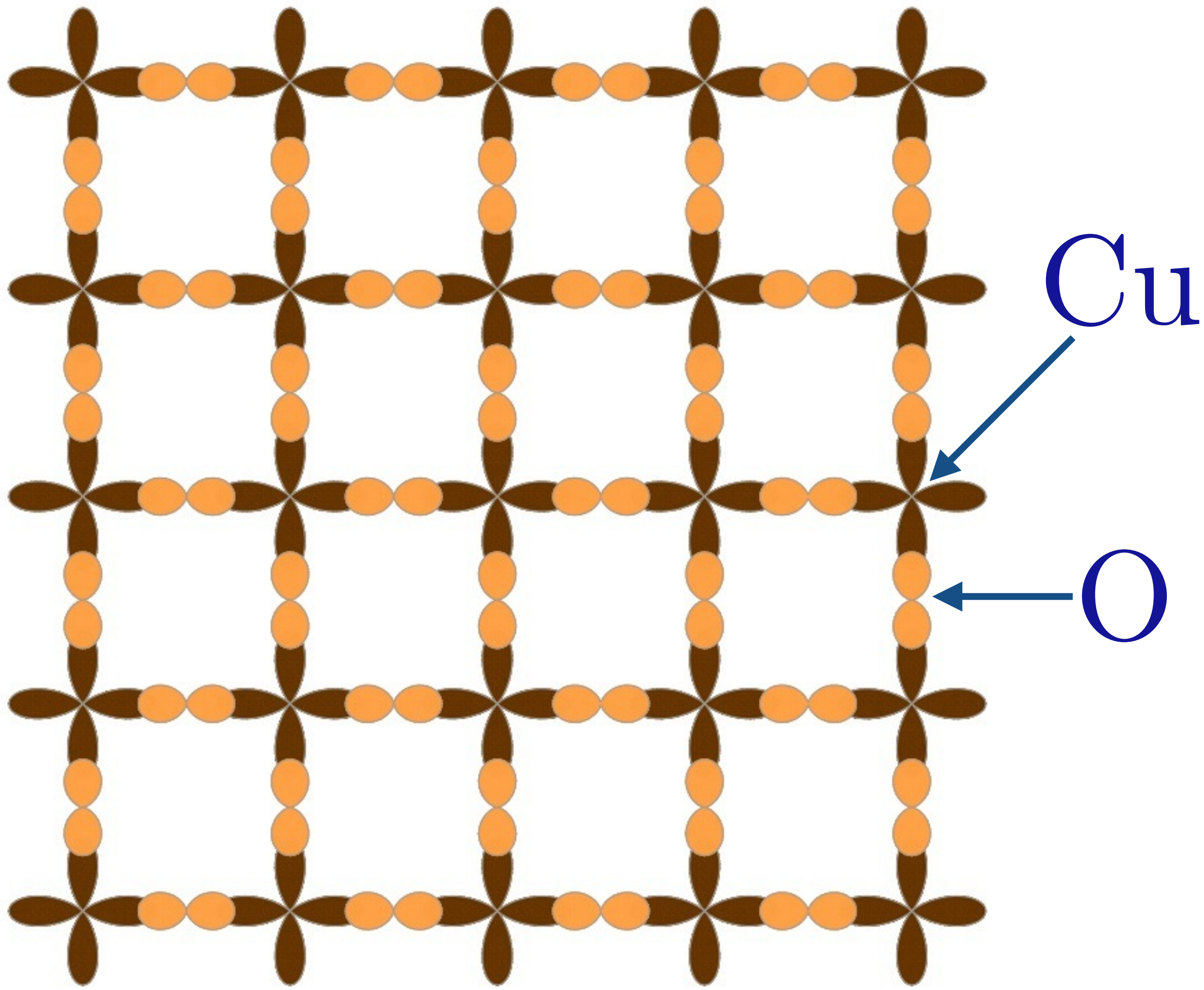

CuO_2 plane

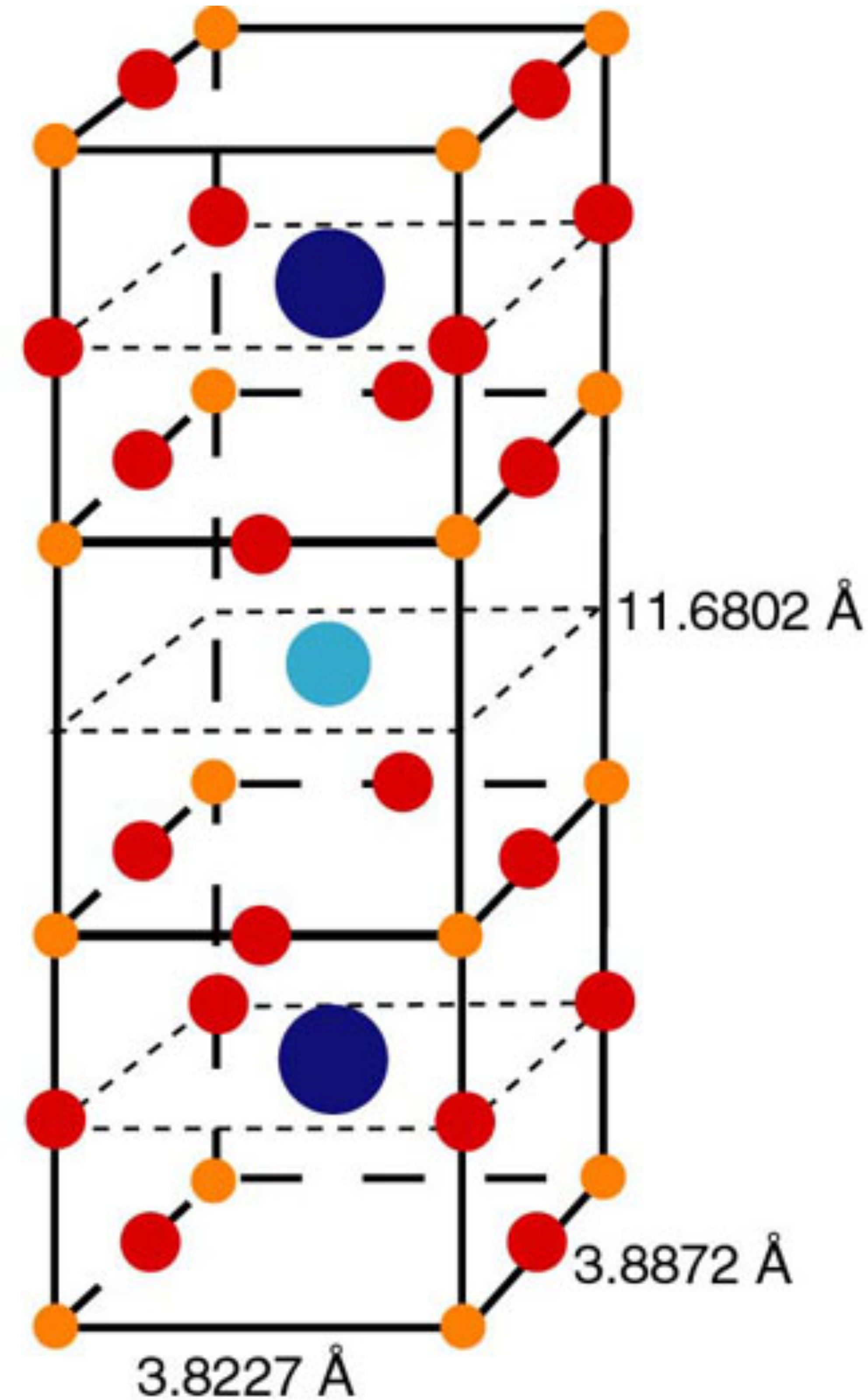

$YBa_2Cu_3O_{6+x}$

Insulating antiferromagnet

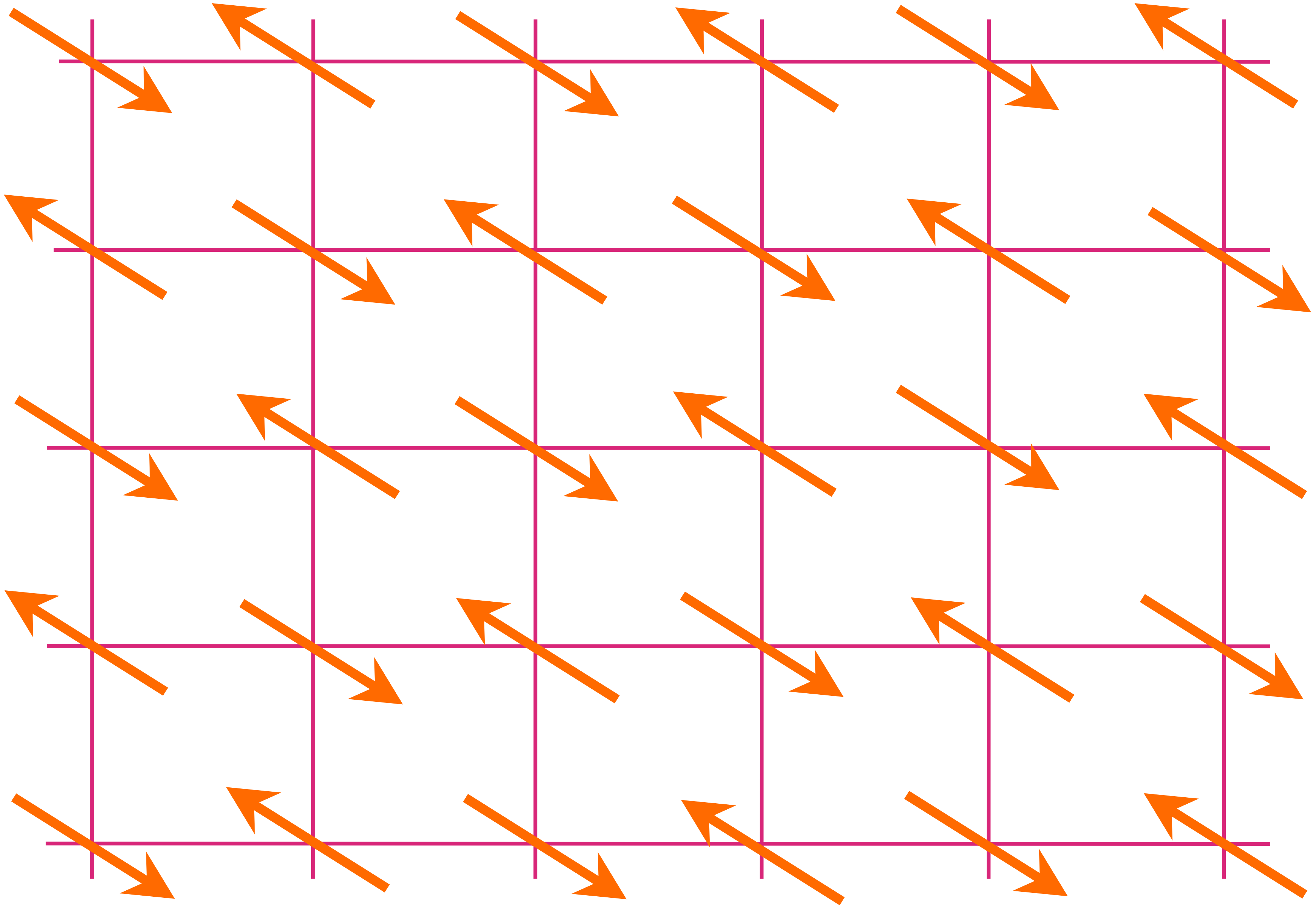

Antiferromagnet doped with hole density p

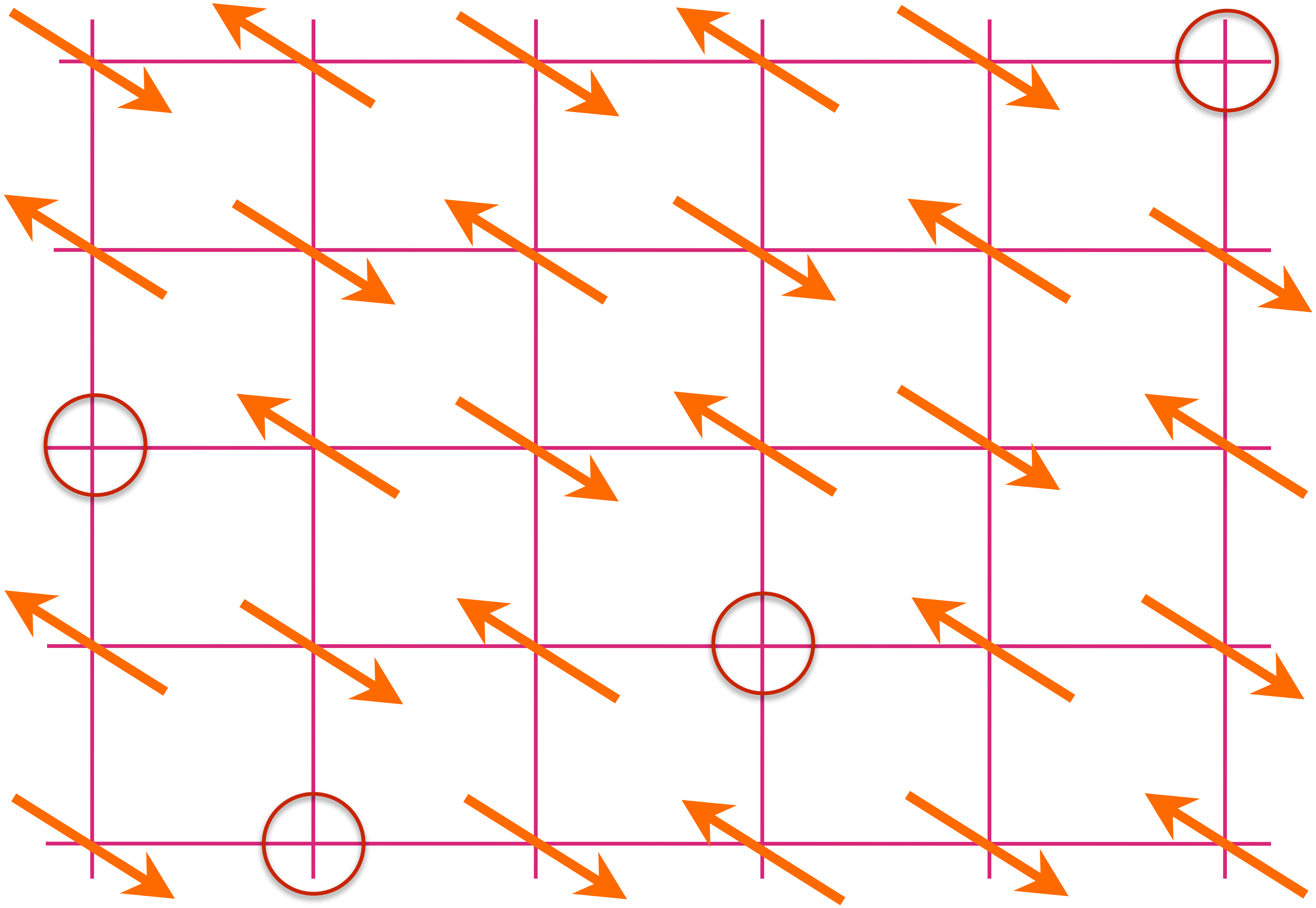

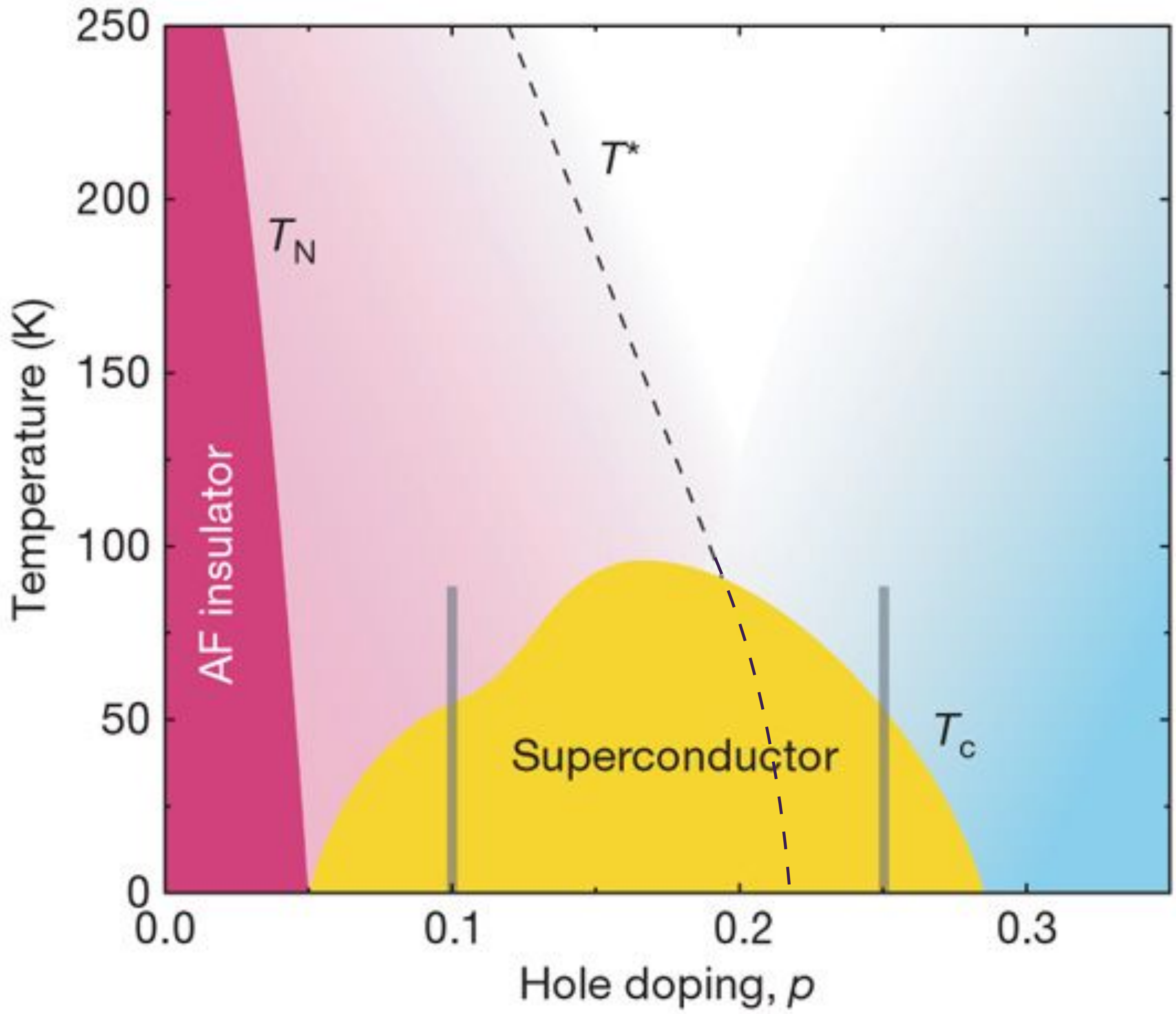
250
200
150
100
50
0
Temperature (K)
0.0
0.1
0.2
0.3
Hole doping, p
AF insulator
T_N
T*
Superconductor
T_c

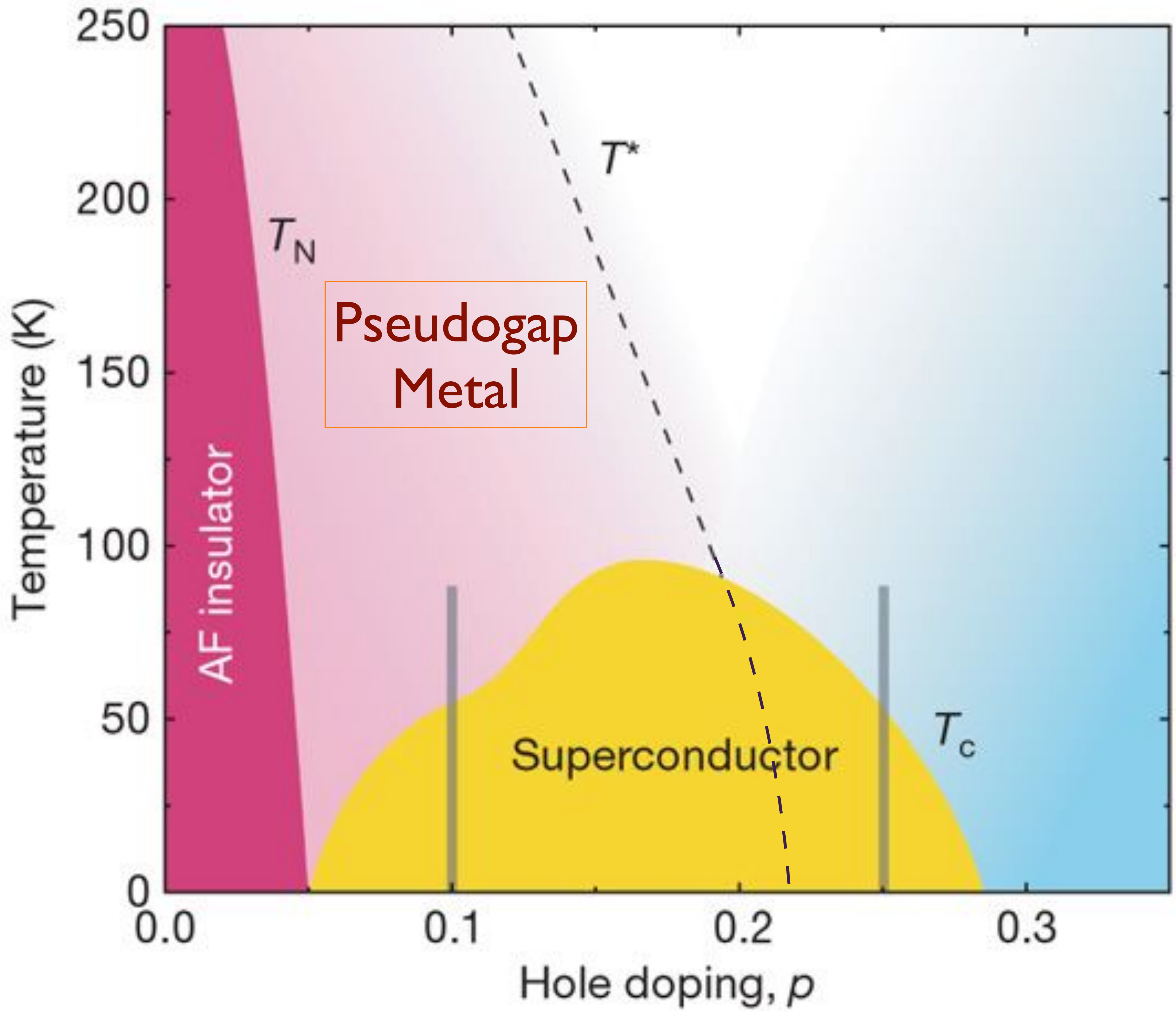
250
200
150
100
50
0
0.0
0.1
0.2
0.3
Temperature (K)
Hole doping, p
AF insulator
T_N
Pseudogap
Metal
T*
Superconductor
T_c

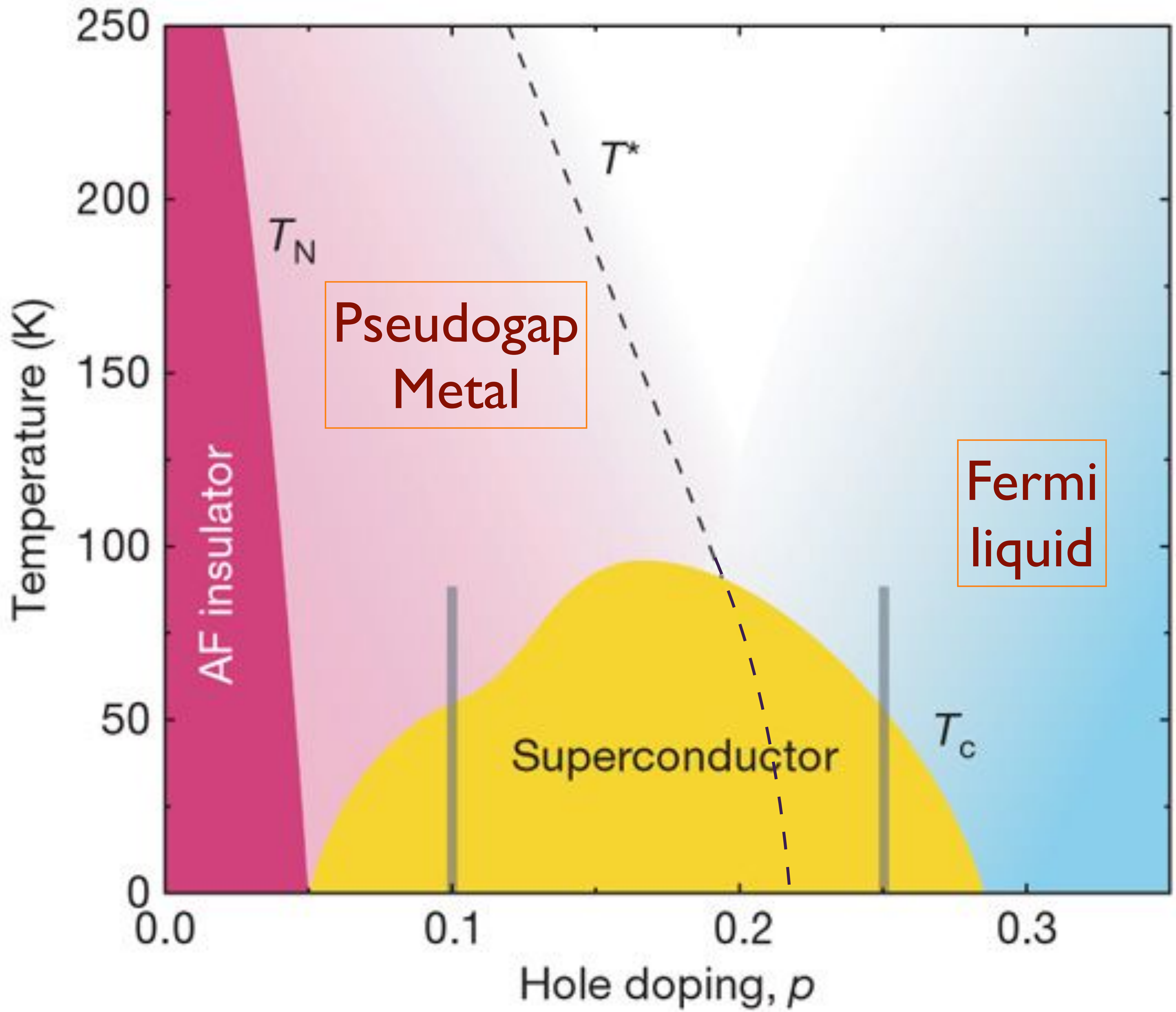
250
200
150
100
50
0
0.0
0.1
0.2
0.3
Temperature (K)
Hole doping, p
AF insulator
T_N
T*
Pseudogap Metal
Fermi liquid
Superconductor
T_c

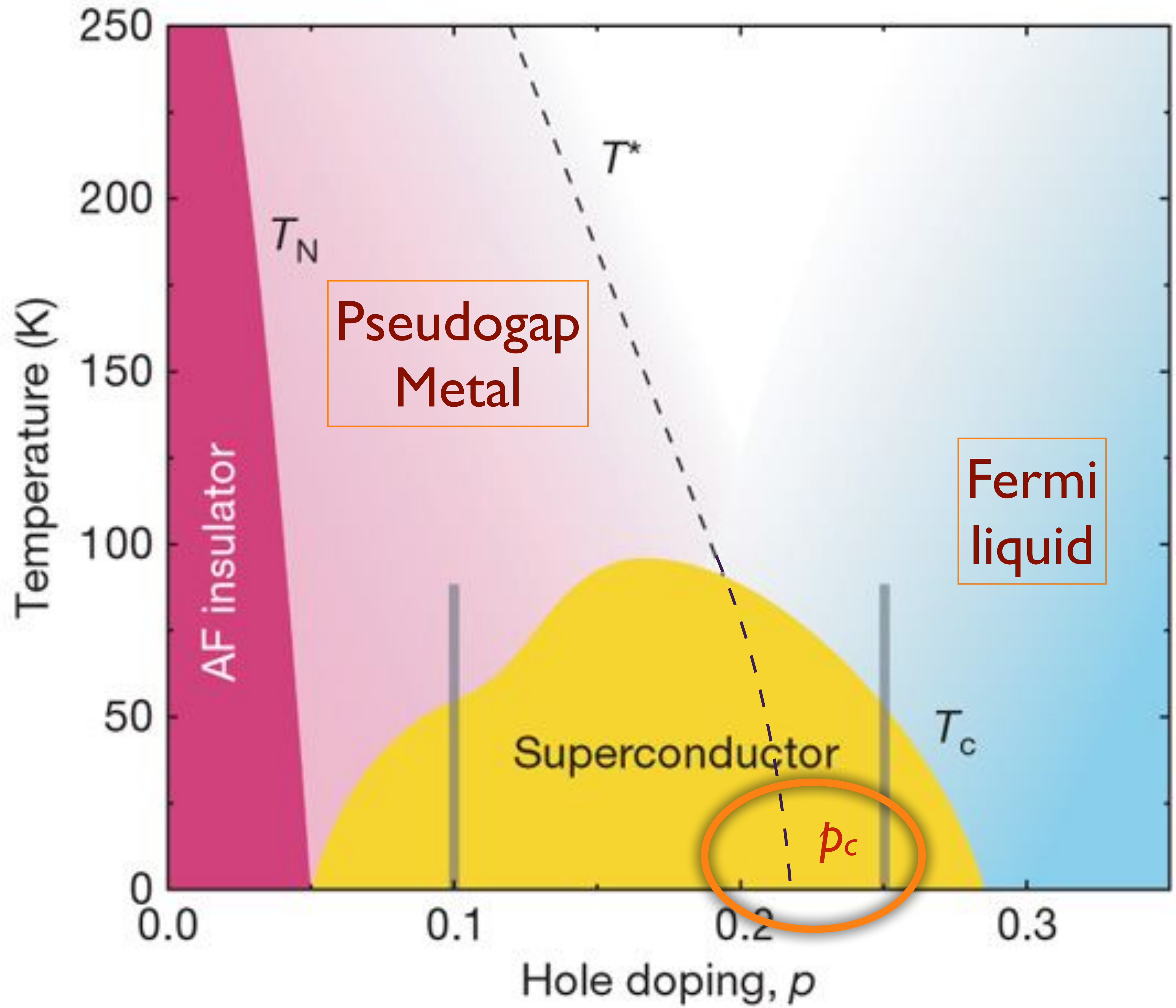

250
200
150
100
50
0
Temperature (K)
0.0
0.1
0.2
0.3
Hole doping, p
AF insulator
T_N
T*
Pseudogap
Metal
Fermi
liquid
Superconductor
T_c
p_c

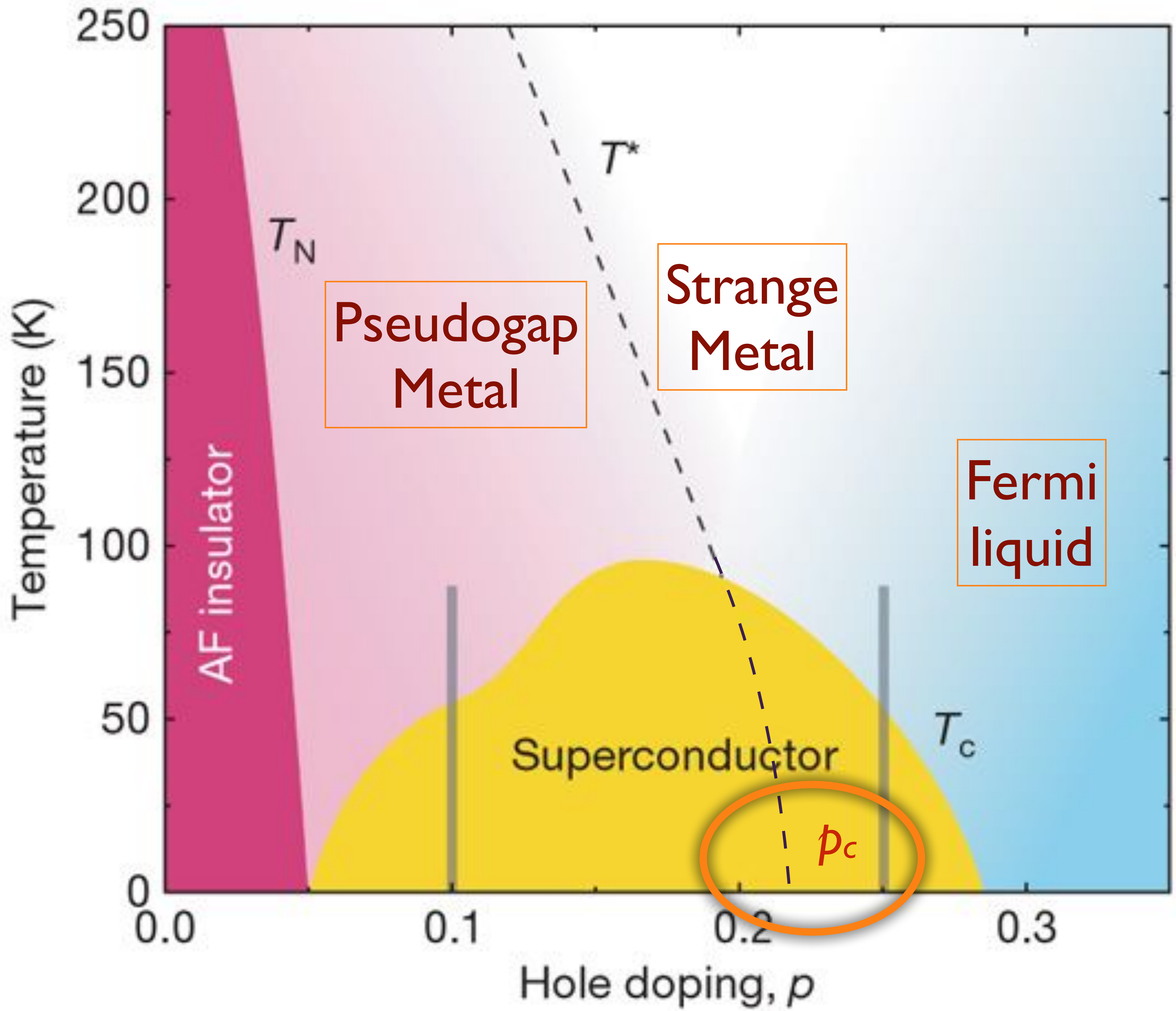

250
200
150
100
50
0
Temperature (K)
0.0
0.1
0.2
0.3
Hole doping, p
AF insulator
T_N
T*
Pseudogap Metal
Strange Metal
Fermi liquid
Superconductor
T_c
p_c

Real-space view at small p

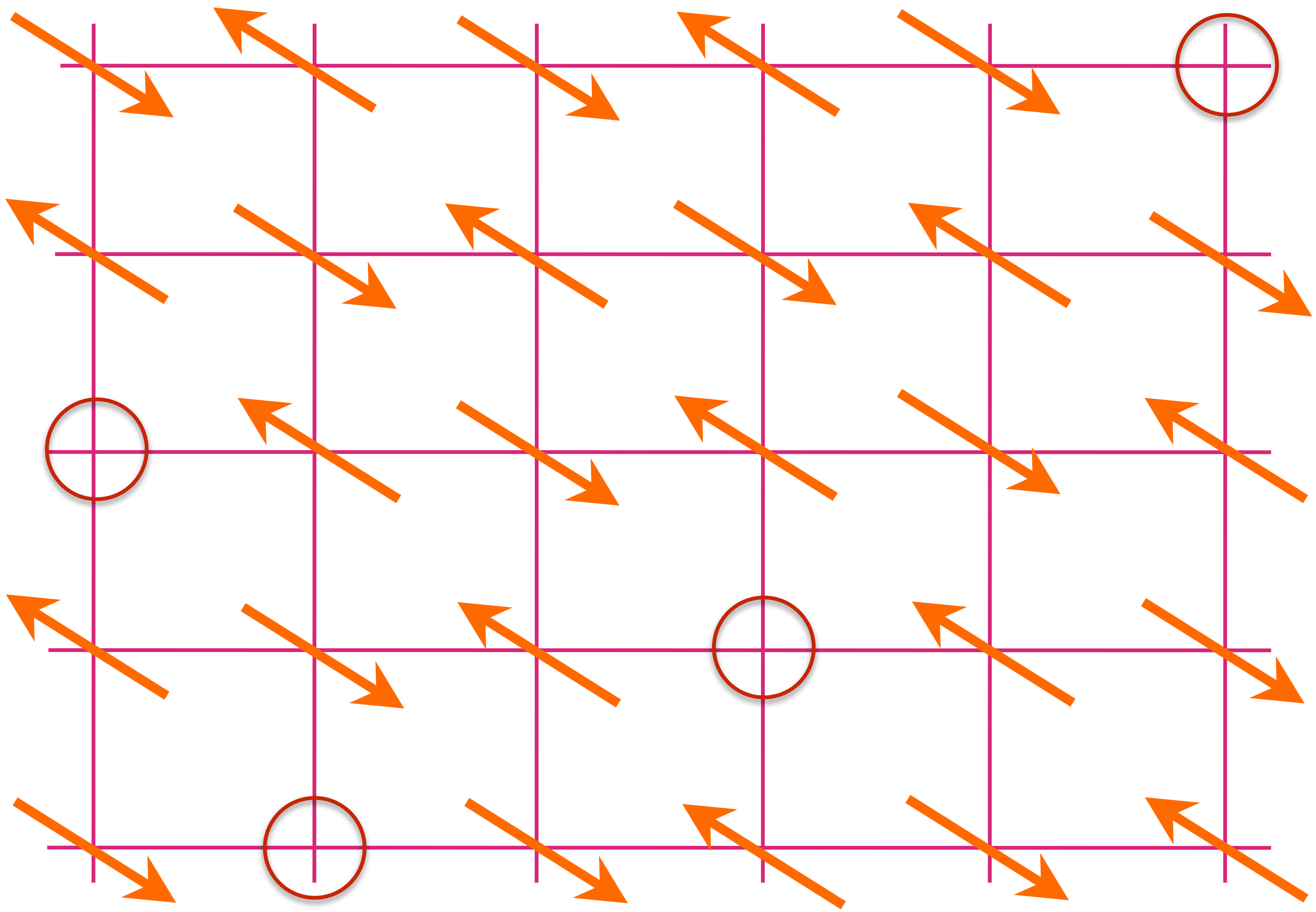

p mobile holes in a background of fluctuating spins

Real-space view at small p

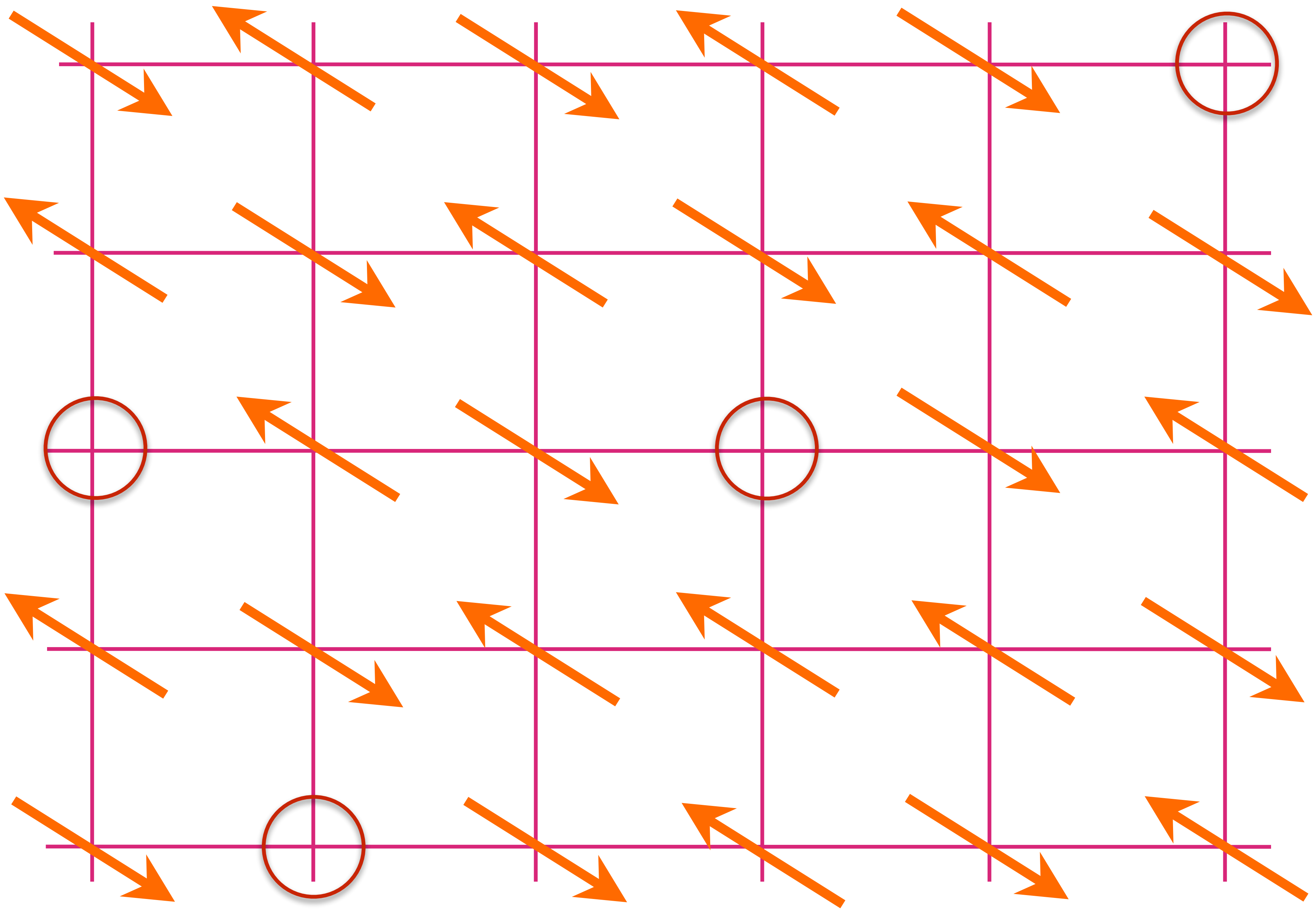

p mobile holes in a background of fluctuating spins

Real-space view at small p

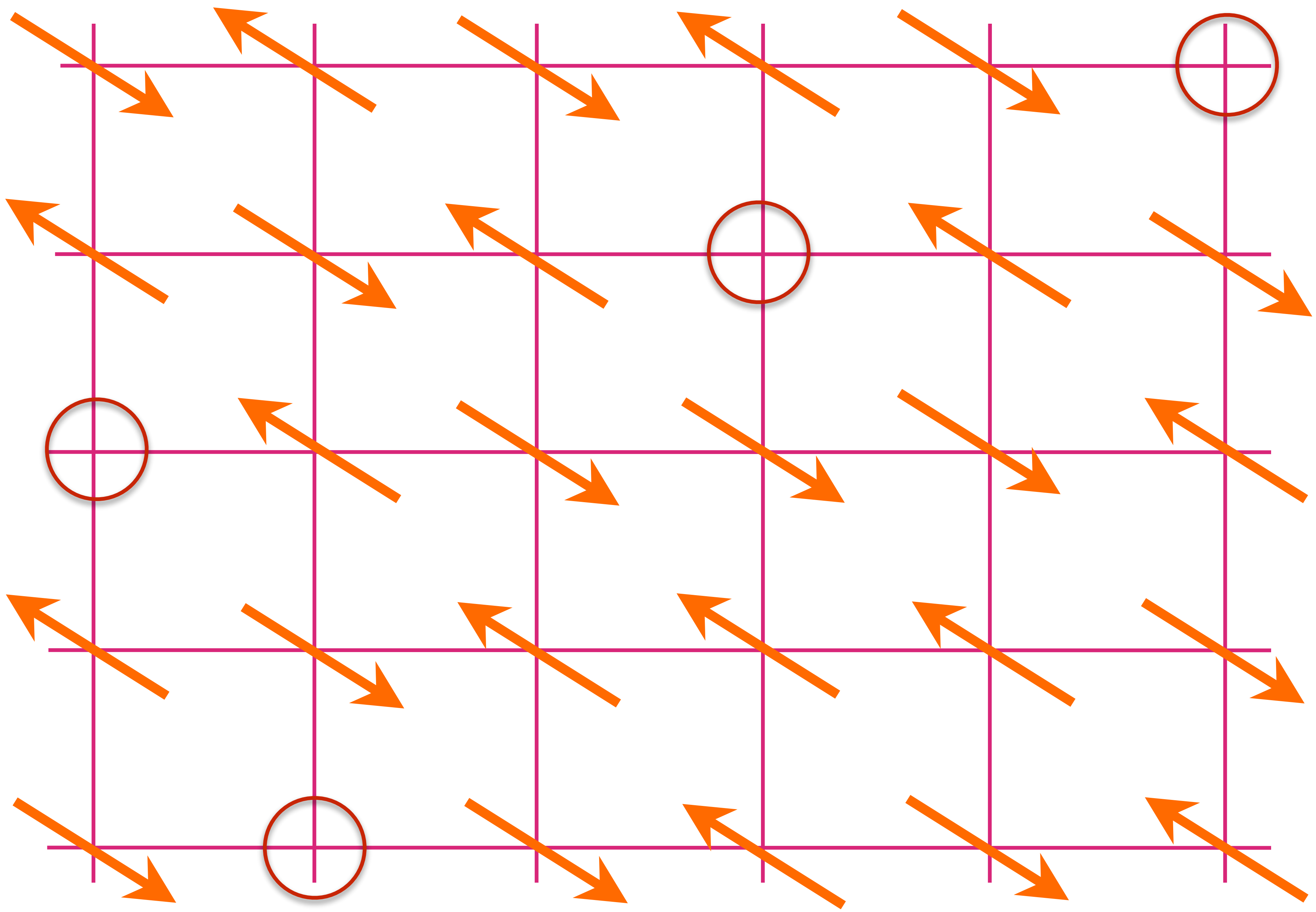

p mobile holes in a background of fluctuating spins

Real-space view at small p

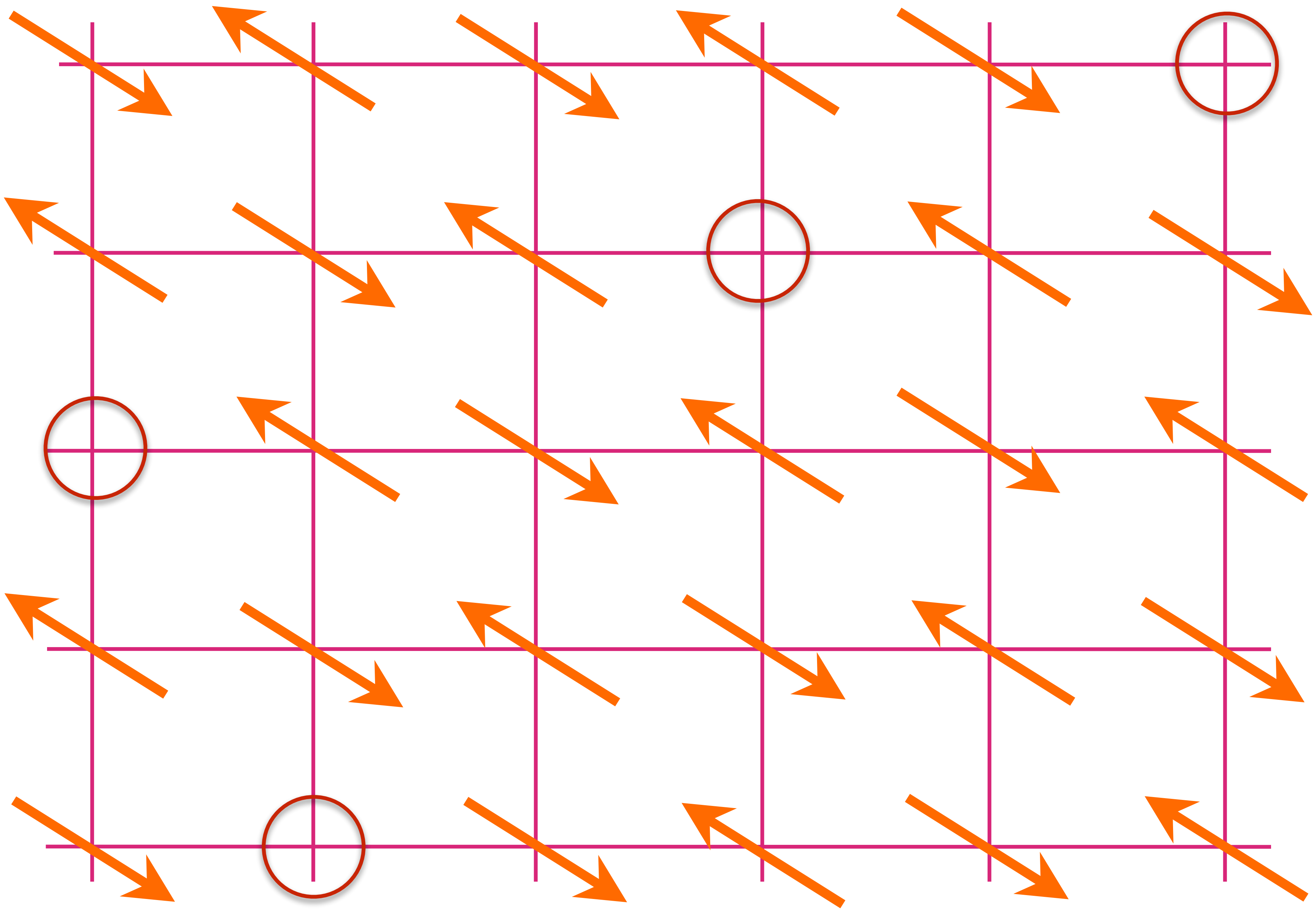

p mobile holes in a background of fluctuating spins

Real-space view at small p

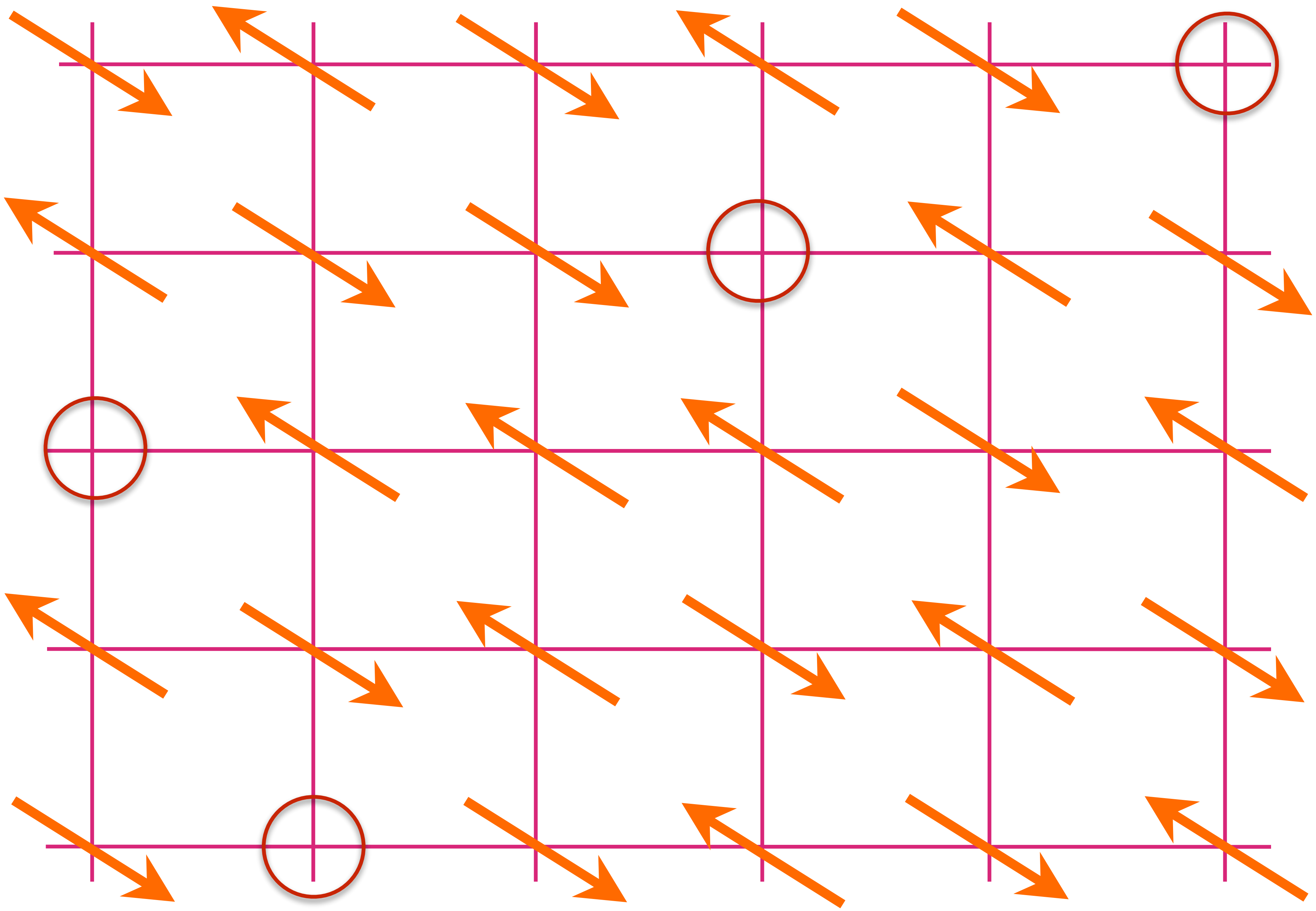

p mobile holes in a background of fluctuating spins

Real-space view at small p

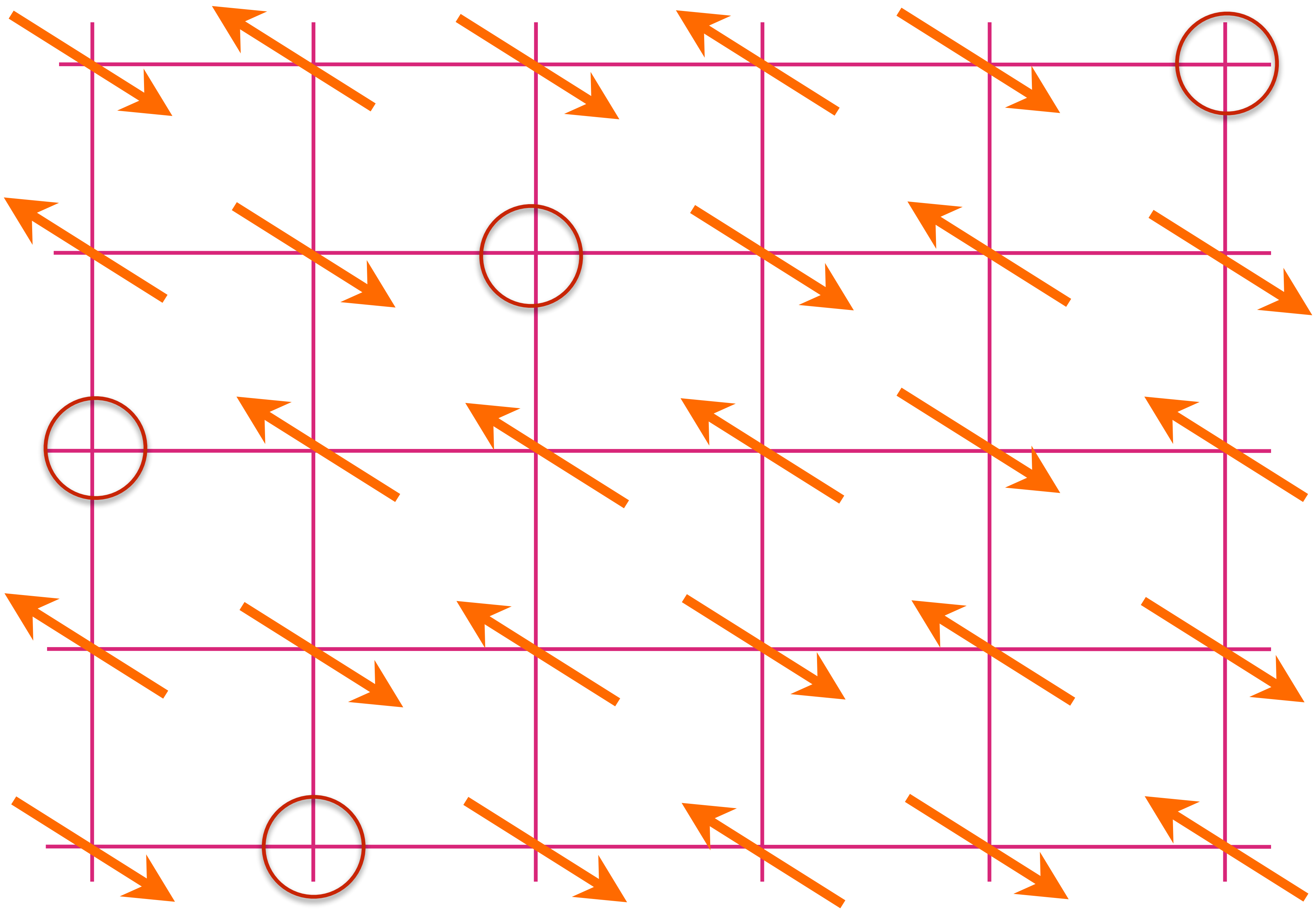

p mobile holes in a background of fluctuating spins

Real-space view at small p

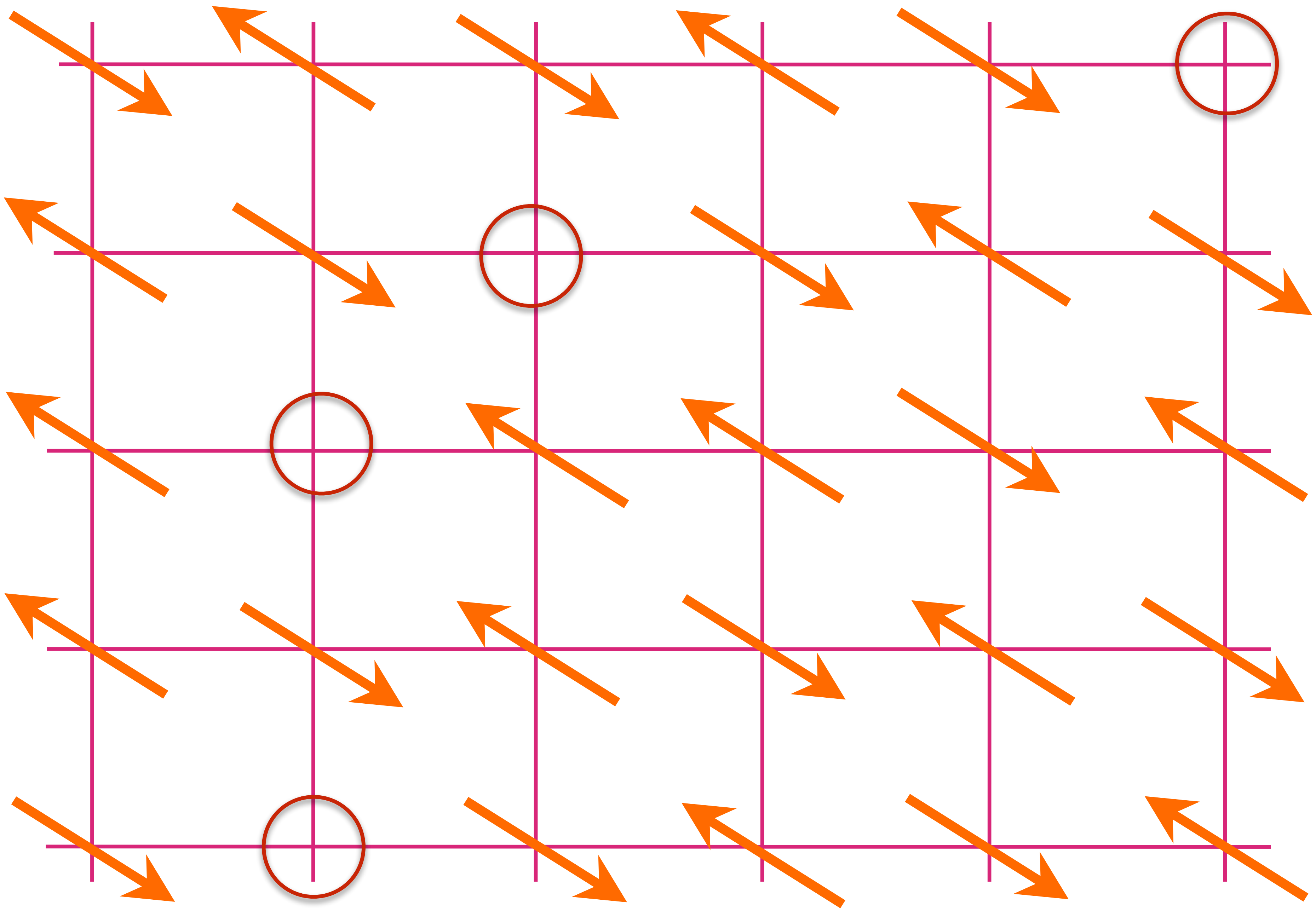

p mobile holes in a background of fluctuating spins

Real-space view at small p

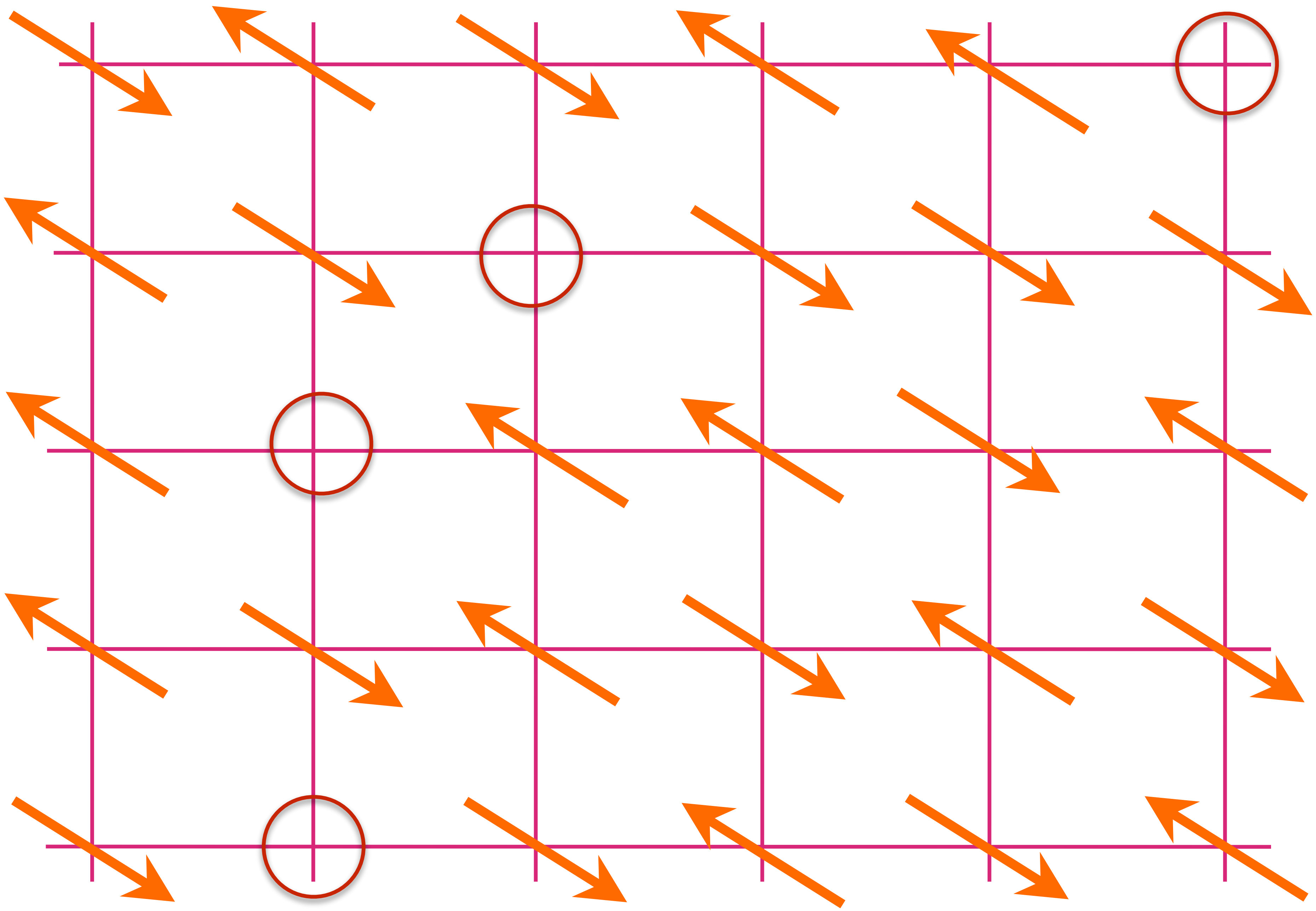

p mobile holes in a background of fluctuating spins

Real-space view at small p

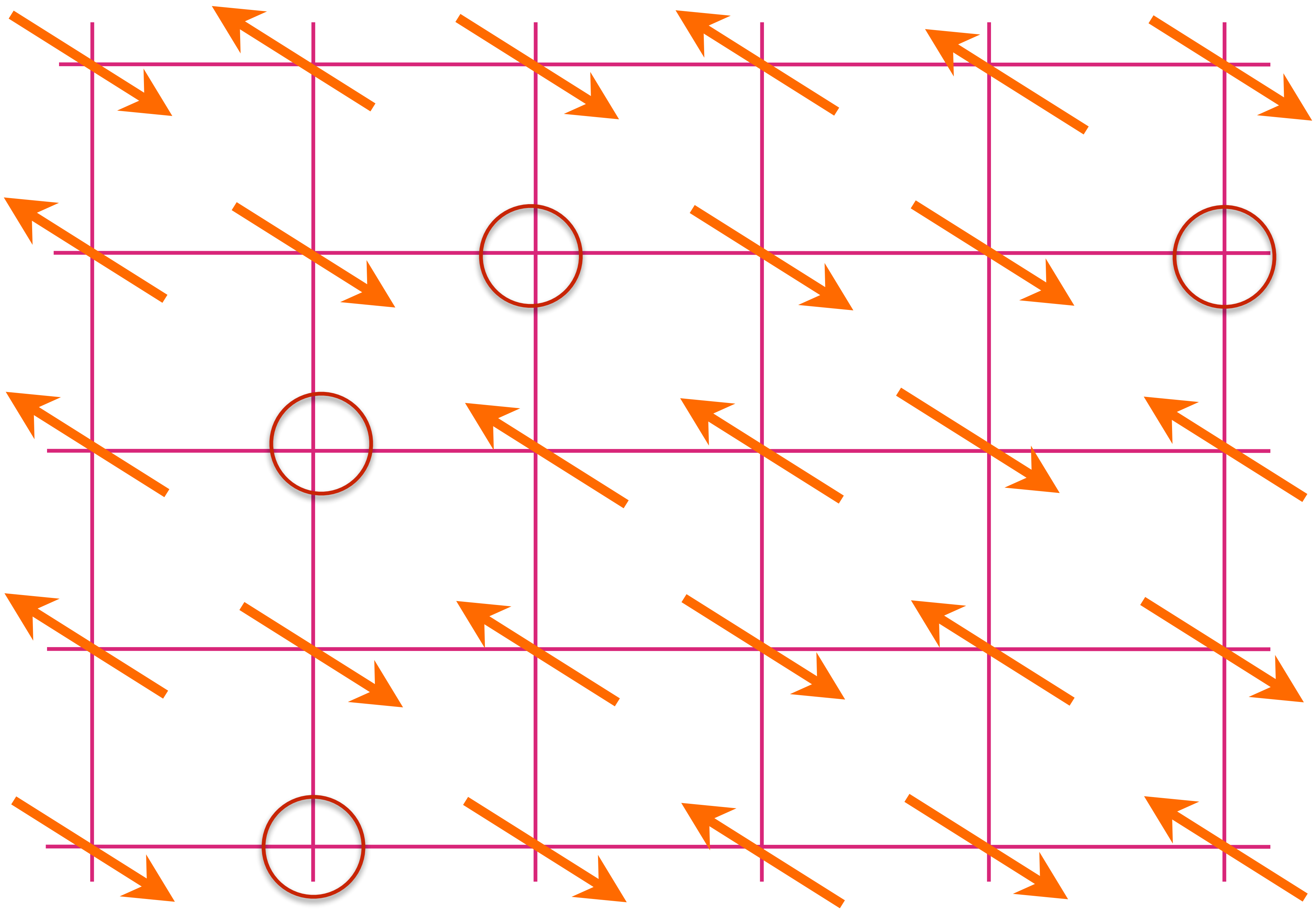

p mobile holes in a background of fluctuating spins

Momentum-space view at large p

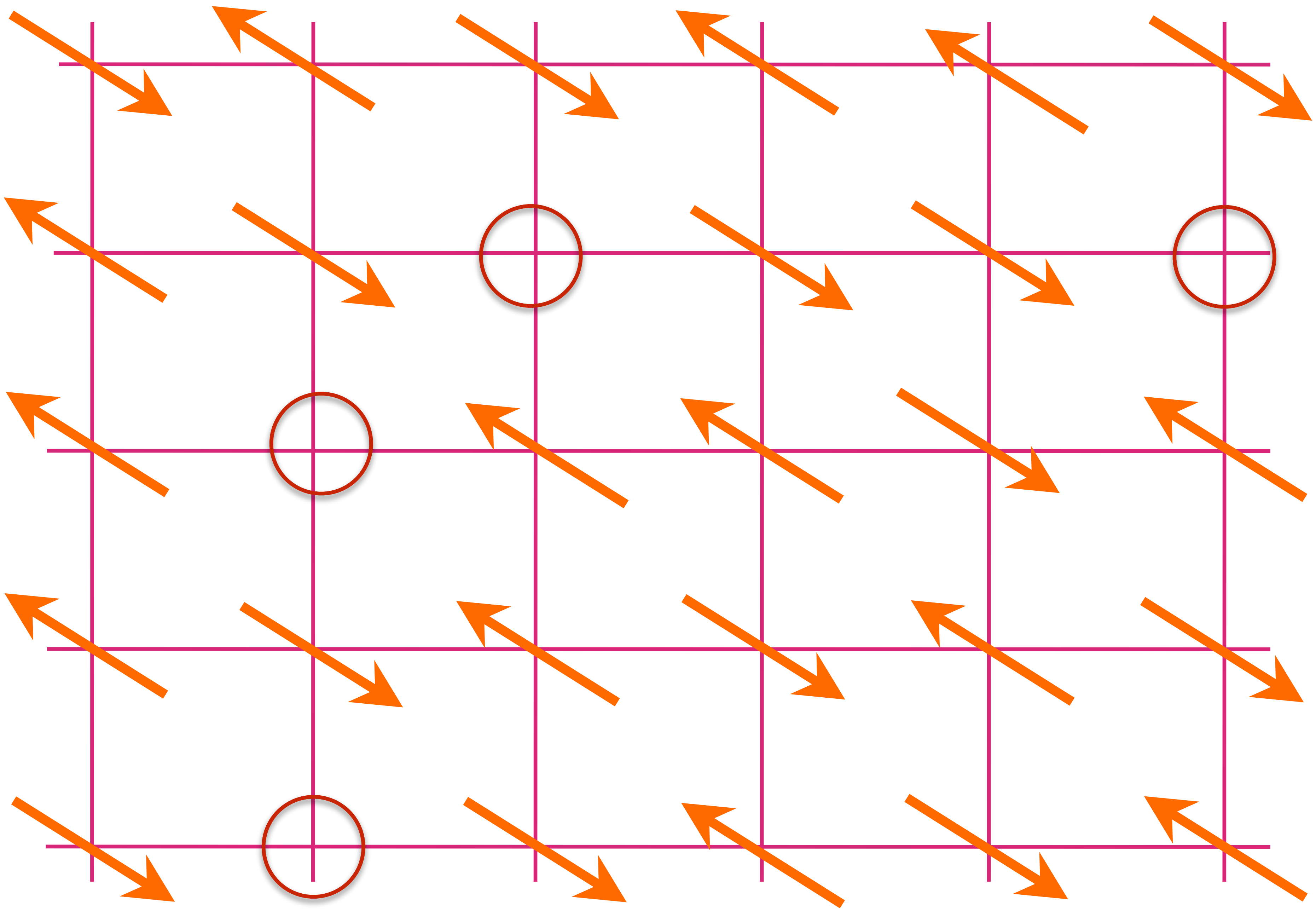

$1\text{-}p$ mobile electrons =
$1+p$ mobile holes in a filled band

Momentum-space view at large p

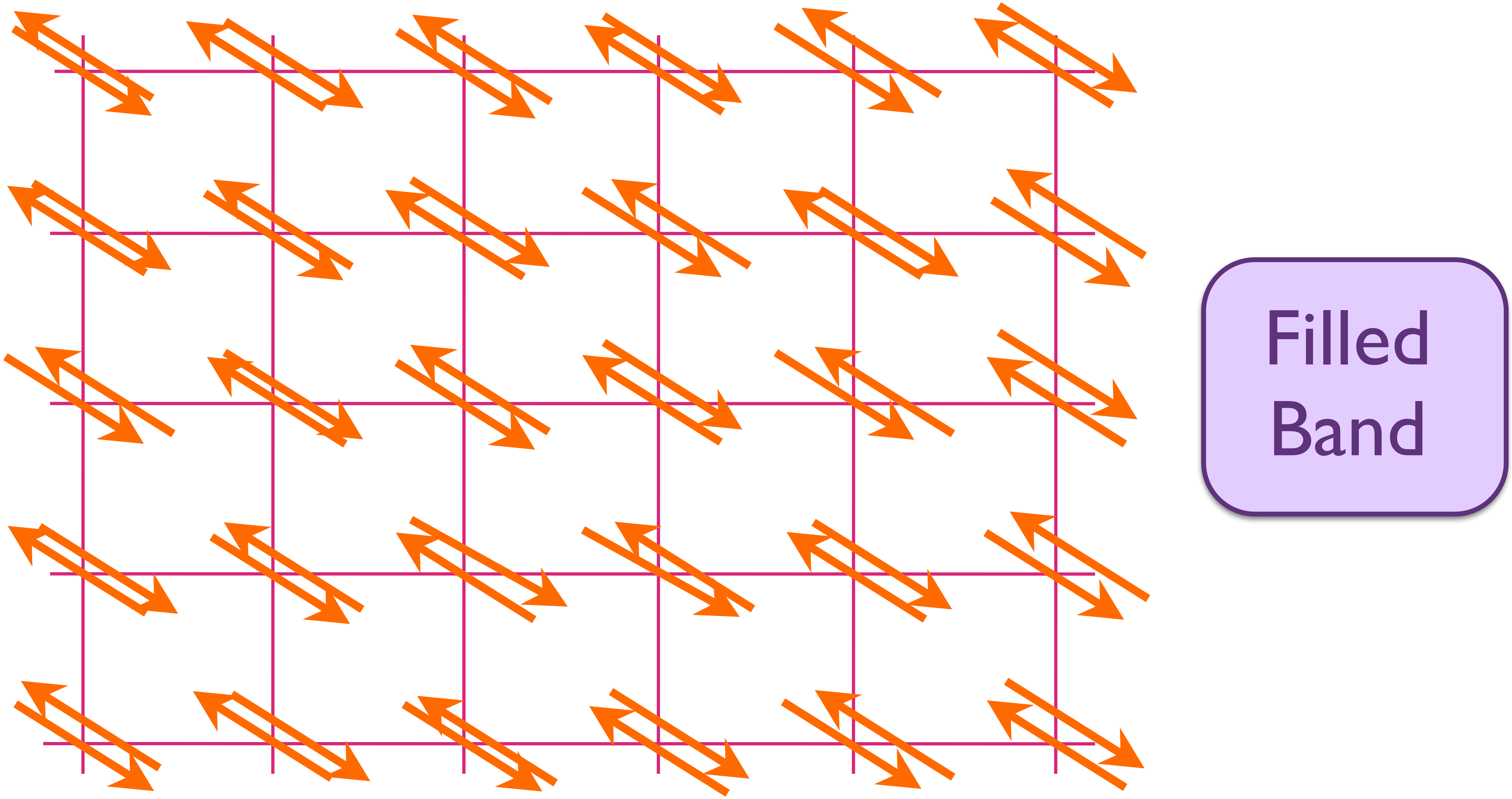

Momentum-space view at large p

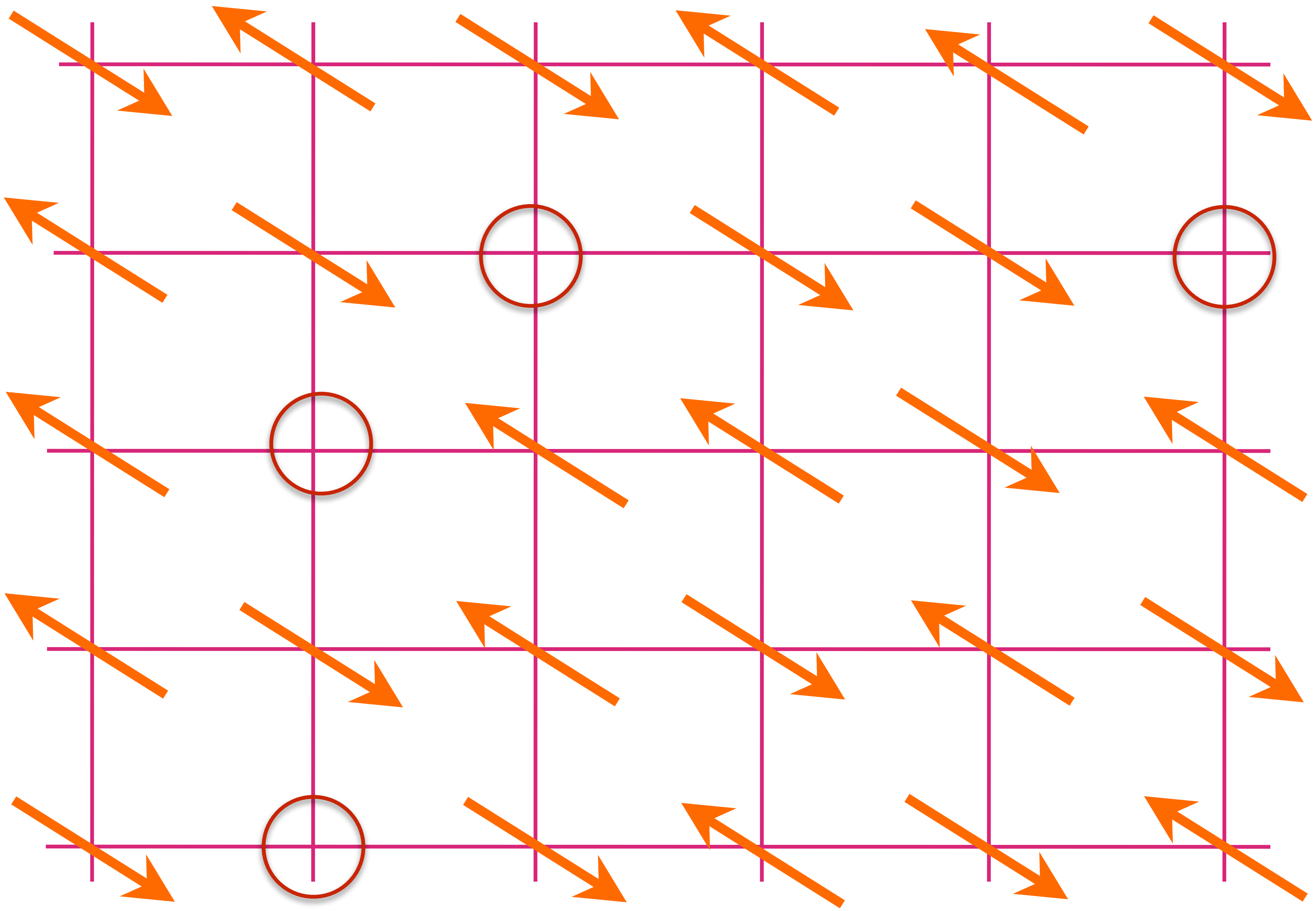

$1-p$ mobile electrons =

$1+p$ mobile holes in a filled band

Momentum-space view at large p

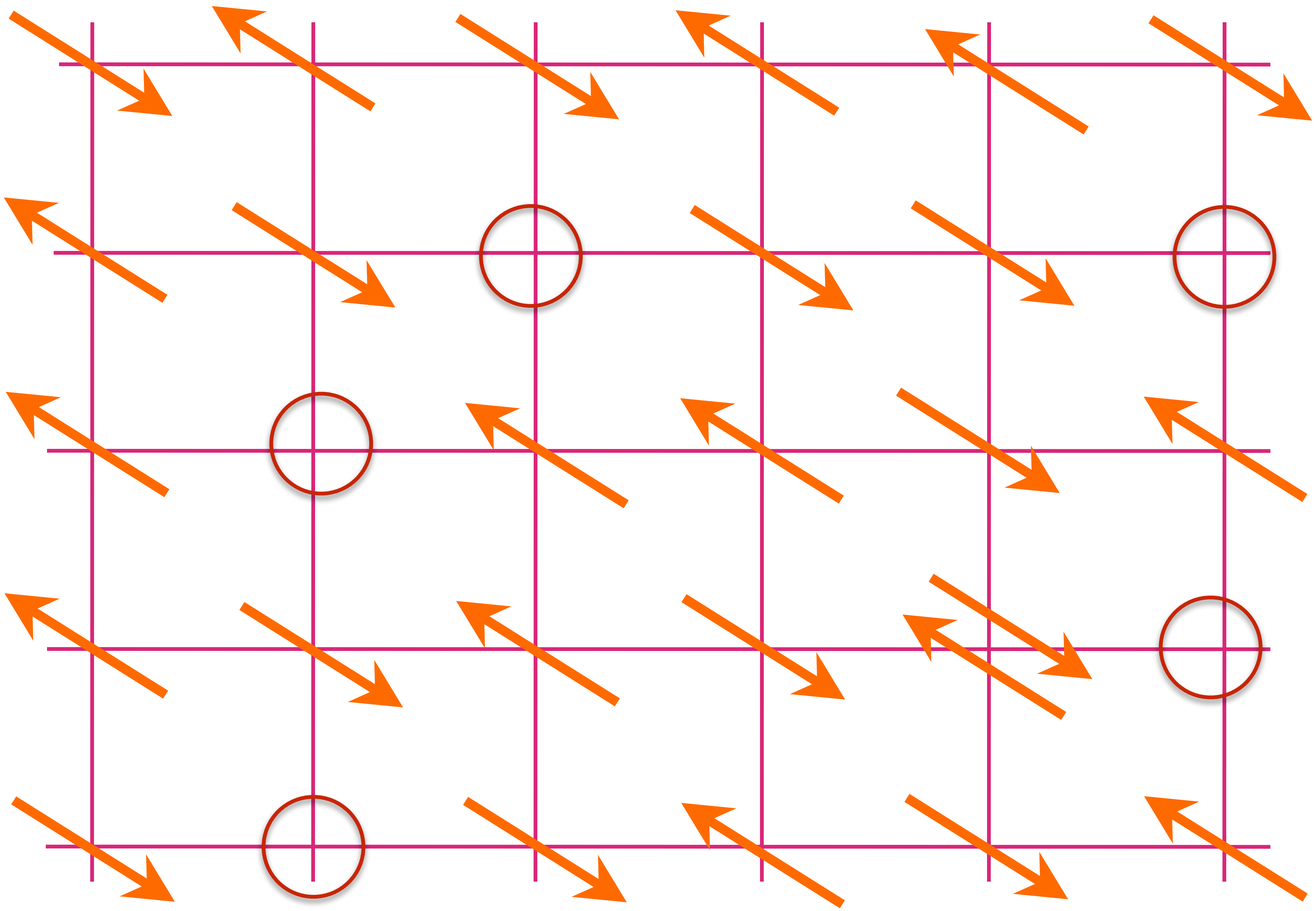

$1\text{-}p$ mobile electrons =

$1+p$ mobile holes in a filled band

Momentum-space view at large p

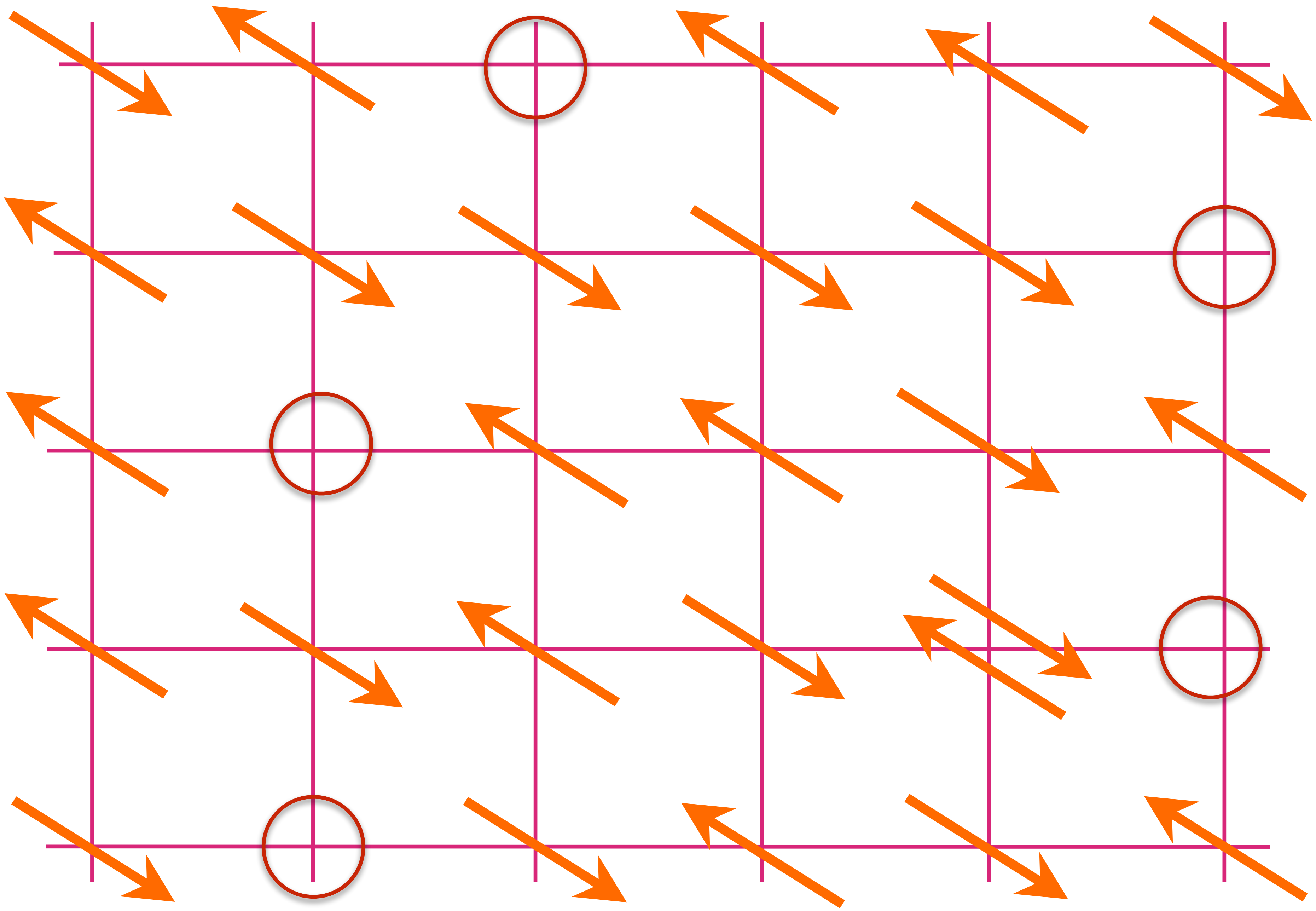

$1-p$ mobile electrons =

$1+p$ mobile holes in a filled band

Momentum-space view at large p

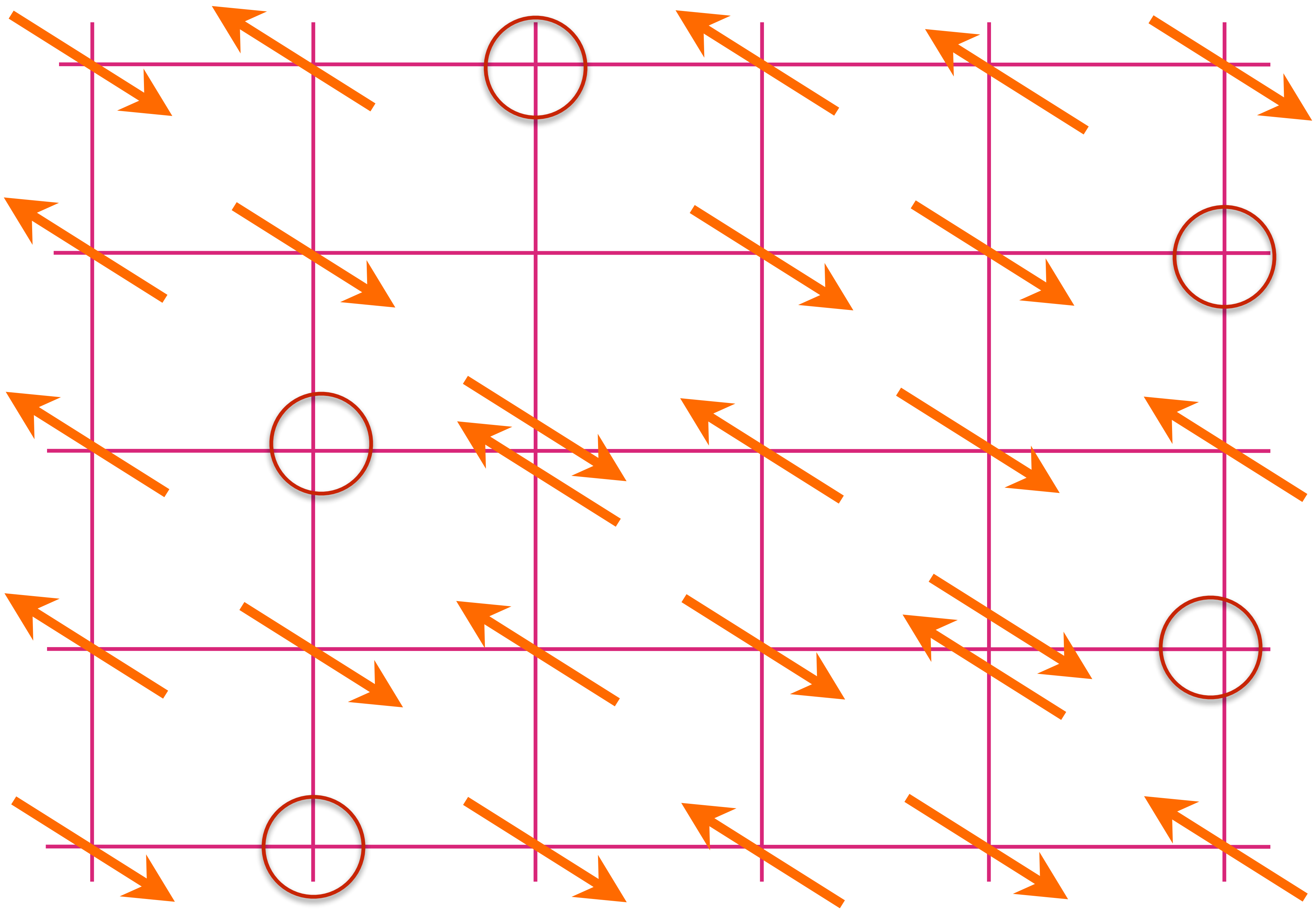

$1\text{-}p$ mobile electrons =
$1+p$ mobile holes in a filled band

Momentum-space view at large p

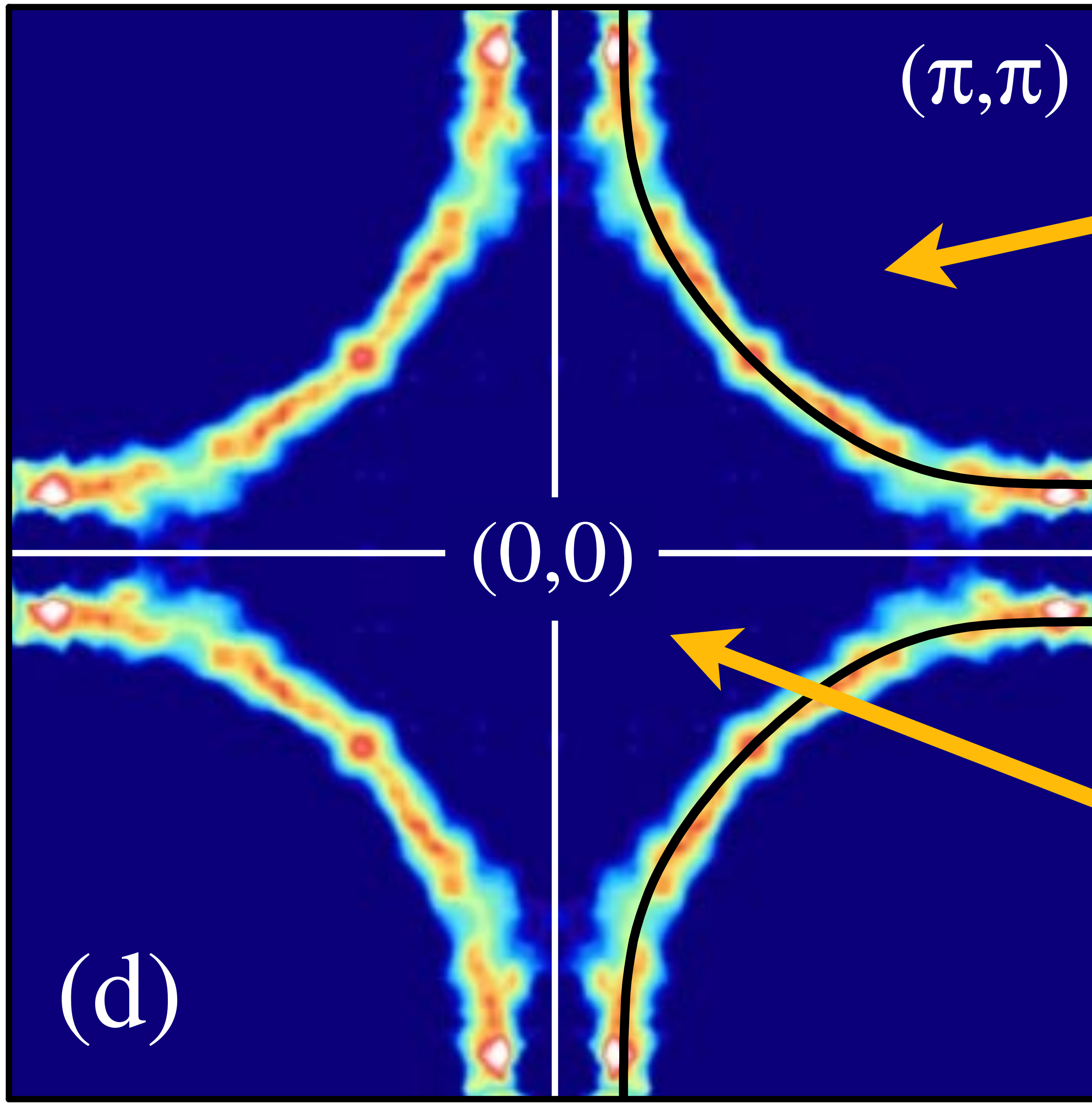

$1+p$ holes

1-p electrons

$1+p$ mobile holes in a filled band

Hole doped cuprates

The remarkable underlying ground states of cuprate superconductors

Cyril Proust and Louis Taillefer, arXiv:1807.0507

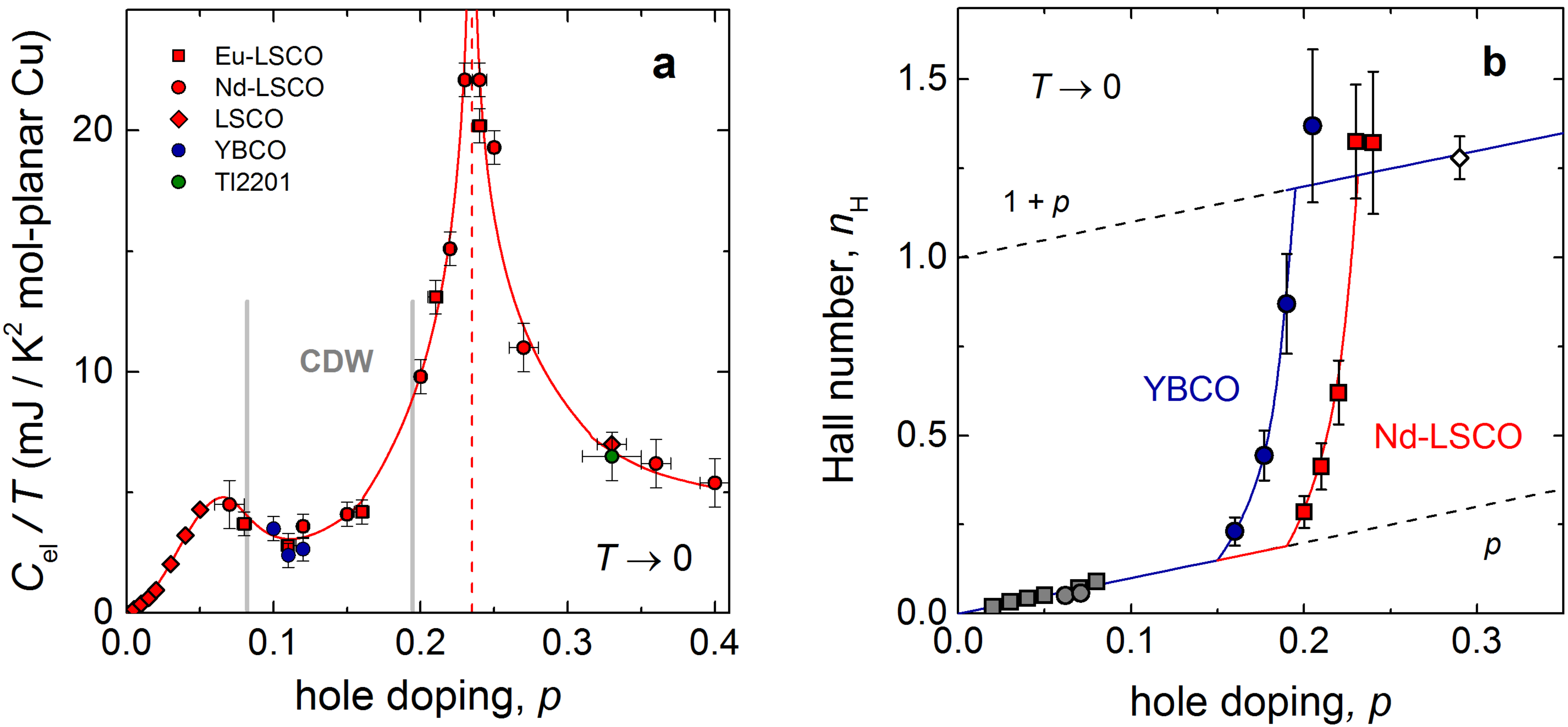

Fermi surface transformation at the pseudogap critical point of a cuprate superconductor

Yawen Fang, Gaël Grissonnanche, Anaëlle Legros, Simon Verret, Francis Laliberté, Clément Collignon, Amirreza Ataei, Maxime Dion, Jianshi Zhou, David Graf, M. J. Lawler, Paul Goddard, Louis Taillefer, and B. J. Ramshaw, arXiv:2004.01725

We use angle-dependent magnetoresistance (ADMR) to measure the Fermi surface of the cuprate $La_{1.6-x}Nd_{0.4}Sr_xCuO_4$. Above the critical doping p*—outside of the pseudogap phase—we find a Fermi surface that is in quantitative agreement with angle-resolved photoemission. Below p*, however, the ADMR is qualitatively different, revealing a clear change in Fermi surface topology. We find that our data is most consistent with a Fermi surface that has been reconstructed by a Q = (π,π) wavevector. While static Q = (π,π) antiferromagnetism is not found at these dopings, our results suggest that this wavevector is a fundamental organizing principle of the pseudogap phase.

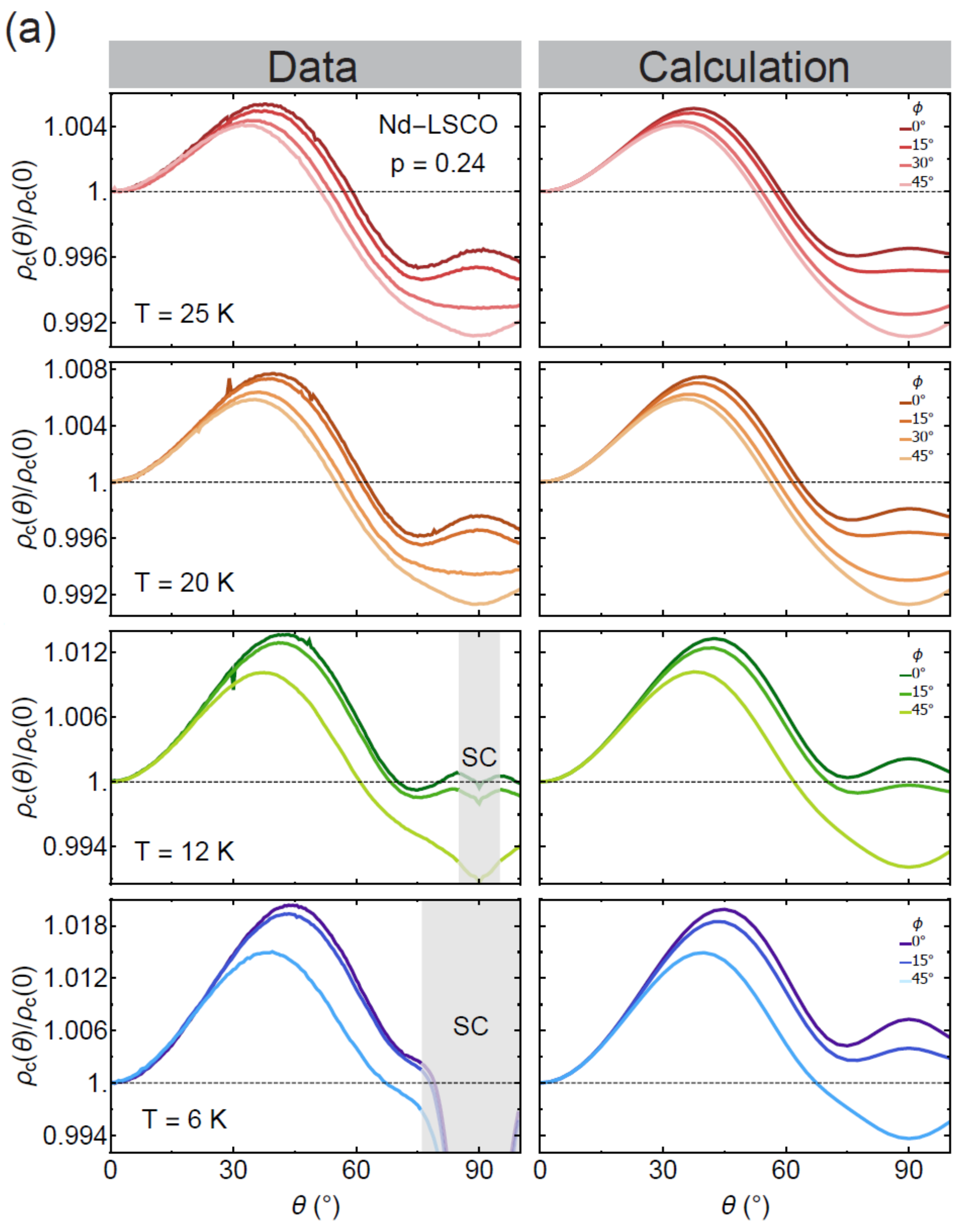

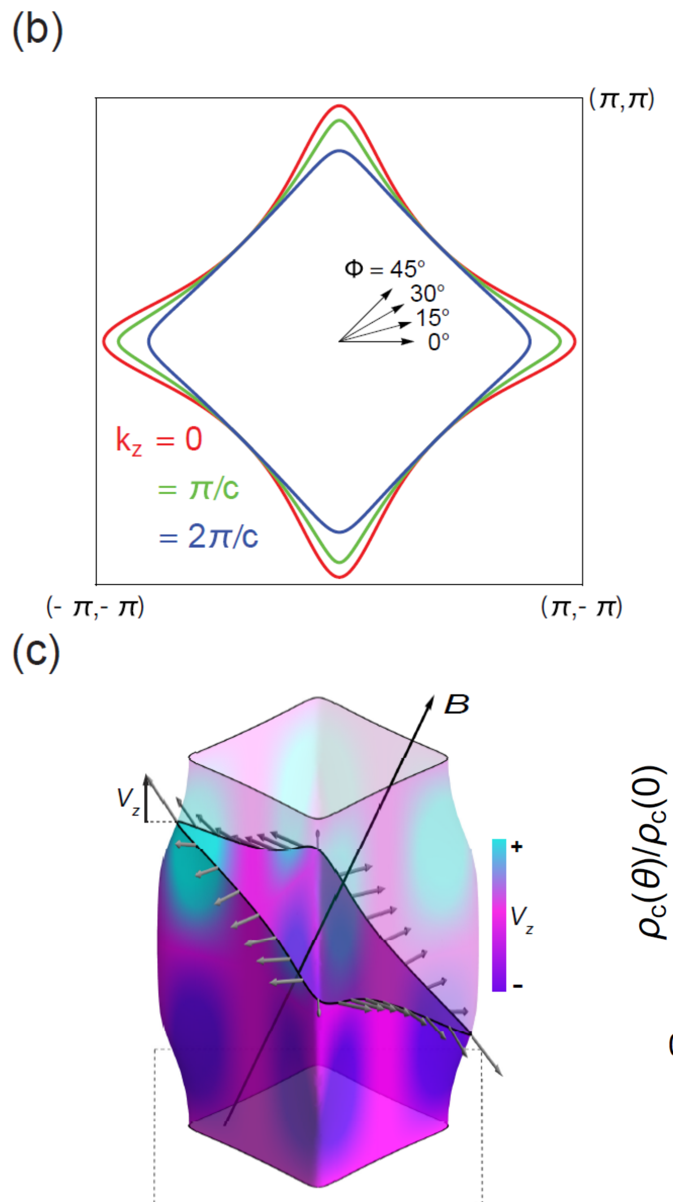

$p > p_c$ Large Fermi surface

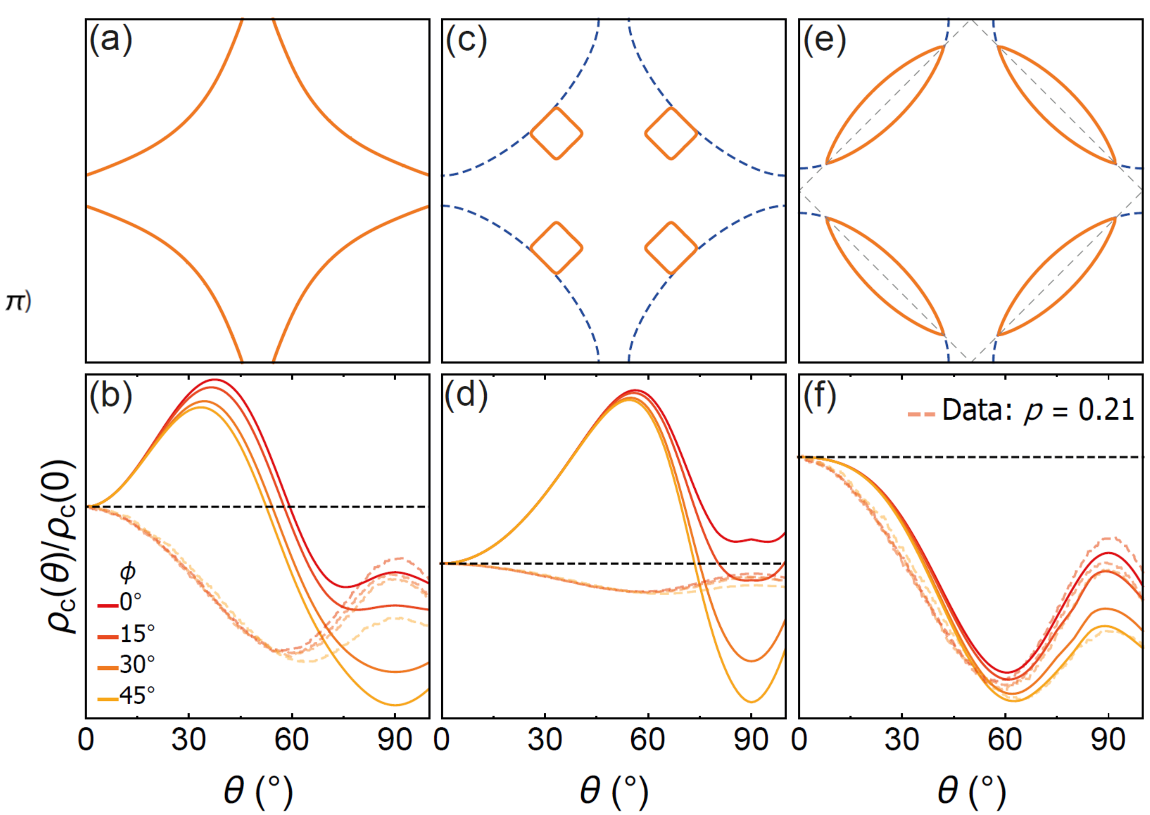

$p < p_c$ Reconstructed Fermi surface

Hidden magnetism at the pseudogap critical point of a high temperature superconductor

Nature Physics doi: 10.1038/s41567-020-0950-5

Mehdi Frachet[1]†, Igor Vinograd[1]†, Rui Zhou[1,2], Siham Benhabib[1], Shangfei Wu[1], Hadrien Mayaffre[1], Steffen Krämer[1], Sanath K. Ramakrishna[3], Arneil P. Reyes[3], Jérôme Debray[4], Tohru Kurosawa[5], Naoki Momono[6], Migaku Oda[5], Seiki Komiya[7], Shimpei Ono[7], Masafumi Horio[8], Johan Chang[8], Cyril Proust[1], David LeBoeuf[1*], Marc-Henri Julien[1*]

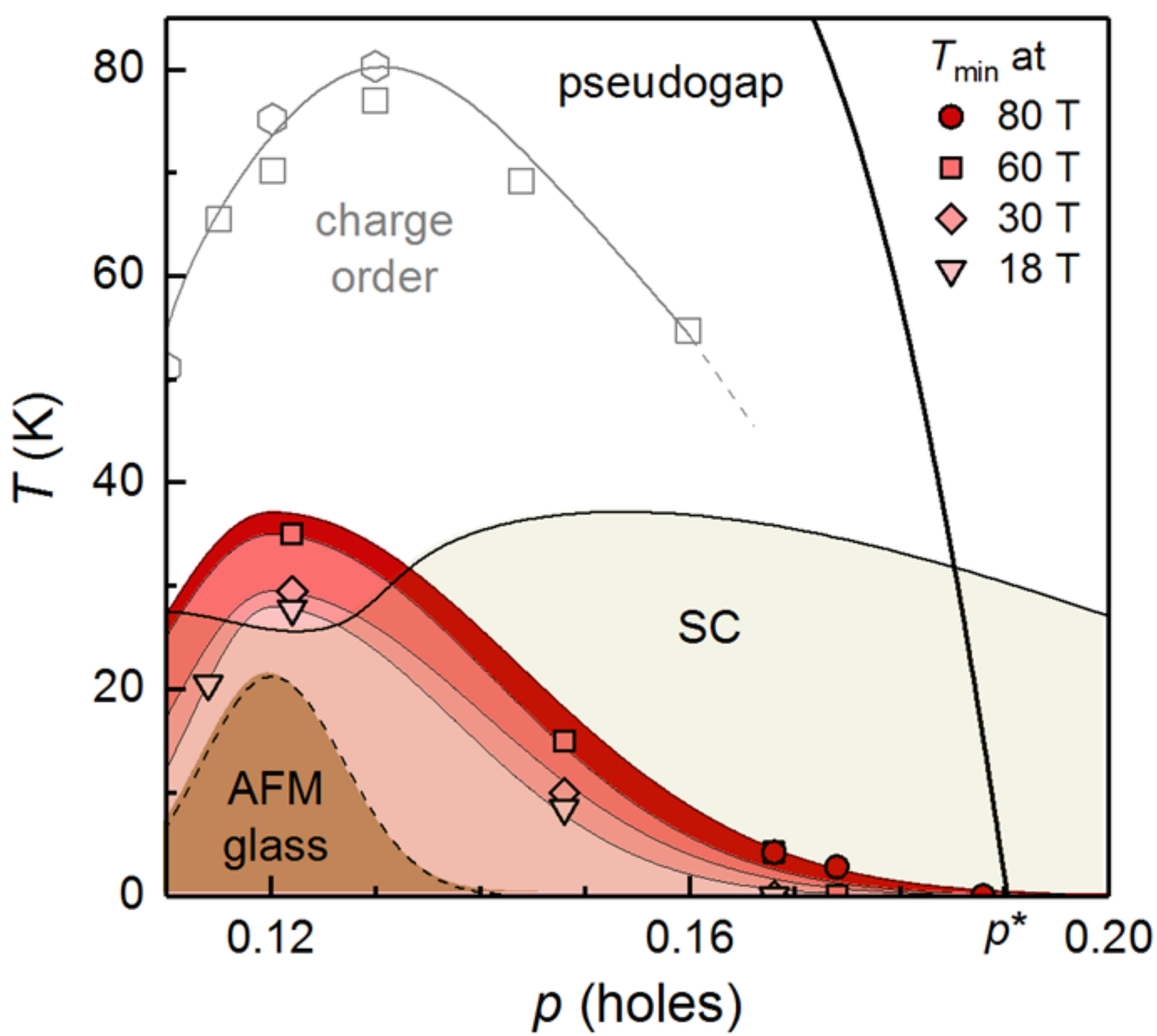

Quasi-static magnetism in the pseudogap state of $La_{2-x}Sr_xCuO_4$. Temperature – doping phase diagram representing T_{min}, the temperature of the minimum in the sound velocity, at different fields. Since superconductivity precludes the observation of T_{min} in zero-field, the dashed line (brown area) represents the extrapolated $T_{min}(B=0)$. While not exactly equal to the freezing temperature T_f (see Fig. 2), T_{min} is closely tied to T_f and so is expected to have the same doping dependence, including a peak around $p = 0.12$ in zero/low fields (ref. 2). Onset temperatures of charge order are from ref. 33 (squares) and 35 (hexagons).

1. Non-random t-*J* model (metals)

   Ancilla qubits and ghost Fermi surfaces

2. All-to-all random Hubbard and *t*-*J* models

   Numerical results

3. Random *J* model (insulator)

   RG analysis and exact exponent

4. Random t-*J* model (metals)

   RG analysis and exact exponents

1. Non-random t-*J* model (metals)

Ancilla qubits and ghost Fermi surfaces

2. All-to-all random Hubbard and *t*-*J* models

Numerical results

3. Random *J* model (insulator)

RG analysis and exact exponent

4. Random t-*J* model (metals)

RG analysis and exact exponents

Metal-metal transitions in ***Kondo lattice*** models

Kondo lattice of f electron spins coupled
to a conduction band of c electrons of density p.

Kondo-breakdown or 'selective Mott' transition

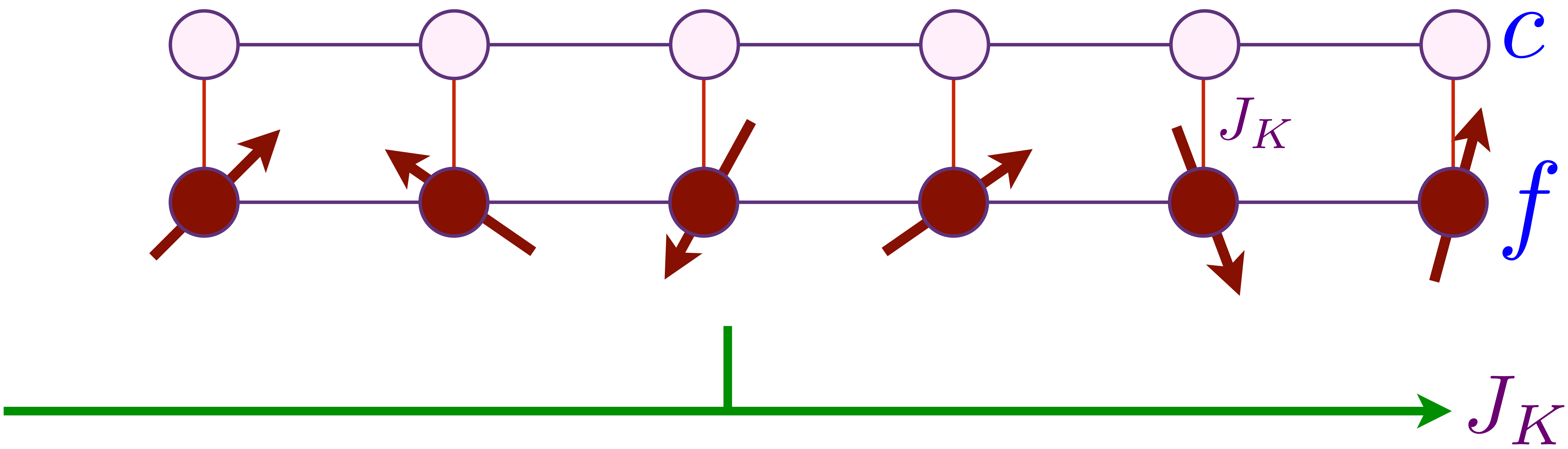

T. Senthil, M. Vojta, and S. Sachdev, PRB **69**, 035111 (2004)

Metal-metal transitions in ***Kondo lattice*** models

Kondo lattice of f electron spins coupled
to a conduction band of c electrons of density p.

Kondo-breakdown or 'selective Mott' transition

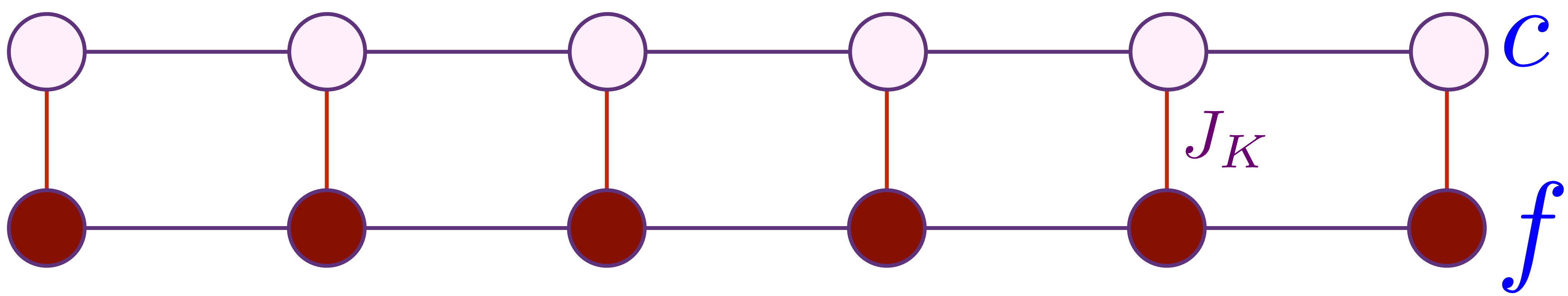

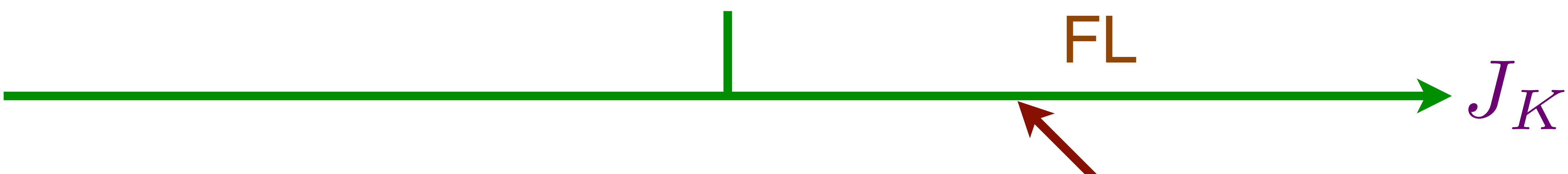

Large Fermi surface of size $1 + p$

$$|\Phi\rangle = [\text{Projection onto one } f \text{ per site}] \bowtie |\text{Slater determinant of } (c, f)\rangle$$

Metal-metal transitions in ***Kondo lattice*** models

Kondo lattice of f electron spins coupled
to a conduction band of c electrons of density p.

Kondo-breakdown or 'selective Mott' transition

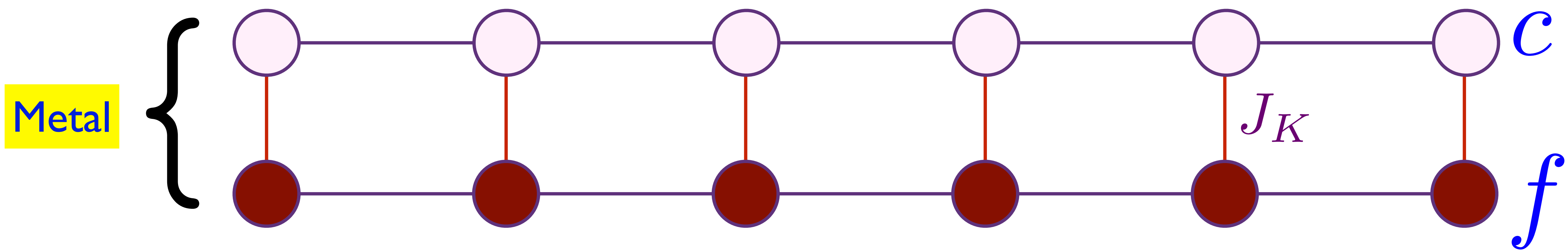

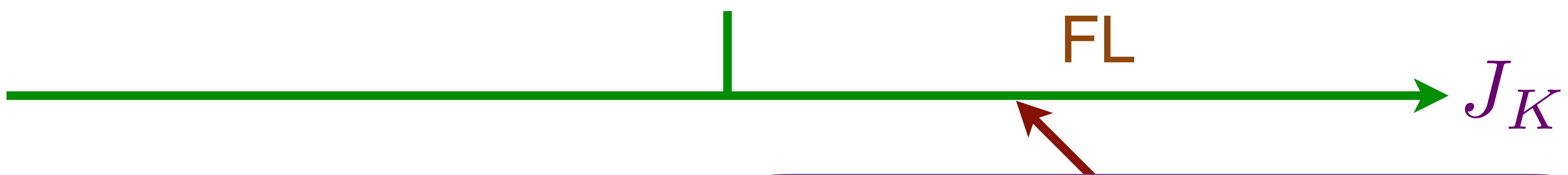

Large Fermi surface of size $1 + p$

$|\Phi\rangle = $ [Projection onto one f per site]
$\bowtie$ $|$Slater determinant of $(c, f)\rangle$

Metal-metal transitions in ***Kondo lattice*** models

Kondo lattice of f electron spins coupled
to a conduction band of c electrons of density p.

Kondo-breakdown or 'selective Mott' transition

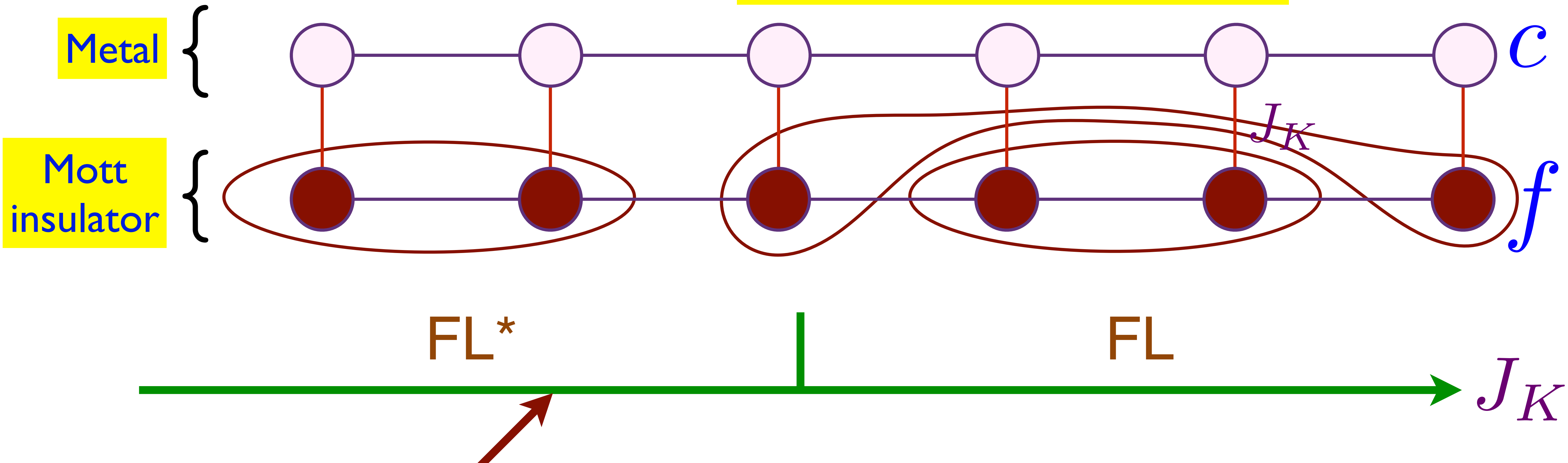

Small Fermi surface of size p

$$|\Phi\rangle = |\text{Spin liquid insulator of } f\rangle \otimes |\text{Slater determinant of } c\rangle$$

T. Senthil, M. Vojta, and S. Sachdev, PRB **69**, 035111 (2004)

Metal-metal transitions in ***Kondo lattice*** models

Kondo lattice of f electron spins coupled
to a conduction band of c electrons of density p.

Kondo-breakdown or 'selective Mott' transition

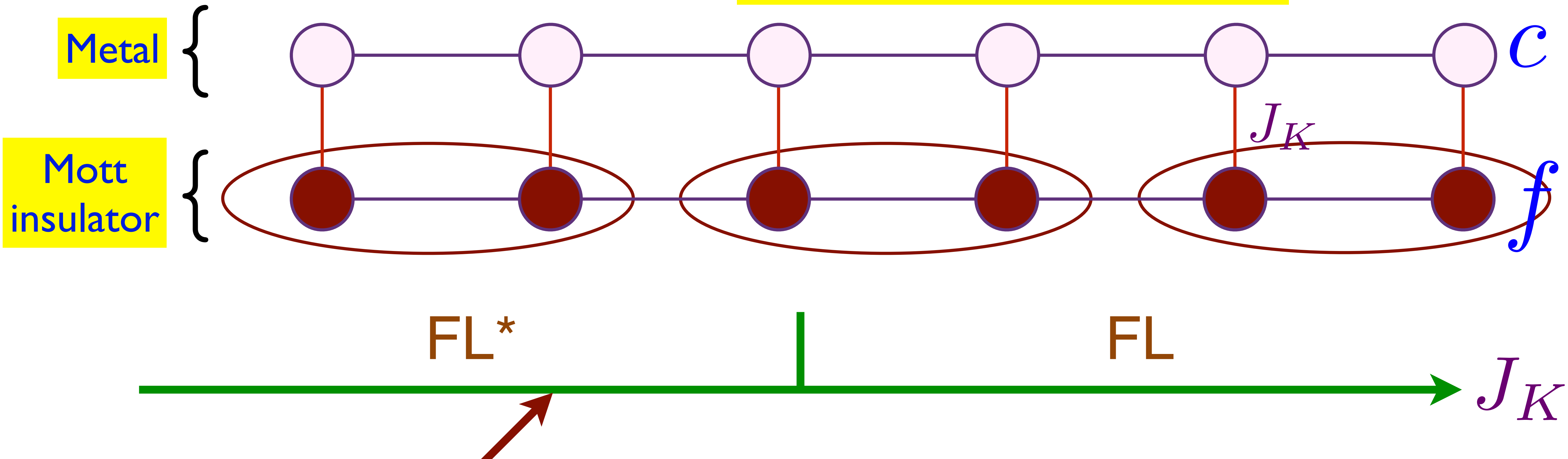

Small Fermi surface of size p

$$|\Phi\rangle = |\text{Spin liquid insulator of } f\rangle \otimes |\text{Slater determinant of } c\rangle$$

T. Senthil, M. Vojta, and S. Sachdev, PRB **69**, 035111 (2004)

Metal-metal transitions in ***Kondo lattice*** models

Kondo lattice of f electron spins coupled
to a conduction band of c electrons of density p.

Kondo-breakdown or 'selective Mott' transition

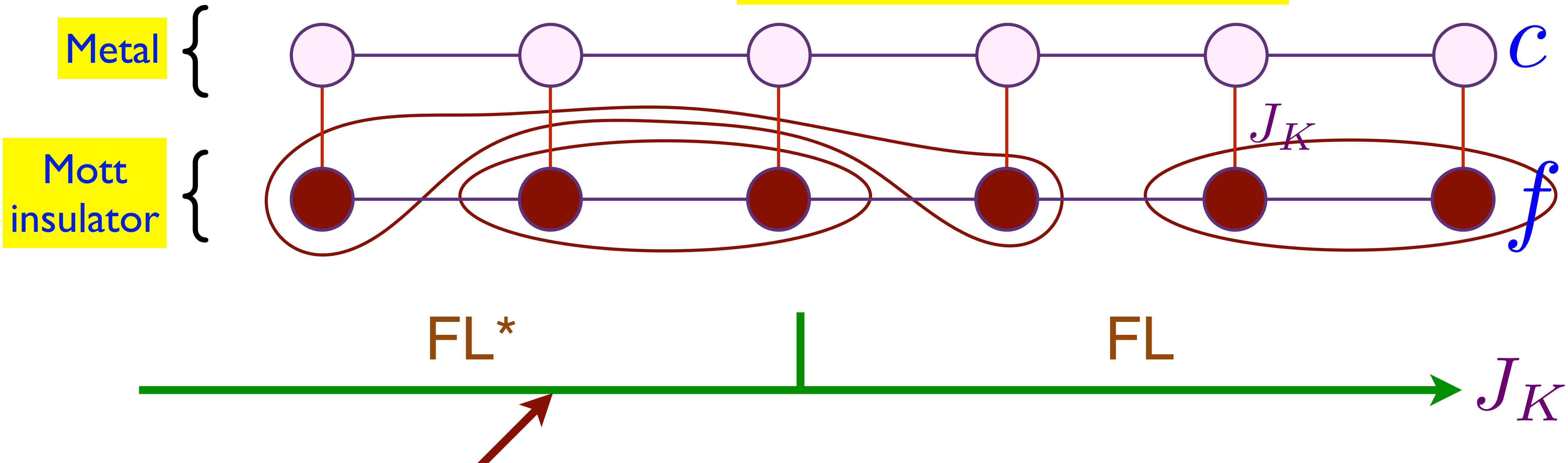

Small Fermi surface of size p

$$|\Phi\rangle = |\text{Spin liquid insulator of } f\rangle \otimes |\text{Slater determinant of } c\rangle$$

T. Senthil, M. Vojta, and S. Sachdev, PRB **69**, 035111 (2004)

Metal-metal transitions in ***Kondo lattice*** models

Kondo lattice of f electron spins coupled
to a conduction band of c electrons of density p.

Kondo-breakdown or 'selective Mott' transition

U(1) gauge theory of a
'hybridization-Higgs' boson
which condenses on the
'Large Fermi surface' side.

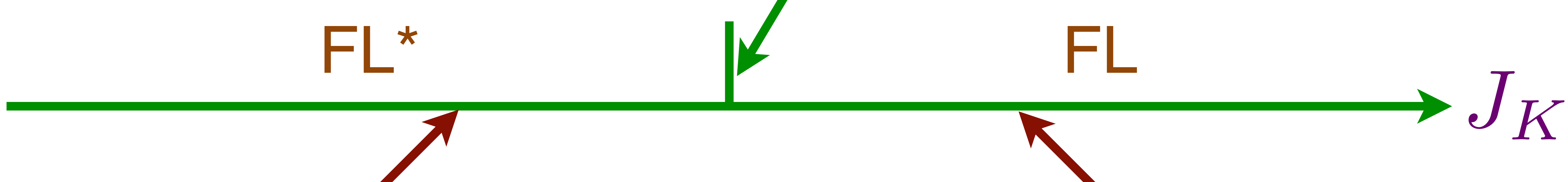

Small Fermi surface of size p

$$|\Phi\rangle = |\text{Spin liquid insulator of } f\rangle \otimes |\text{Slater determinant of } c\rangle$$

Large Fermi surface of size $1+p$

$$|\Phi\rangle = [\text{Projection onto one } f \text{ per site}] \bowtie |\text{Slater determinant of } (c, f)\rangle$$

T. Senthil, M. Vojta, and S. Sachdev, PRB **69**, 035111 (2004)

Metal-metal transitions in a ***one-band*** model

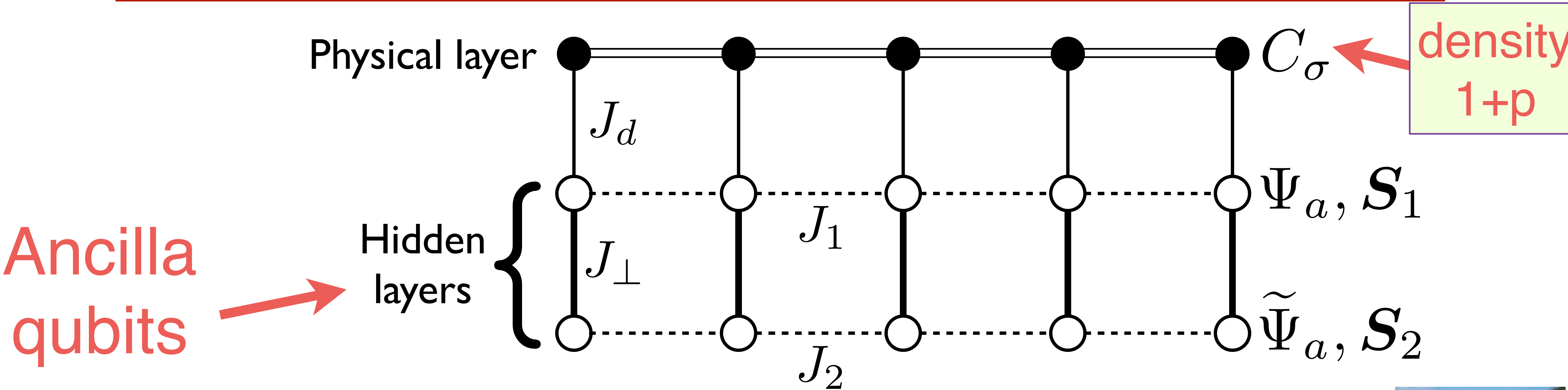


Yahui Zhang

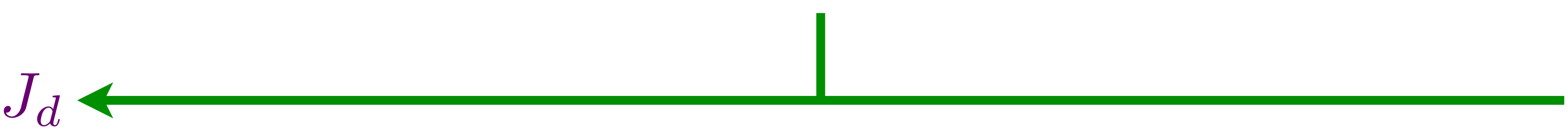

Ya-Hui Zhang, S. Sachdev, PRR **2**, 023172 (2020); arXiv:2006.01140.

Metal-metal transitions in a ***one-band*** model

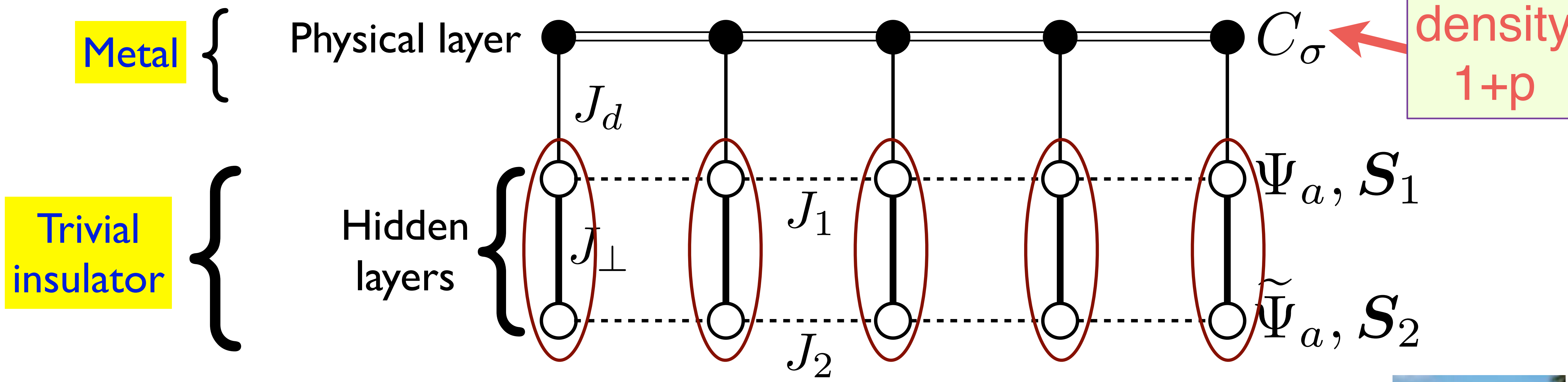

Yahui Zhang

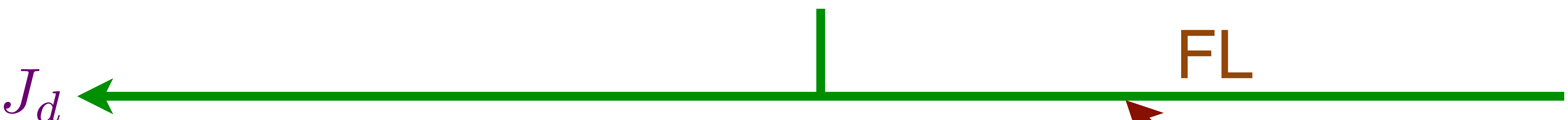

Large Fermi surface of size $1 + p$

$$|\Phi\rangle = \left|\text{Rung singlets of } \Psi, \widetilde{\Psi}\right\rangle \otimes |\text{Slater determinant of } C\rangle$$

Ya-Hui Zhang, S. Sachdev, PRR **2**, 023172 (2020); arXiv:2006.01140.

Metal-metal transitions in a *one-band* model

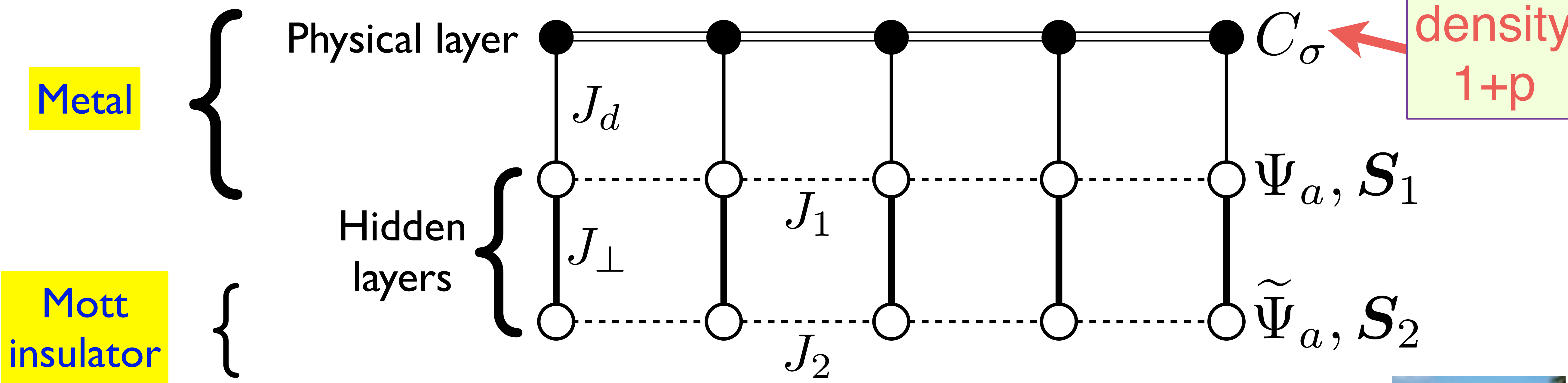

Yahui Zhang

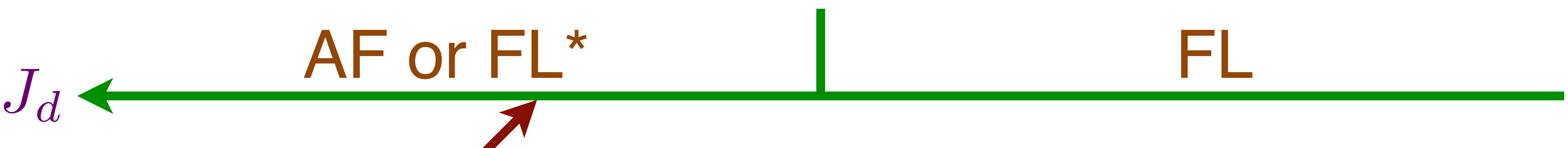

Small Fermi surface of size p

$$|\Phi\rangle = \left[\text{Projection onto rung singlets of } \Psi, \widetilde{\Psi}\right] \bowtie |\text{Slater determinant of } (C, \Psi)\rangle \otimes \left|\text{Slater determinant of } \widetilde{\Psi}\right\rangle$$

Ya-Hui Zhang, S. Sachdev, PRR **2**, 023172 (2020); arXiv:2006.01140.

Metal-metal transitions in a ***one-band*** model

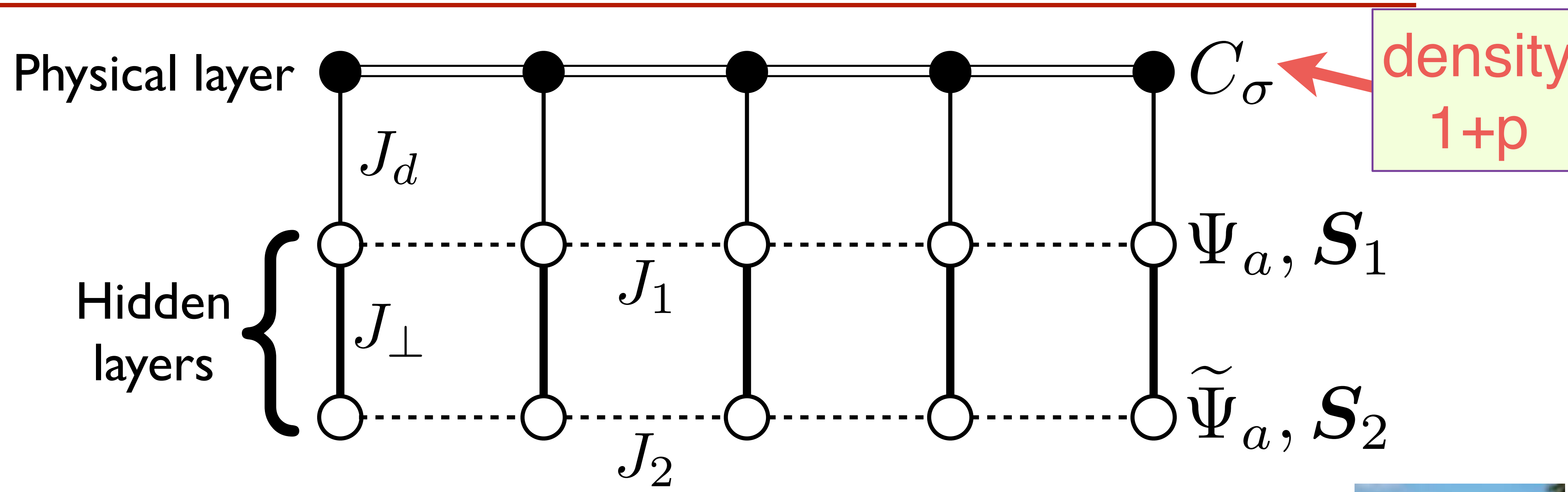

$(U(1) \times U(1))/Z_2$ or $(SU(2) \times U(1))/Z_2$ gauge theory of a ghost Fermi surface and a 'hybridization-Higgs' boson which condenses on the 'Small Fermi surface' side.


Yahui Zhang

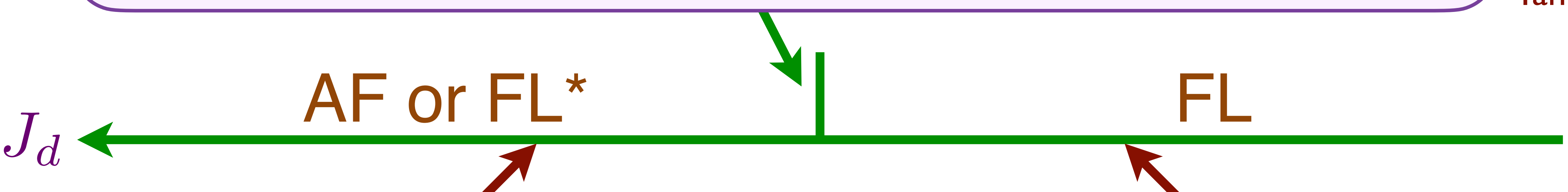

Small Fermi surface of size p

$$|\Phi\rangle = \left[\text{Projection onto rung singlets of } \Psi, \widetilde{\Psi}\right] \bowtie |\text{Slater determinant of } (C, \Psi)\rangle \otimes \left|\text{Slater determinant of } \widetilde{\Psi}\right\rangle$$

Large Fermi surface of size $1 + p$

$$|\Phi\rangle = \left|\text{Rung singlets of } \Psi, \widetilde{\Psi}\right\rangle \otimes |\text{Slater determinant of } C\rangle$$

Ya-Hui Zhang, S. Sachdev, PRR **2**, 023172 (2020); arXiv:2006.01140.

1. Non-random t-*J* model (metals)

Ancilla qubits and ghost Fermi surfaces

2. All-to-all random Hubbard and *t*-*J* models

Numerical results

3. Random *J* model (insulator)

RG analysis and exact exponent

4. Random t-*J* model (metals)

RG analysis and exact exponents

Random t-J-U_H model

$$H = -\frac{1}{\sqrt{N}} \sum_{i,j=1}^{N} t_{ij}\, c_{i\alpha}^\dagger c_{j\alpha} + \frac{1}{\sqrt{N}} \sum_{i<j=1}^{N} J_{ij}\, \vec{S}_i \cdot \vec{S}_j + U_H \sum_{i=1}^{N} n_{i\uparrow} n_{i\downarrow}$$

$$\alpha = \uparrow, \downarrow, \quad \vec{S}_i = \frac{1}{2} c_{i\alpha}^\dagger \vec{\sigma}_{\alpha\beta} c_{i\beta}, \quad n_{i\alpha} = c_{i\alpha}^\dagger c_{i\alpha},$$

$$J_{ij} \text{ random}, \overline{J_{ij}} = 0, \overline{J_{ij}^2} = J^2$$
$$t_{ij} \text{ random}, \overline{t_{ij}} = 0, \overline{t_{ij}^2} = t^2$$

$$U_H > 0 \text{ non-random}$$

Random t-J-U_H model

$$H = -\frac{1}{\sqrt{N}} \sum_{i,j=1}^{N} t_{ij}\, c_{i\alpha}^{\dagger} c_{j\alpha} + \frac{1}{\sqrt{N}} \sum_{i<j=1}^{N} J_{ij}\, \vec{S}_i \cdot \vec{S}_j + U_H \sum_{i=1}^{N} n_{i\uparrow} n_{i\downarrow}$$

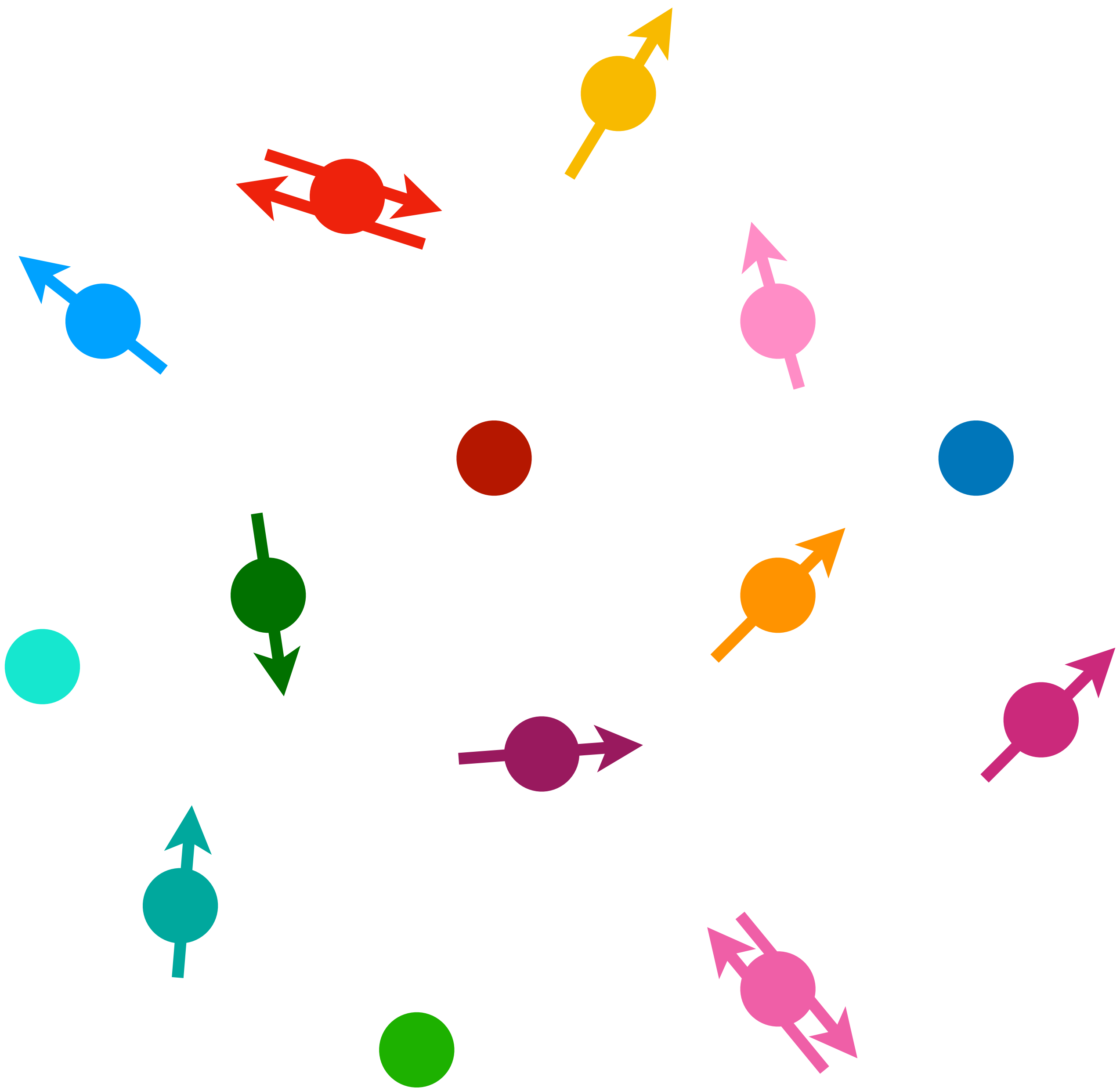

Random *t-J-U*

$$H = -\frac{1}{\sqrt{N}} \sum_{i,j=1}^{N} t_{ij}\, c^{\dagger}_{i\alpha} c_{j\alpha} + \frac{1}{\sqrt{N}} \sum_{i<j=1}^{N} J_{ij}\, \vec{S}_i \cdot \vec{S}_j + U_H \sum_{i=1}^{N} n_{i\uparrow} n_{i\downarrow}$$

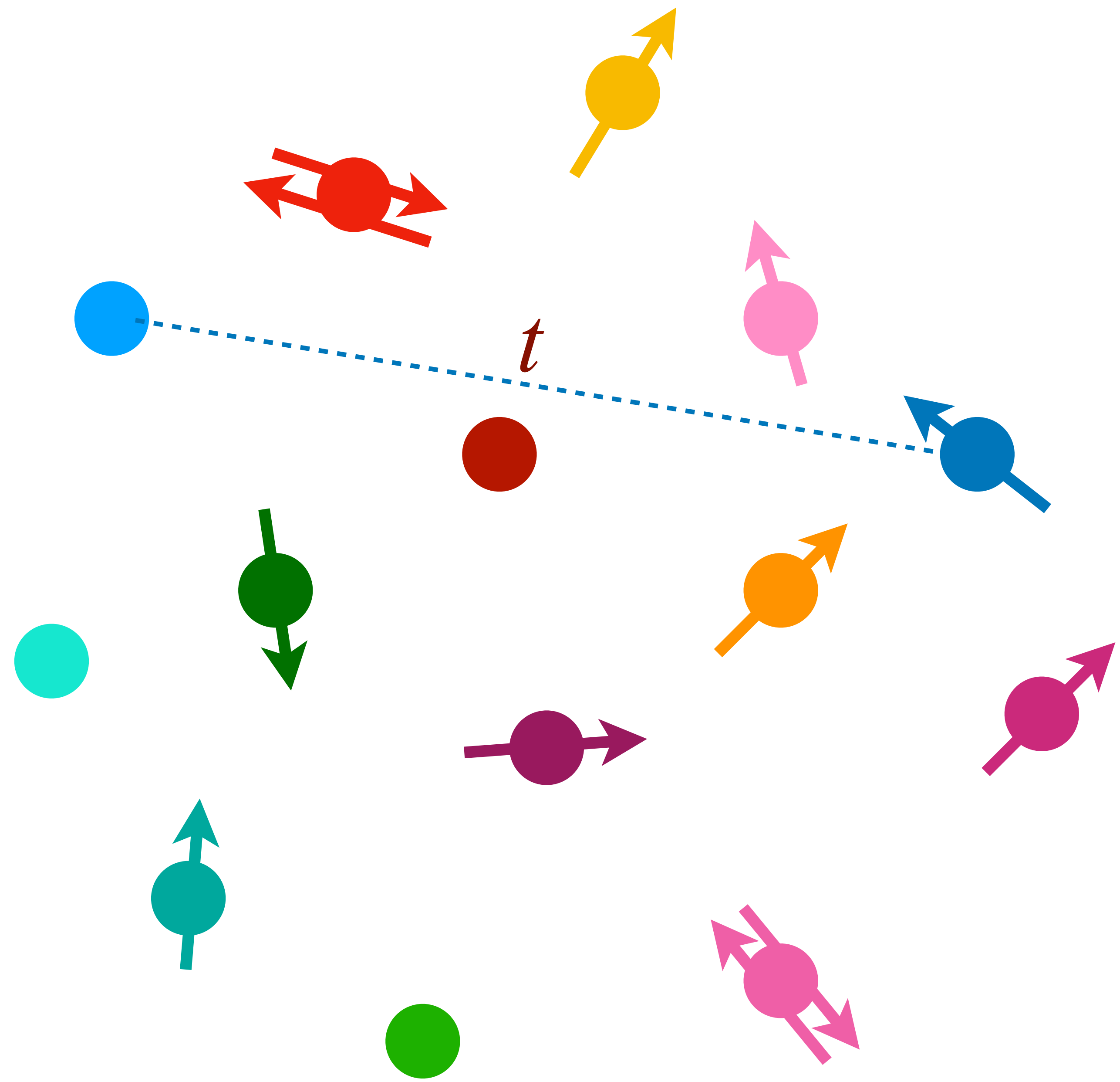

Random t-J-U_H model

$$H = -\frac{1}{\sqrt{N}} \sum_{i,j=1}^{N} t_{ij}\, c_{i\alpha}^{\dagger} c_{j\alpha} + \frac{1}{\sqrt{N}} \sum_{i<j=1}^{N} J_{ij}\, \vec{S}_i \cdot \vec{S}_j + U_H \sum_{i=1}^{N} n_{i\uparrow} n_{i\downarrow}$$

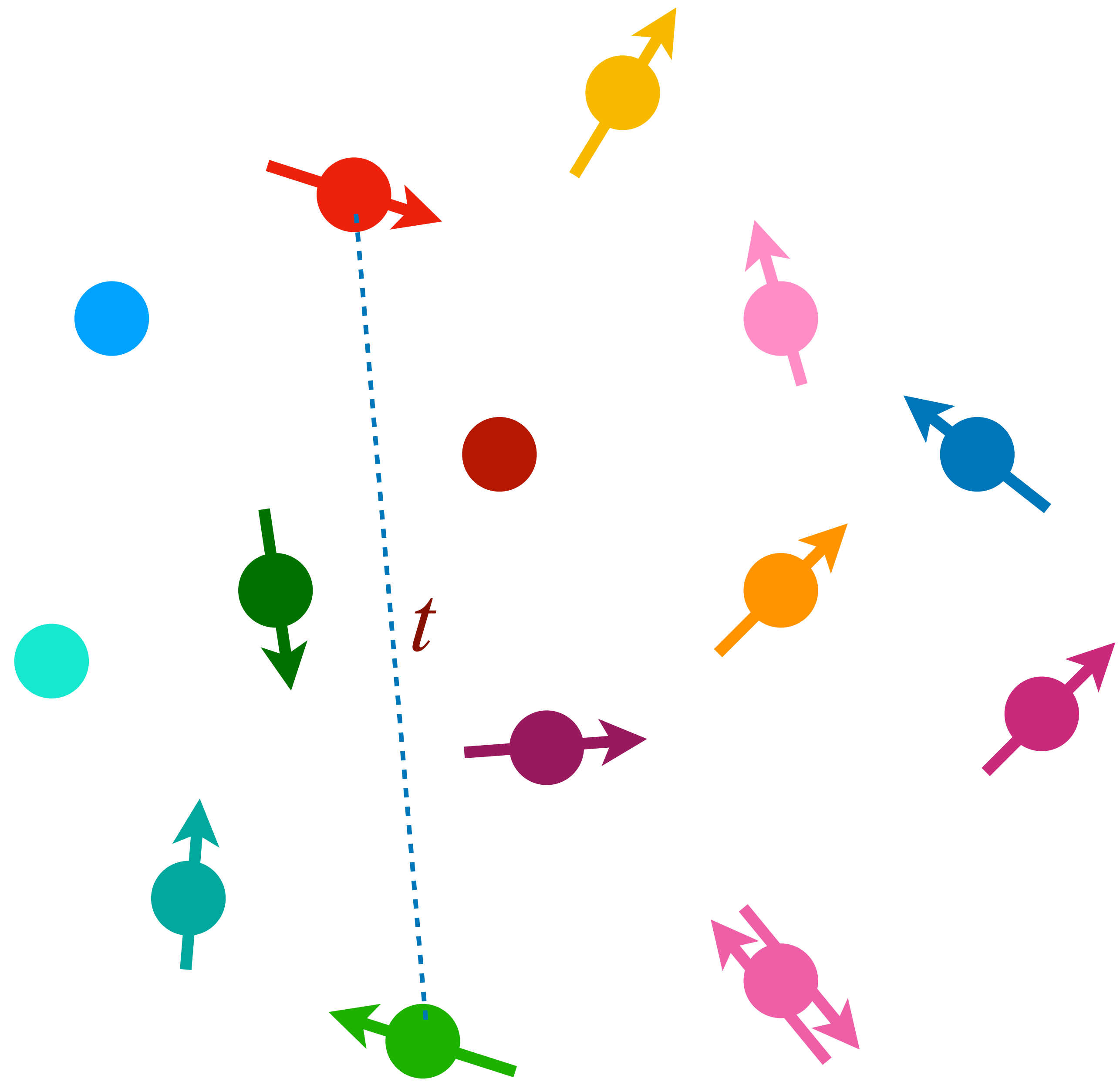

Random t-J-U_H model

$$H = -\frac{1}{\sqrt{N}} \sum_{i,j=1}^{N} t_{ij}\, c_{i\alpha}^{\dagger} c_{j\alpha} + \frac{1}{\sqrt{N}} \sum_{i<j=1}^{N} J_{ij}\, \vec{S}_i \cdot \vec{S}_j + U_H \sum_{i=1}^{N} n_{i\uparrow} n_{i\downarrow}$$

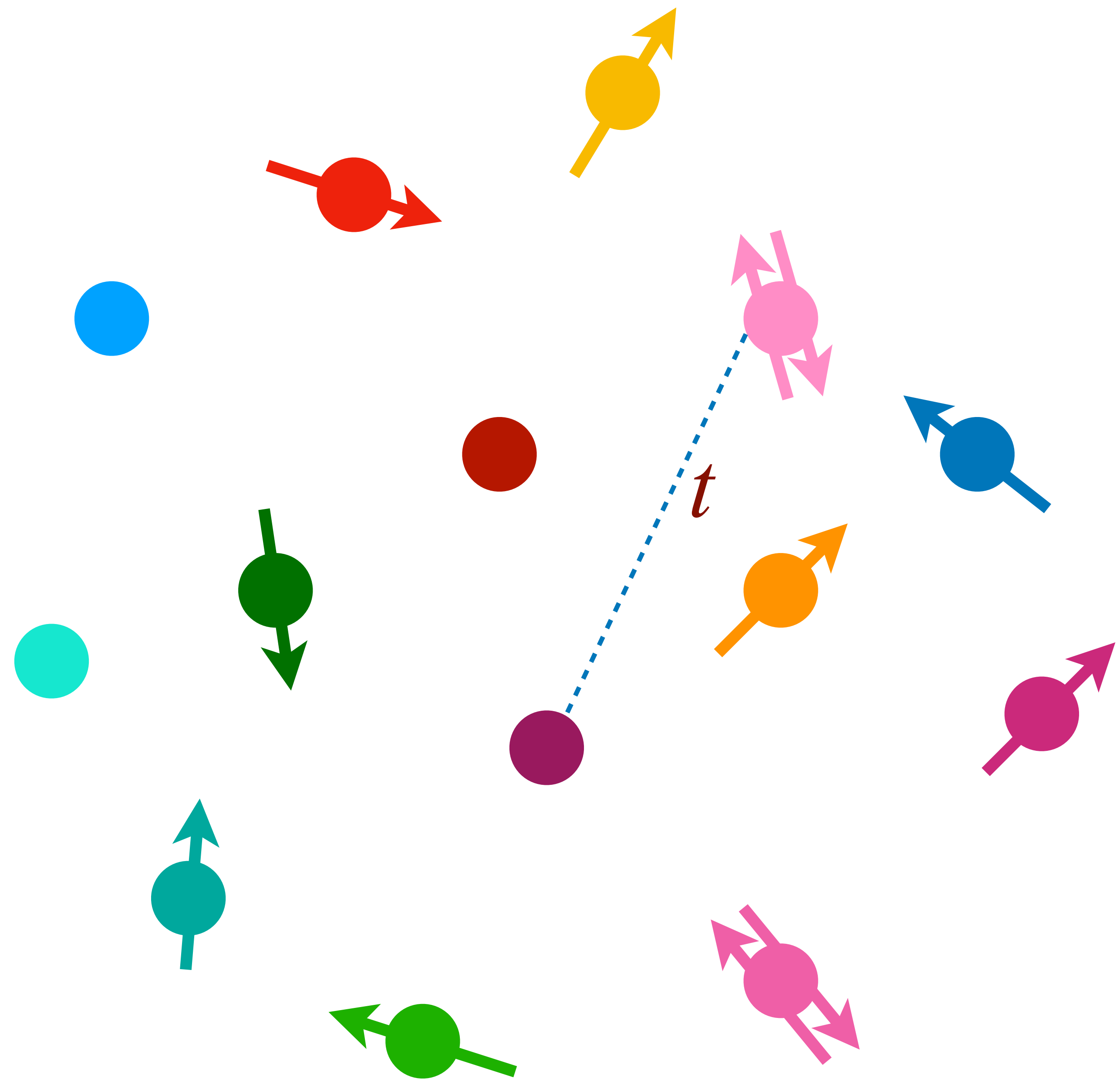

Random *t-J-U_H* model

$$H = -\frac{1}{\sqrt{N}} \sum_{i,j=1}^{N} t_{ij}\, c_{i\alpha}^{\dagger} c_{j\alpha} + \frac{1}{\sqrt{N}} \sum_{i<j=1}^{N} J_{ij}\, \vec{S}_i \cdot \vec{S}_j + U_H \sum_{i=1}^{N} n_{i\uparrow} n_{i\downarrow}$$

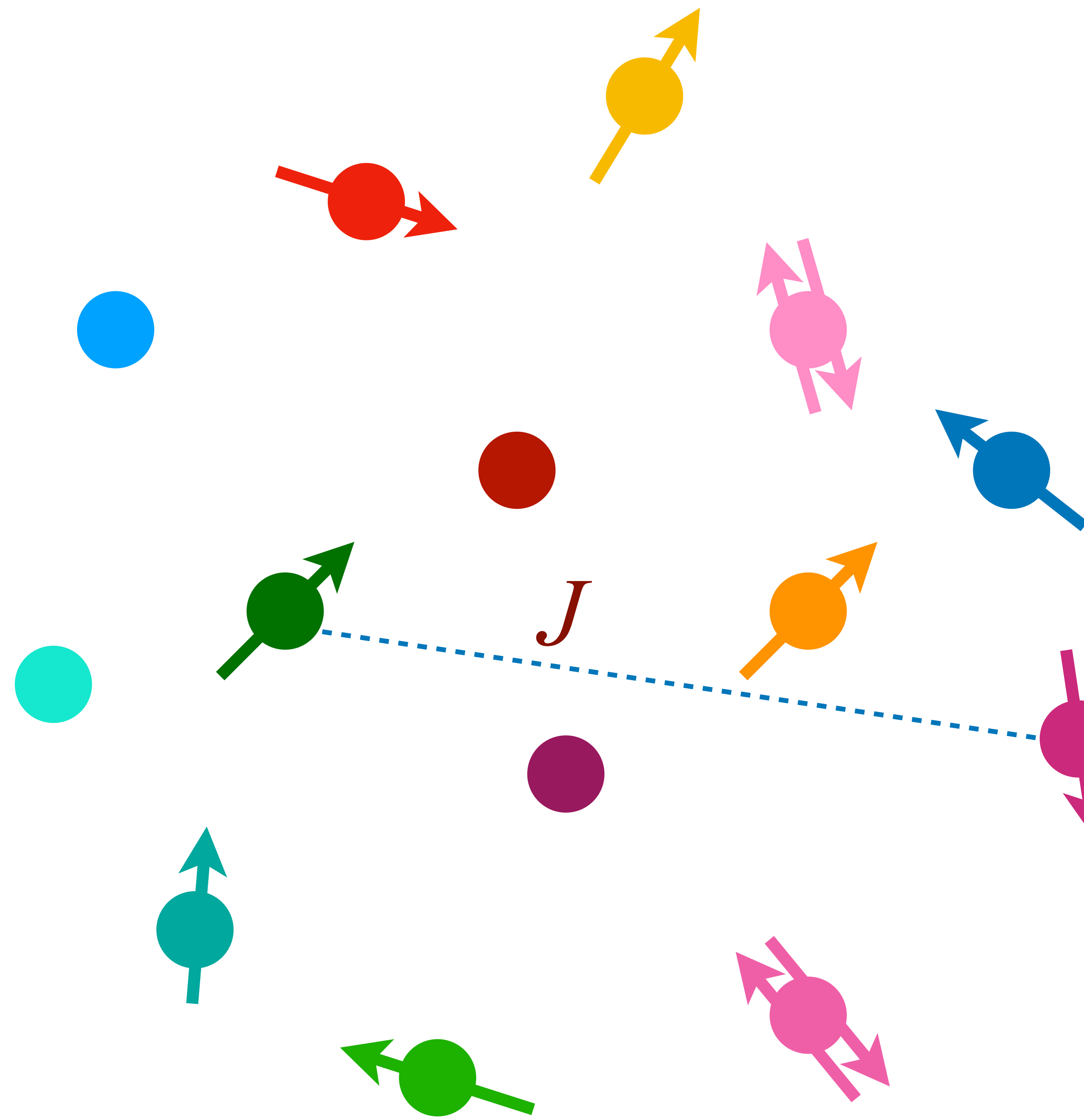

Random t-J-U_H model

$$H = -\frac{1}{\sqrt{N}} \sum_{i,j=1}^{N} t_{ij}\, c^\dagger_{i\alpha} c_{j\alpha} + \frac{1}{\sqrt{N}} \sum_{i<j=1}^{N} J_{ij}\, \vec{S}_i \cdot \vec{S}_j + U_H \sum_{i=1}^{N} n_{i\uparrow} n_{i\downarrow}$$

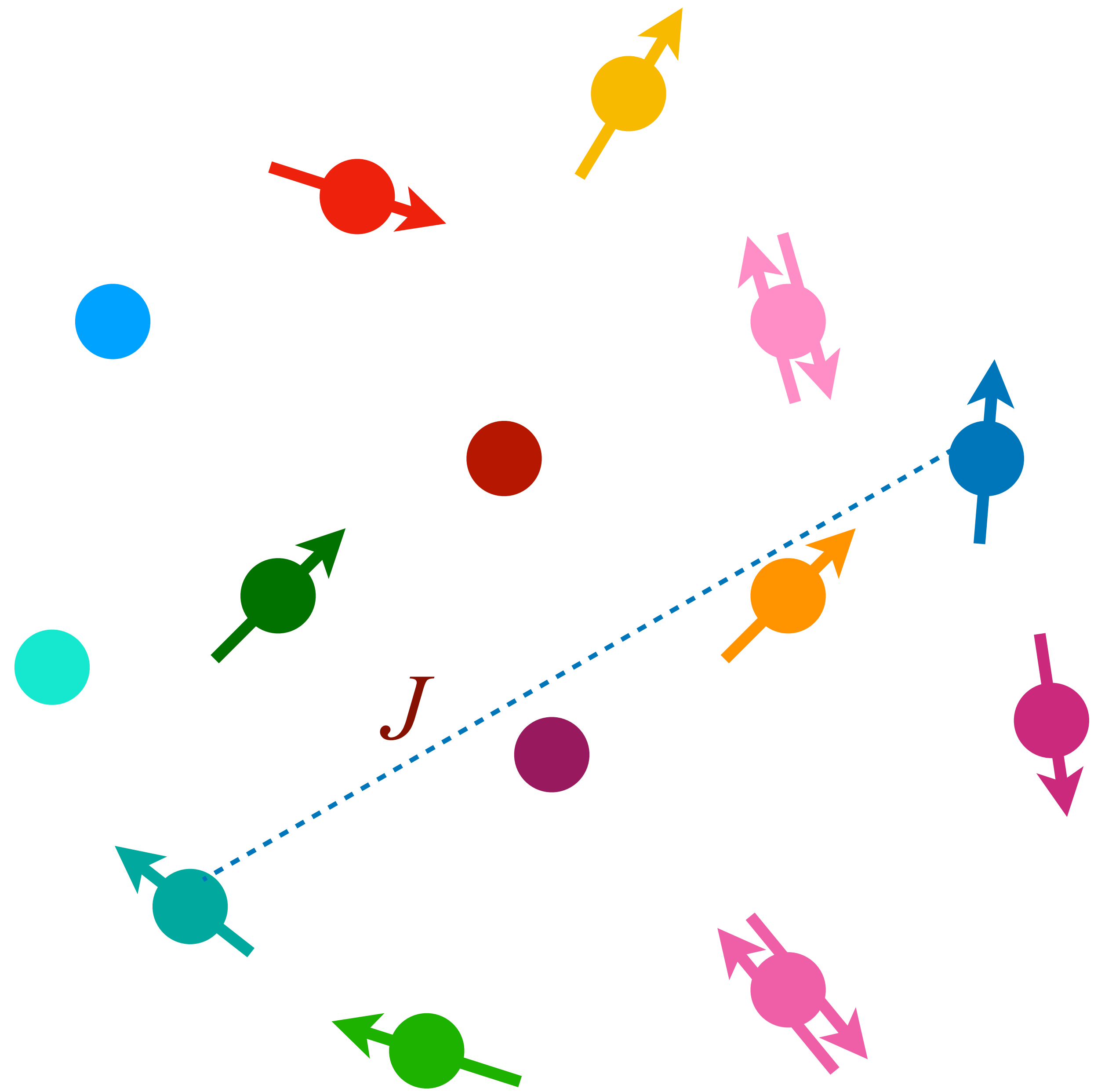

Random *t-J-U_H* model

$$H = -\frac{1}{\sqrt{N}} \sum_{i,j=1}^{N} t_{ij}\, c^\dagger_{i\alpha} c_{j\alpha} + \frac{1}{\sqrt{N}} \sum_{i<j=1}^{N} J_{ij}\, \vec{S}_i \cdot \vec{S}_j + U_H \sum_{i=1}^{N} n_{i\uparrow} n_{i\downarrow}$$

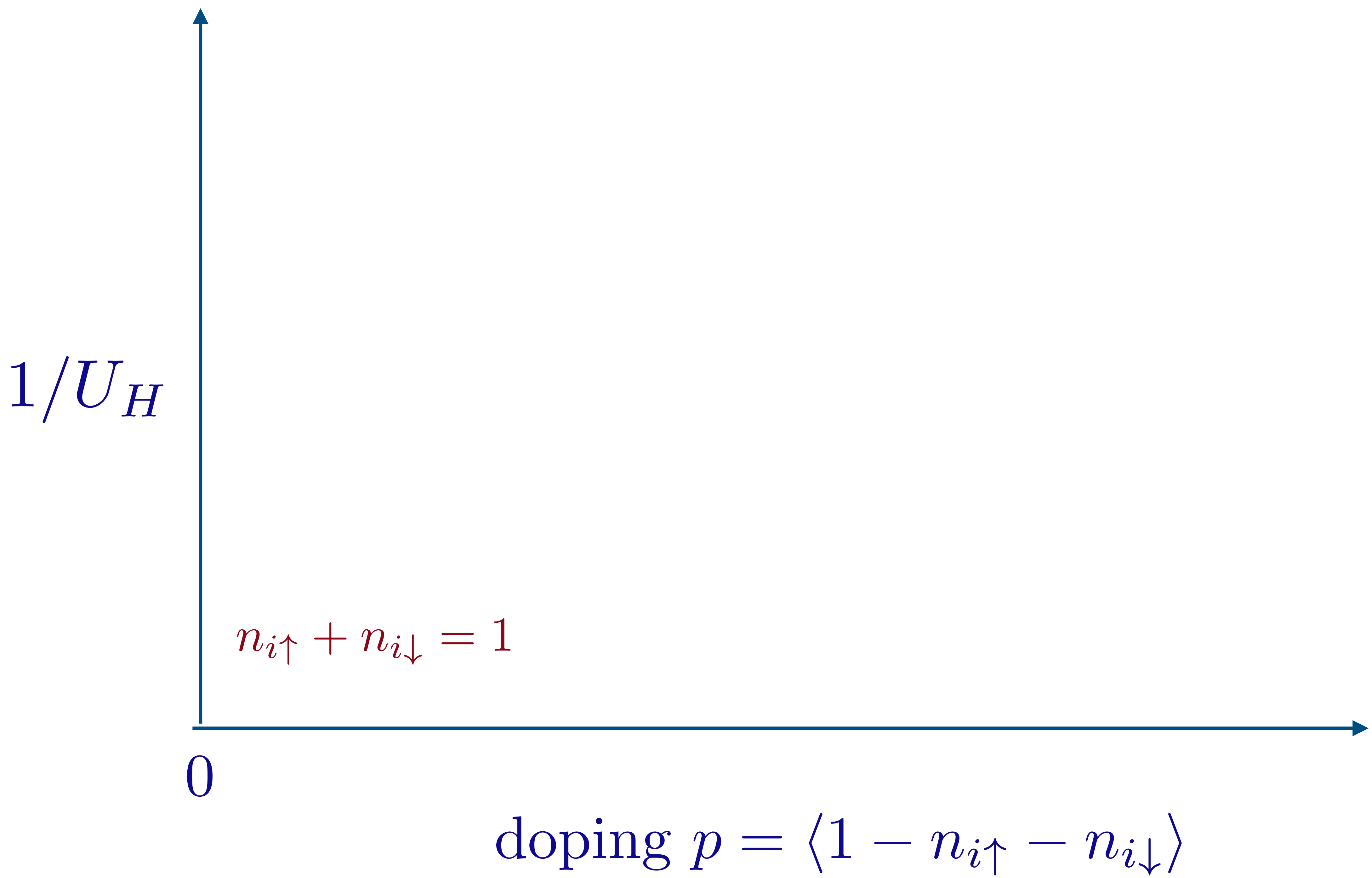

Random t-J-U_H model

$$H = -\frac{1}{\sqrt{N}} \sum_{i,j=1}^{N} t_{ij}\, c_{i\alpha}^{\dagger} c_{j\alpha} + \frac{1}{\sqrt{N}} \sum_{i<j=1}^{N} J_{ij}\, \vec{S}_i \cdot \vec{S}_j + U_H \sum_{i=1}^{N} n_{i\uparrow} n_{i\downarrow}$$

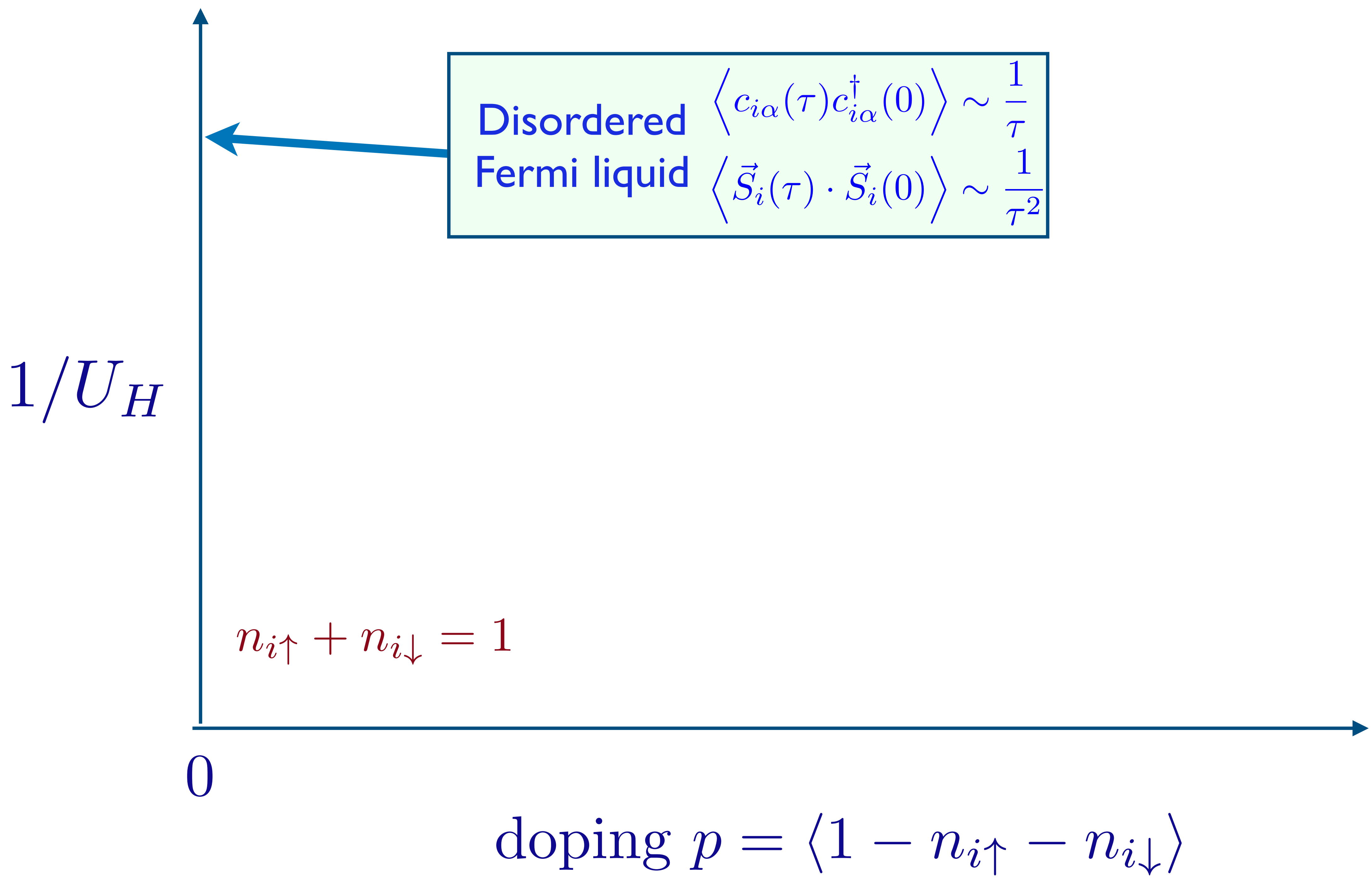

Random t-J-U_H model

$$H = -\frac{1}{\sqrt{N}} \sum_{i,j=1}^{N} t_{ij}\, c_{i\alpha}^{\dagger} c_{j\alpha} + \frac{1}{\sqrt{N}} \sum_{i<j=1}^{N} J_{ij}\, \vec{S}_i \cdot \vec{S}_j + U_H \sum_{i=1}^{N} n_{i\uparrow} n_{i\downarrow}$$

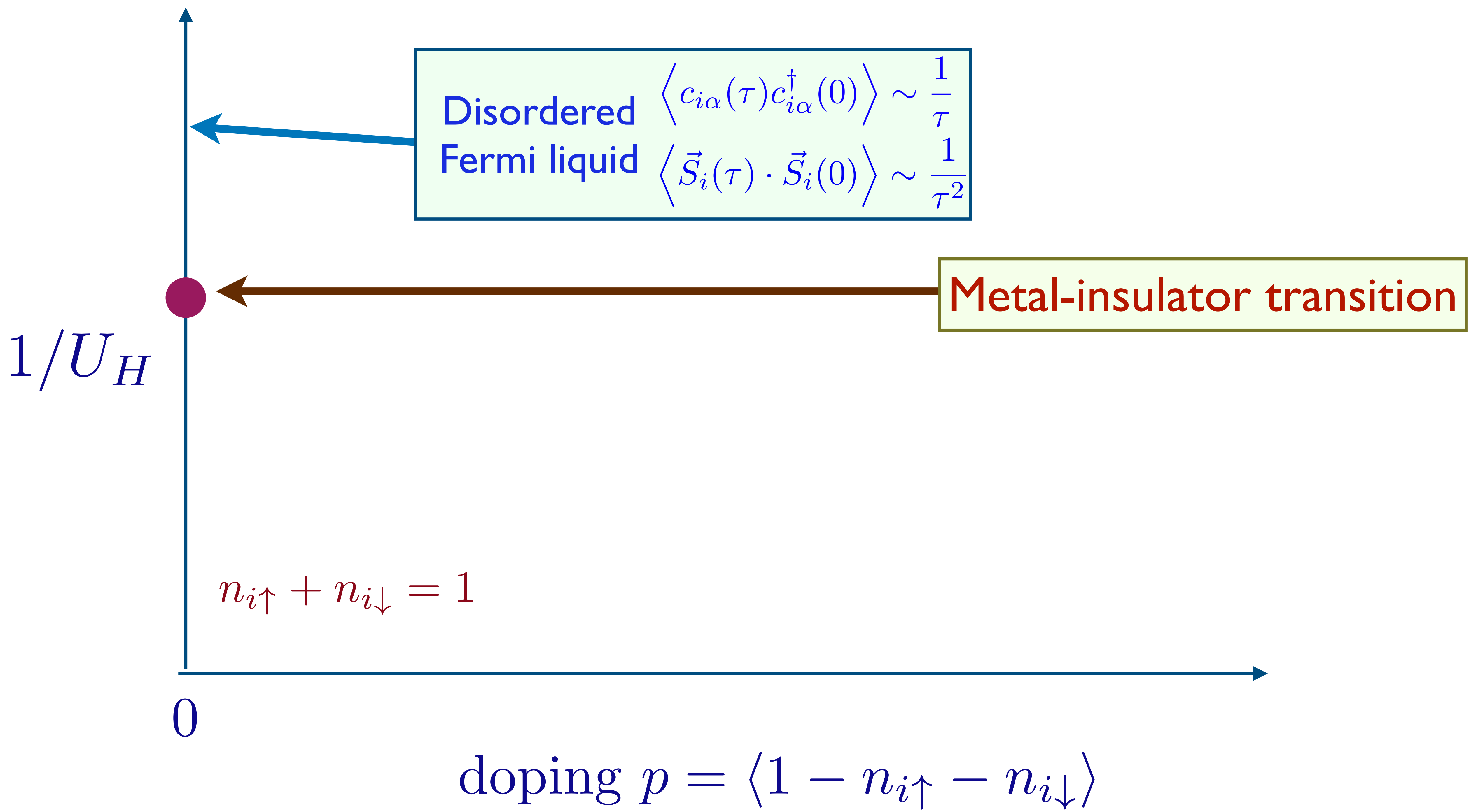

Random t-J-U_H model

$$H = -\frac{1}{\sqrt{N}} \sum_{i,j=1}^{N} t_{ij}\, c_{i\alpha}^{\dagger} c_{j\alpha} + \boxed{\frac{1}{\sqrt{N}} \sum_{i<j=1}^{N} J_{ij}\, \vec{S}_i \cdot \vec{S}_j} + U_H \sum_{i=1}^{N} n_{i\uparrow} n_{i\downarrow}$$

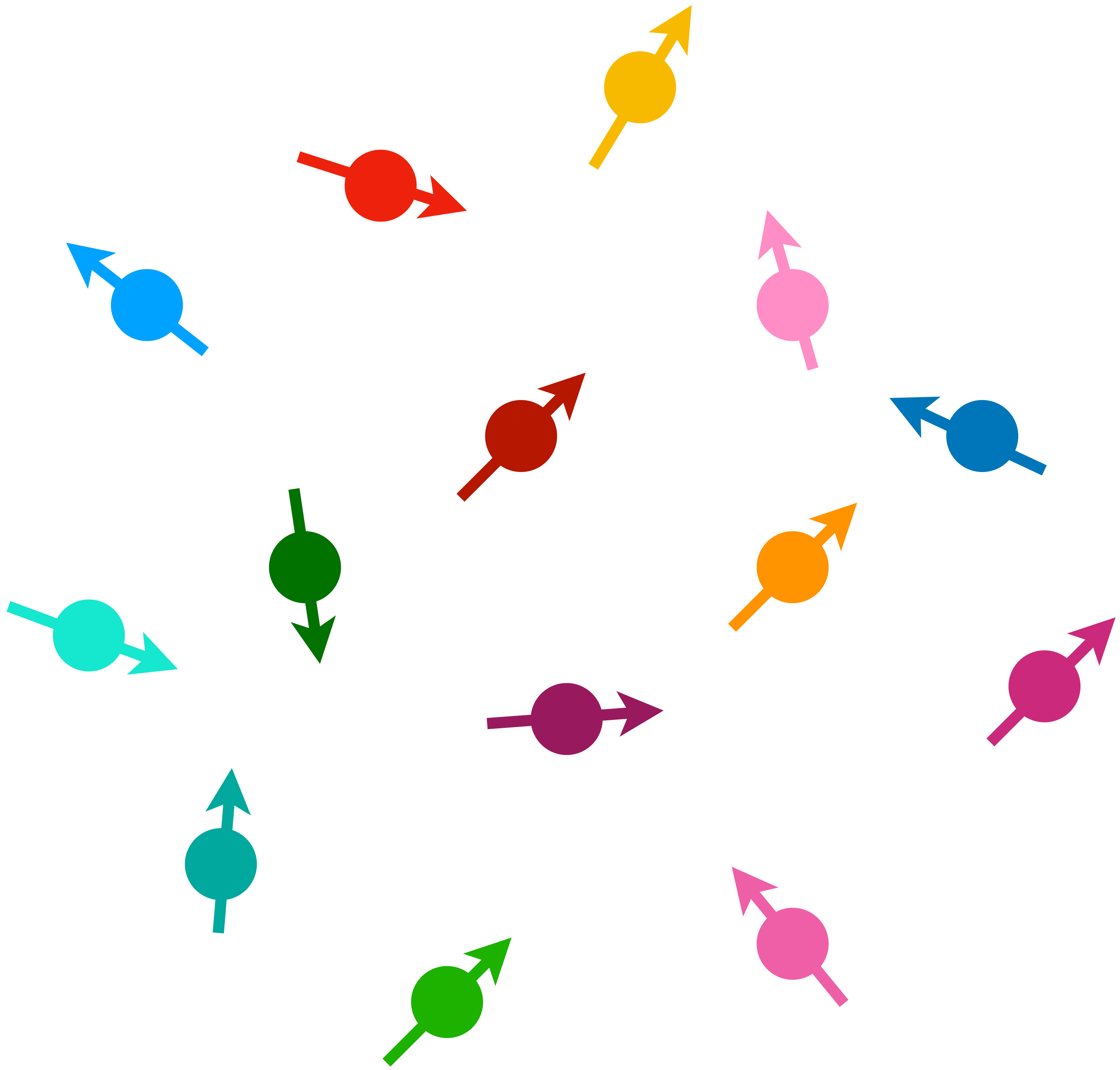

doping $p = \langle 1 - n_{i\uparrow} - n_{i\downarrow} \rangle = 0;\ U_H \to \infty$

Random *t-J-U_H* model

$$H = -\frac{1}{\sqrt{N}} \sum_{i,j=1}^{N} t_{ij}\, c_{i\alpha}^{\dagger} c_{j\alpha} + \frac{1}{\sqrt{N}} \sum_{i<j=1}^{N} J_{ij}\, \vec{S}_i \cdot \vec{S}_j + U_H \sum_{i=1}^{N} n_{i\uparrow} n_{i\downarrow}$$

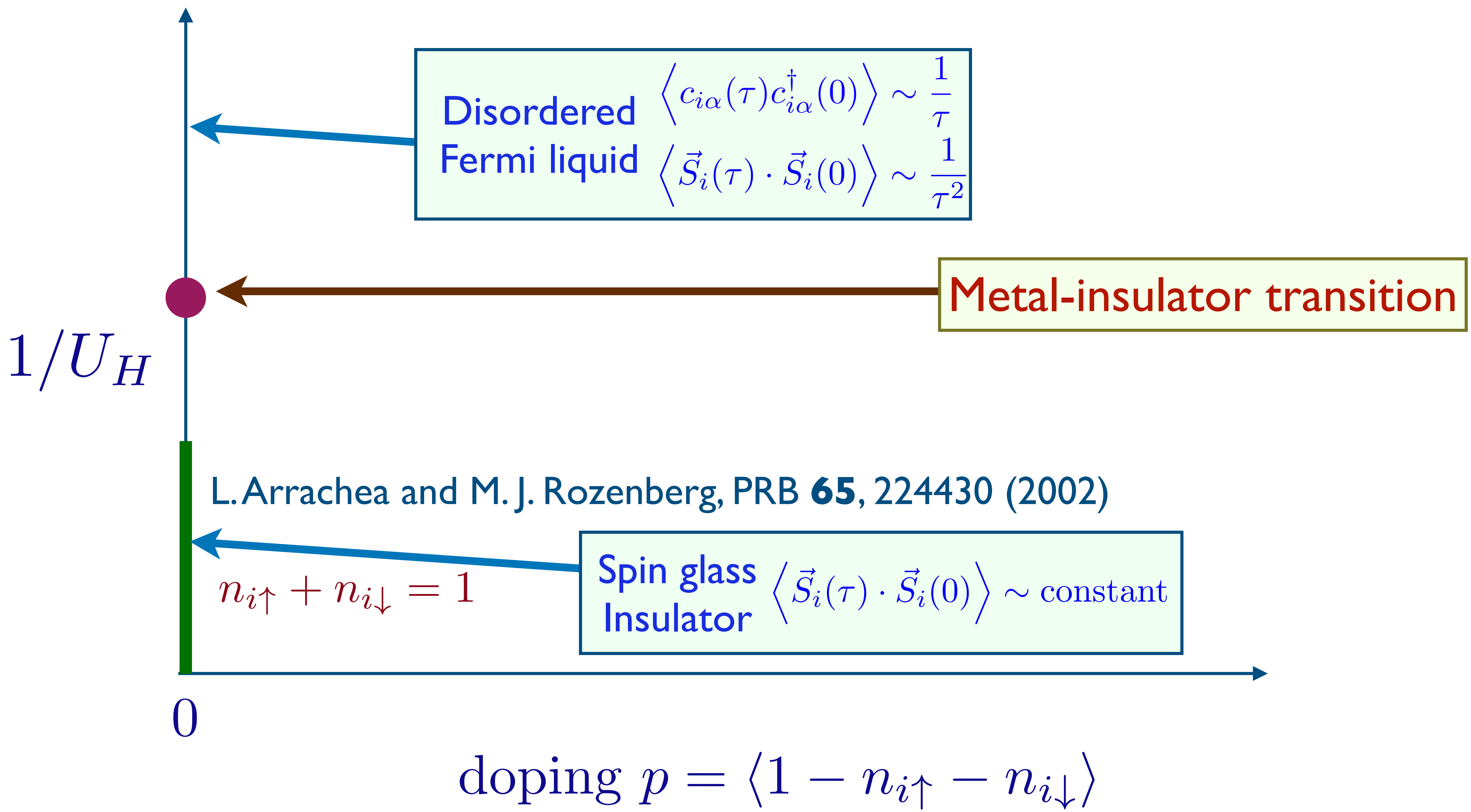

Random t-J-U_H model

$$H = -\frac{1}{\sqrt{N}} \sum_{i,j=1}^{N} t_{ij}\, c_{i\alpha}^{\dagger} c_{j\alpha} + \frac{1}{\sqrt{N}} \sum_{i<j=1}^{N} J_{ij}\, \vec{S}_i \cdot \vec{S}_j + U_H \sum_{i=1}^{N} n_{i\uparrow} n_{i\downarrow}$$

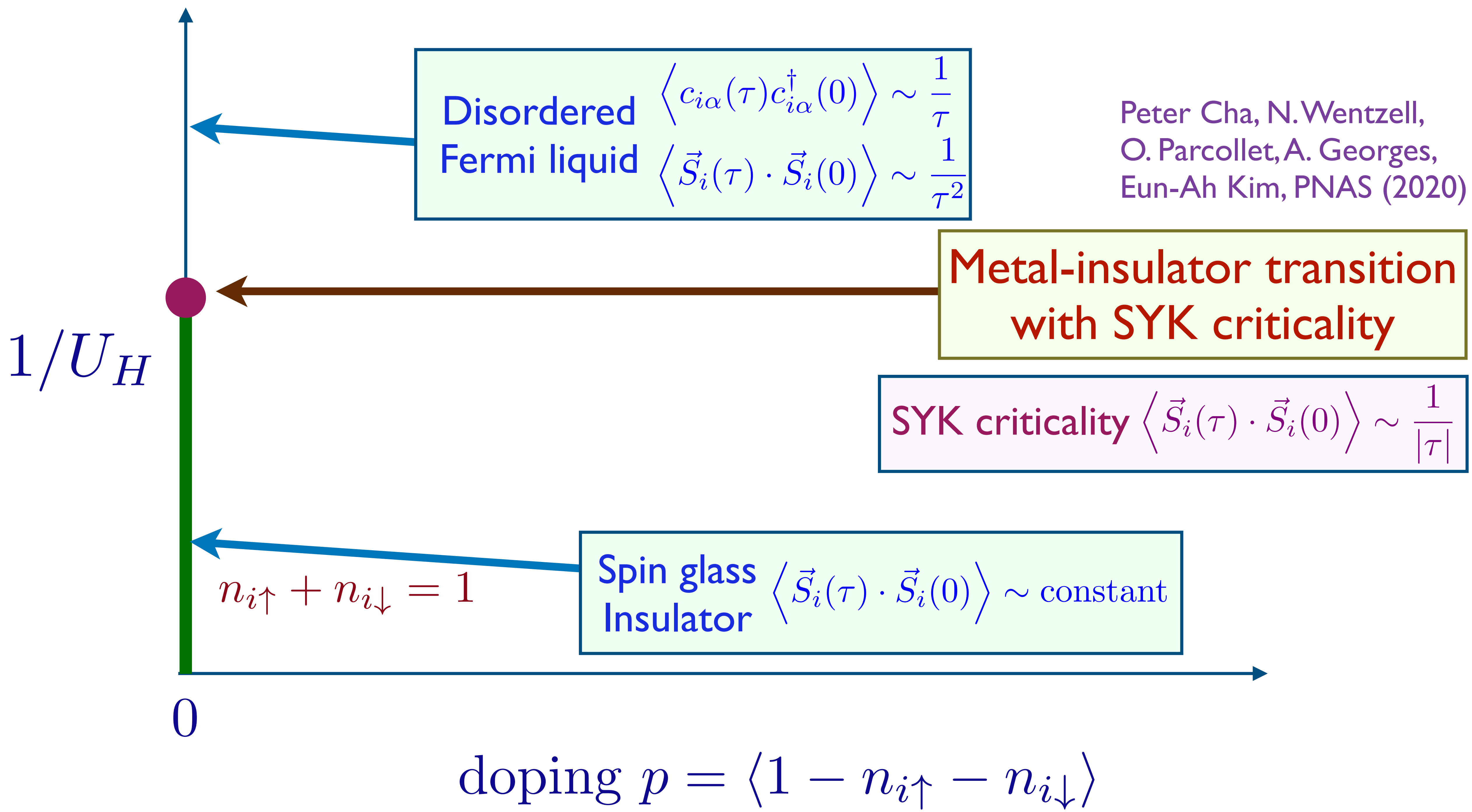

Linear resistivity and Sachdev-Ye-Kitaev (SYK) spin liquid behavior in a quantum critical metal with spin-1/2 fermions

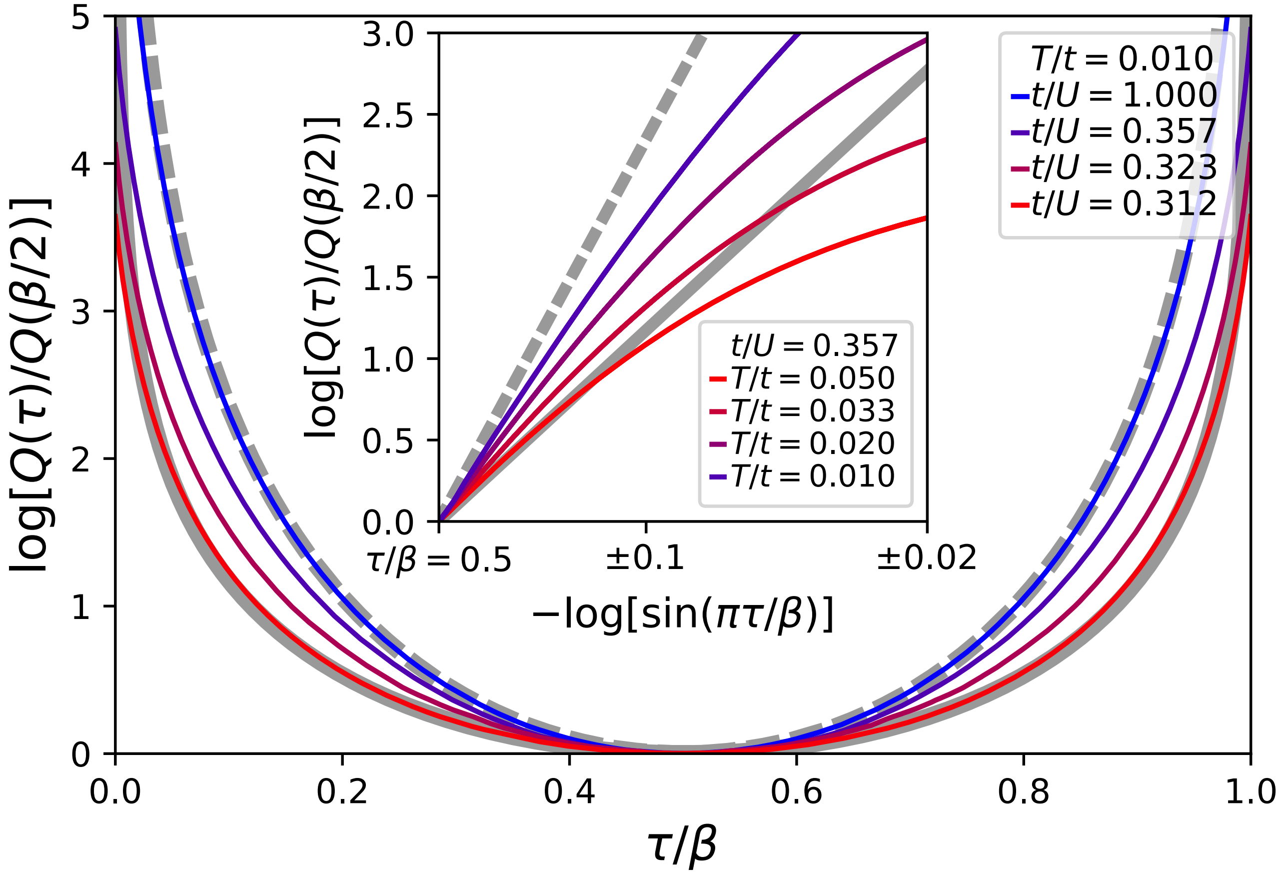

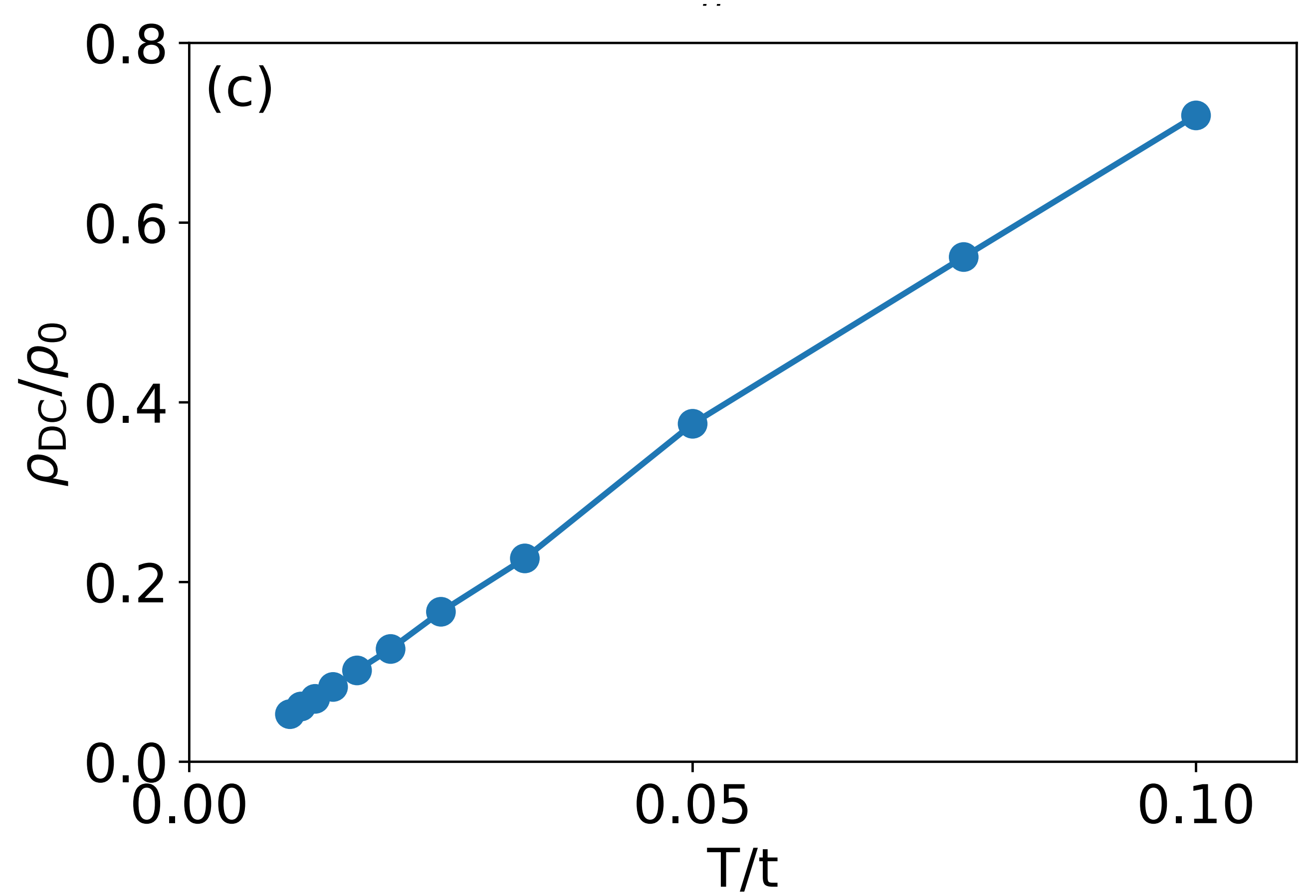

Critical spin correlations:

$$\left\langle \vec{S}(\tau) \cdot \vec{S}(0) \right\rangle \sim \frac{1}{|\tau|}$$

Resisitivity $\rho \sim T$ to the lowest T at the critical point

Onset of insulating gap and spin glass order co-incide.

Peter Cha, N. Wentzell, O. Parcollet, A. Georges, Eun-Ah Kim, PNAS (2020)

Random t-J-U_H model

$$H = -\frac{1}{\sqrt{N}} \sum_{i,j=1}^{N} t_{ij}\, c_{i\alpha}^\dagger c_{j\alpha} + \frac{1}{\sqrt{N}} \sum_{i<j=1}^{N} J_{ij}\, \vec{S}_i \cdot \vec{S}_j + U_H \sum_{i=1}^{N} n_{i\uparrow} n_{i\downarrow}$$

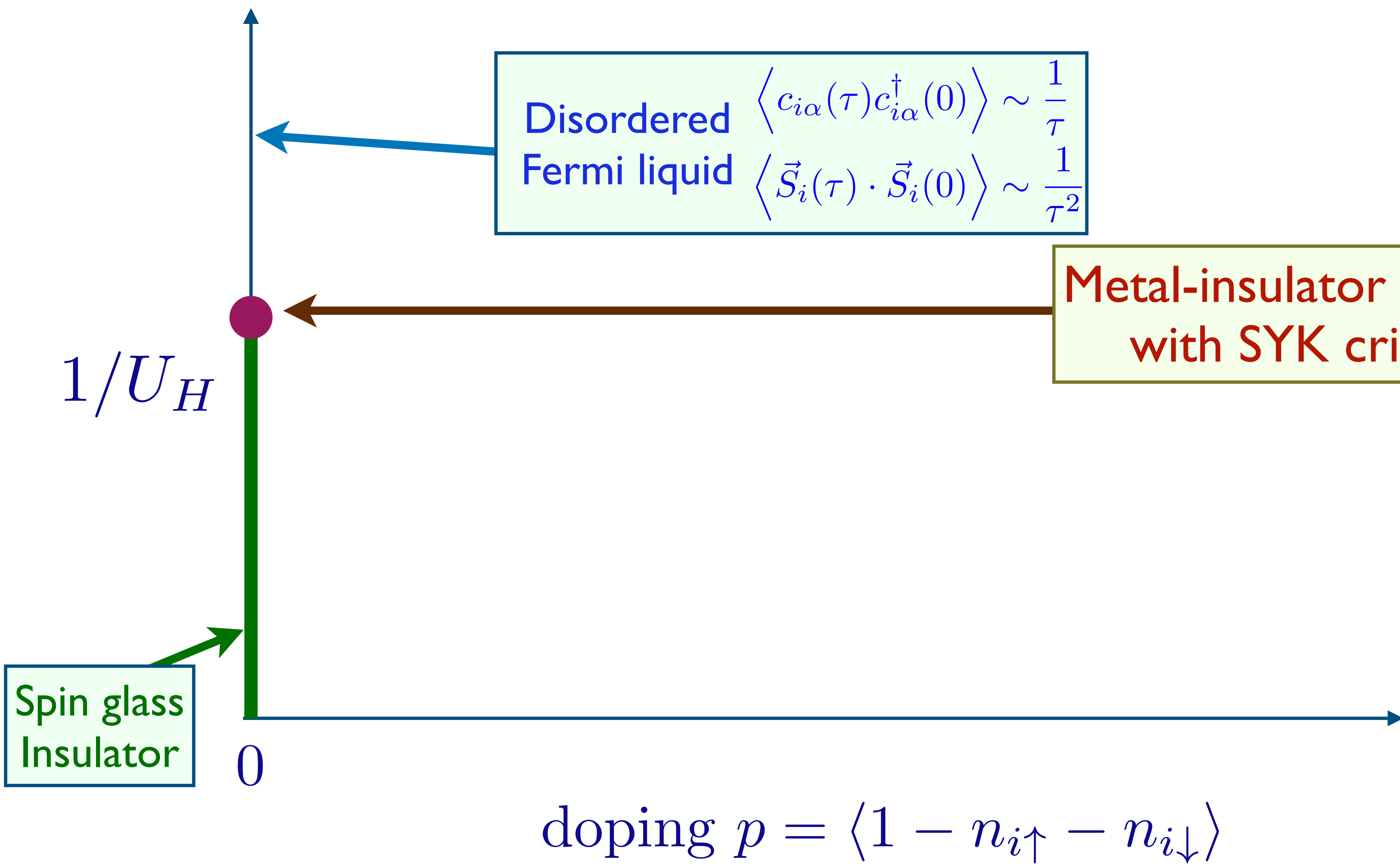

Random t-J-U_H model

$$H = -\frac{1}{\sqrt{N}} \sum_{i,j=1}^{N} t_{ij}\, c_{i\alpha}^{\dagger} c_{j\alpha} + \frac{1}{\sqrt{N}} \sum_{i<j=1}^{N} J_{ij}\, \vec{S}_i \cdot \vec{S}_j + U_H \sum_{i=1}^{N} n_{i\uparrow} n_{i\downarrow}$$

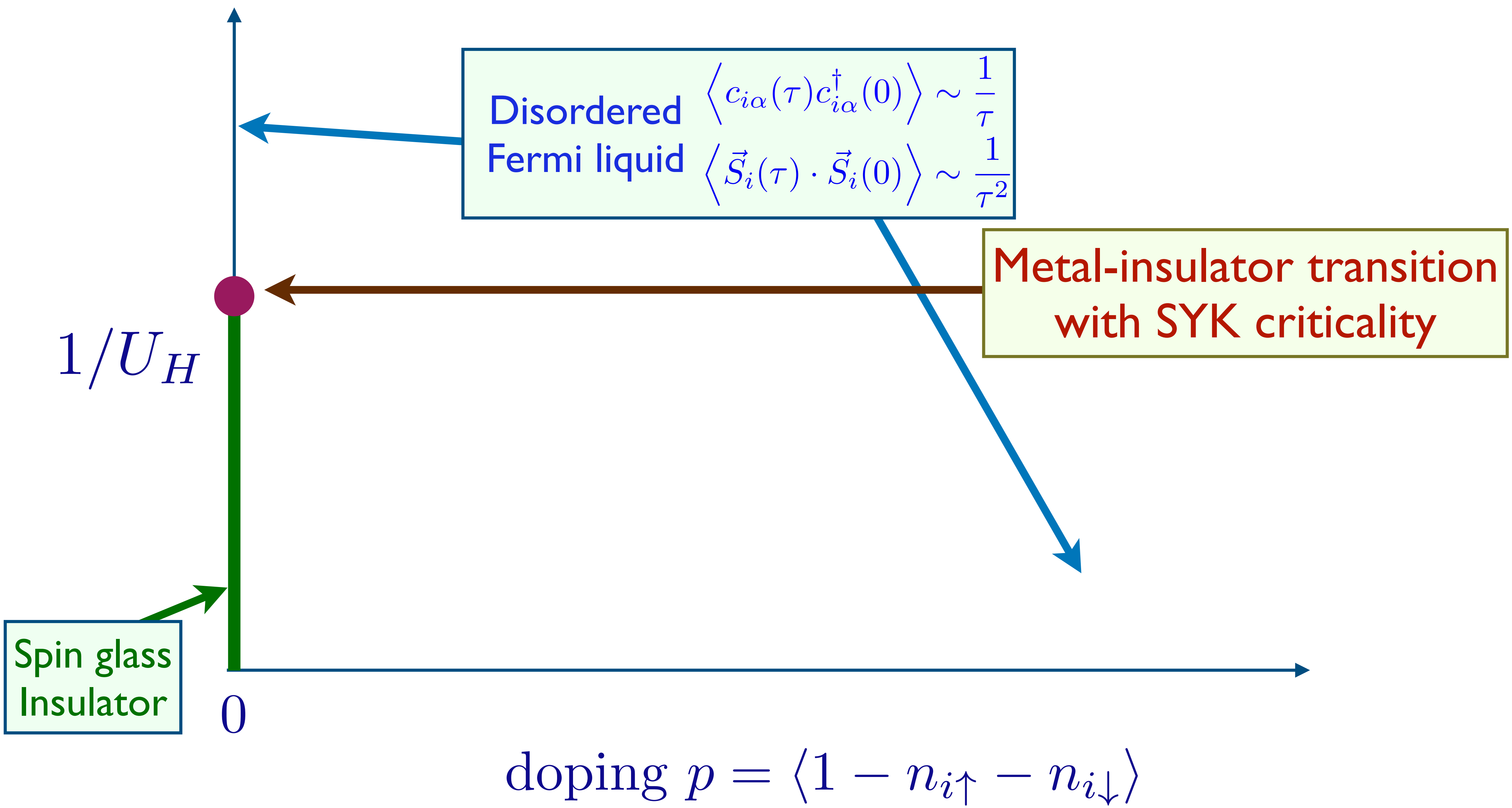

Random t-J-U_H model

$$H = -\frac{1}{\sqrt{N}} \sum_{i,j=1}^{N} t_{ij}\, c_{i\alpha}^{\dagger} c_{j\alpha} + \frac{1}{\sqrt{N}} \sum_{i<j=1}^{N} J_{ij}\, \vec{S}_i \cdot \vec{S}_j + U_H \sum_{i=1}^{N} n_{i\uparrow} n_{i\downarrow}$$

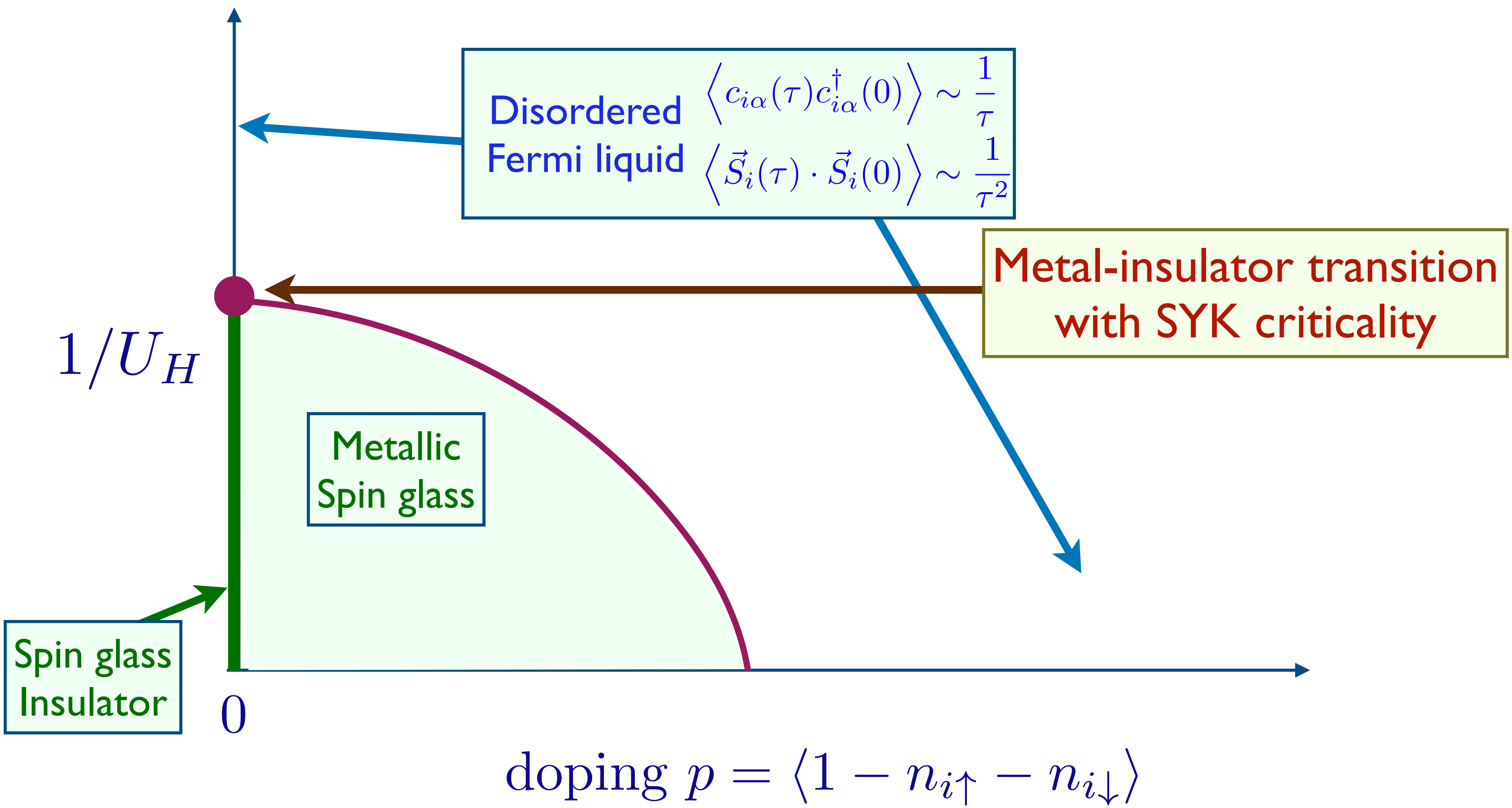

Random t-J-U_H model

$$H = -\frac{1}{\sqrt{N}} \sum_{i,j=1}^{N} t_{ij}\, c_{i\alpha}^{\dagger} c_{j\alpha} + \frac{1}{\sqrt{N}} \sum_{i<j=1}^{N} J_{ij}\, \vec{S}_i \cdot \vec{S}_j + U_H \sum_{i=1}^{N} n_{i\uparrow} n_{i\downarrow}$$

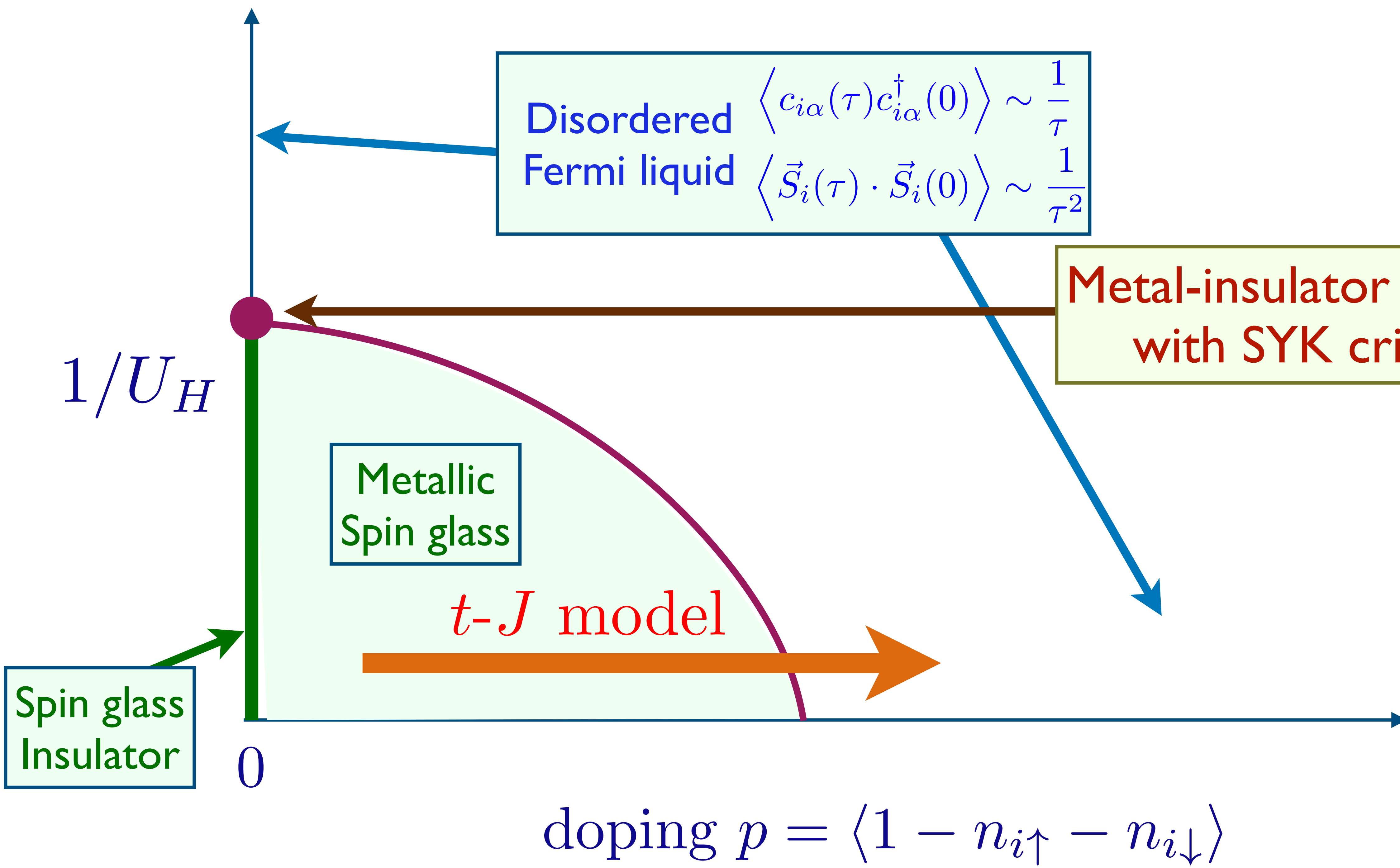

Random *t-J* model $(U_H \to \infty)$

$$H = -\frac{1}{\sqrt{N}} \sum_{i,j=1}^{N} t_{ij}\, c_{i\alpha}^\dagger c_{j\alpha} + \frac{1}{\sqrt{N}} \sum_{i<j=1}^{N} J_{ij}\, \vec{S}_i \cdot \vec{S}_j$$

We consider the hole-doped case, with no double occupancy.

$$\alpha = \uparrow, \downarrow, \quad \{c_{i\alpha}, c_{j\beta}^\dagger\} = \delta_{ij}\delta_{\alpha\beta}, \quad \{c_{i\alpha}, c_{j\beta}\} = 0$$

$$\vec{S}_i = \frac{1}{2} c_{i\alpha}^\dagger \vec{\sigma}_{\alpha\beta} c_{i\beta}, \quad \sum_{\alpha} c_{i\alpha}^\dagger c_{i\alpha} \leq 1, \quad \frac{1}{N}\sum_{i\alpha} c_{i\alpha}^\dagger c_{i\alpha} = 1 - p$$

$$J_{ij} \text{ random}, \ \overline{J_{ij}} = 0, \ \overline{J_{ij}^2} = J^2$$
$$t_{ij} \text{ random}, \ \overline{t_{ij}} = 0, \ \overline{t_{ij}^2} = t^2$$

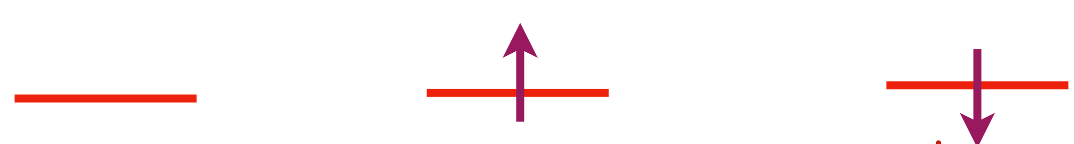

$|0\rangle$ $\quad c_\uparrow^\dagger |0\rangle$ $\quad c_\downarrow^\dagger |0\rangle$

Random *t-J* model $(U_H \to \infty)$

$$H = -\frac{1}{\sqrt{N}} \sum_{i,j=1}^{N} t_{ij}\, c^\dagger_{i\alpha} c_{j\alpha} + \frac{1}{\sqrt{N}} \sum_{i<j=1}^{N} J_{ij}\, \vec{S}_i \cdot \vec{S}_j$$

We consider the hole-doped case, with no double occupancy.

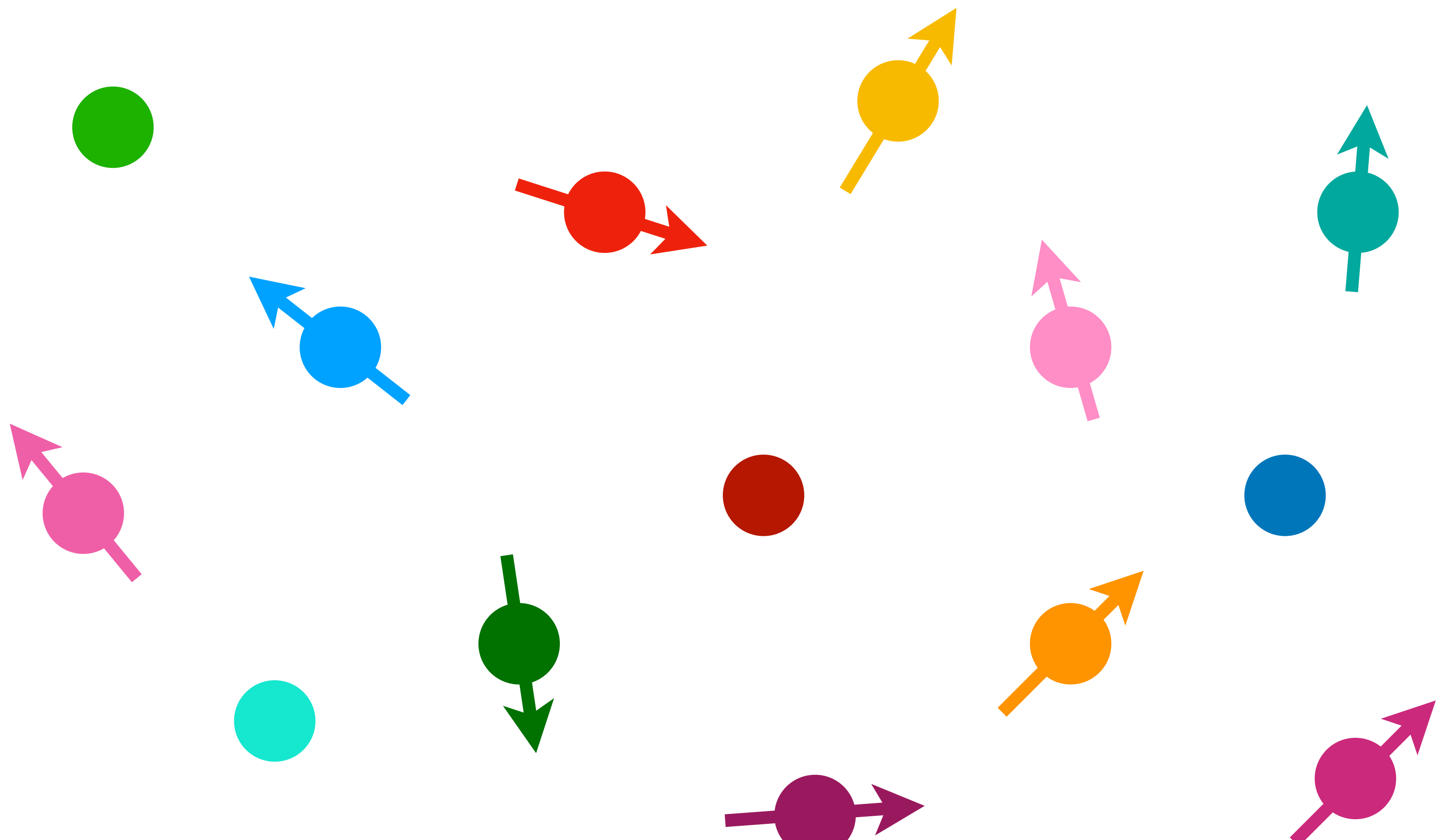

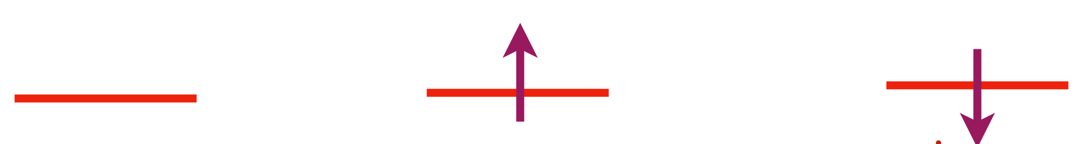

$|0\rangle$ $\quad c^\dagger_\uparrow |0\rangle$ $\quad c^\dagger_\downarrow |0\rangle$

Random *t-J* model

Local dynamic spin susceptibility $\chi''(\omega)$

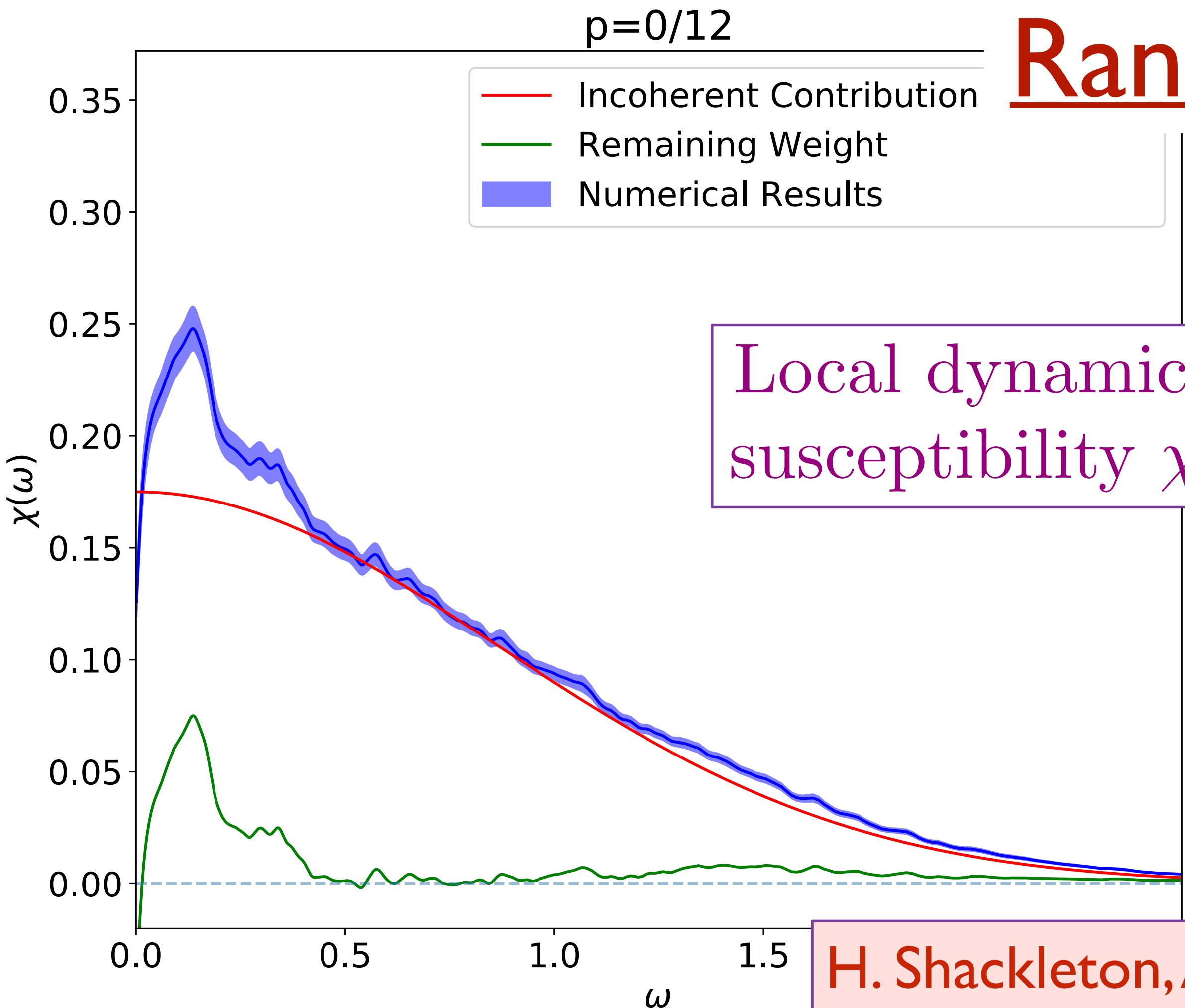

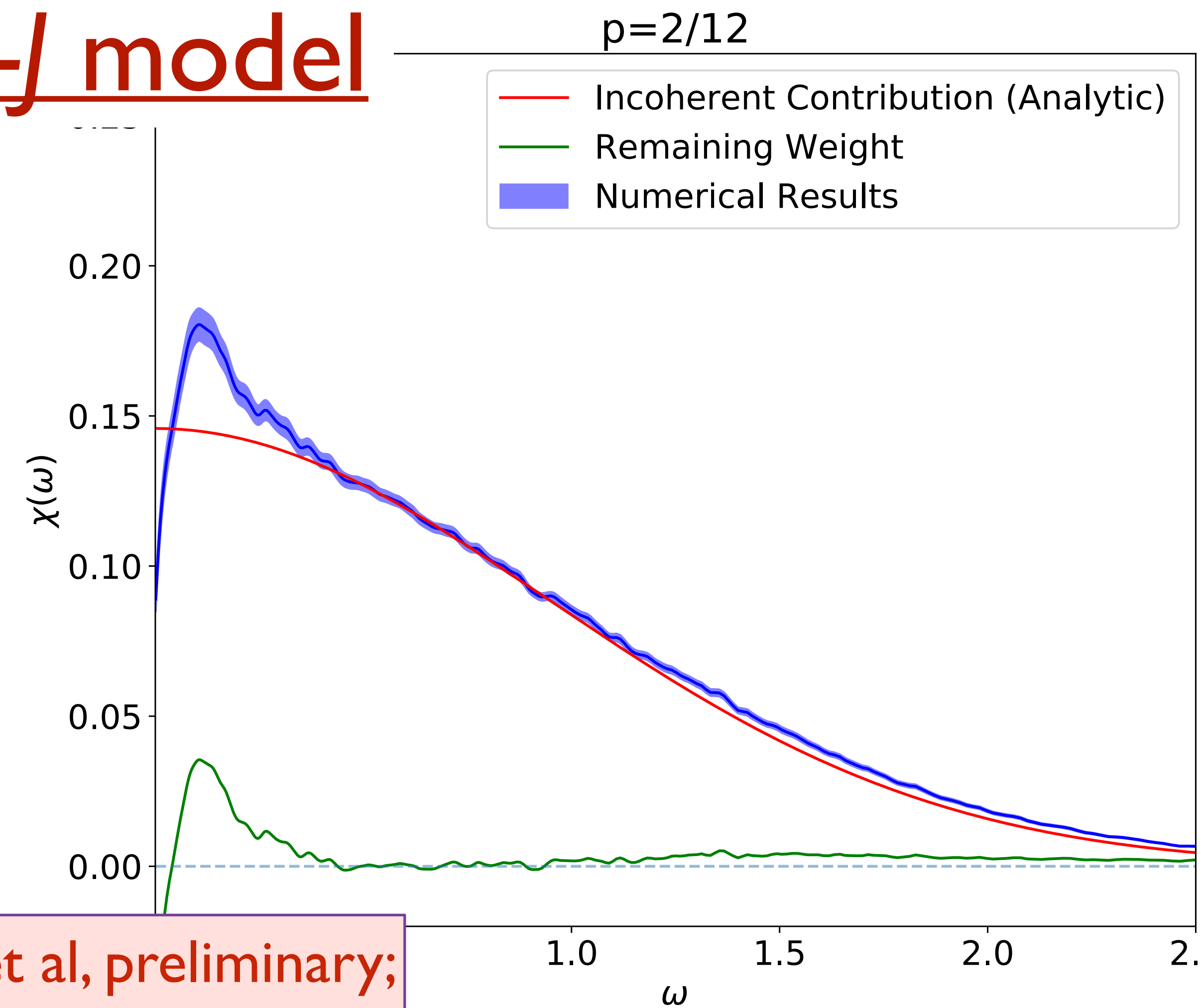

H. Shackleton, A. Wietek et al, preliminary;
Exact diagonalization of clusters

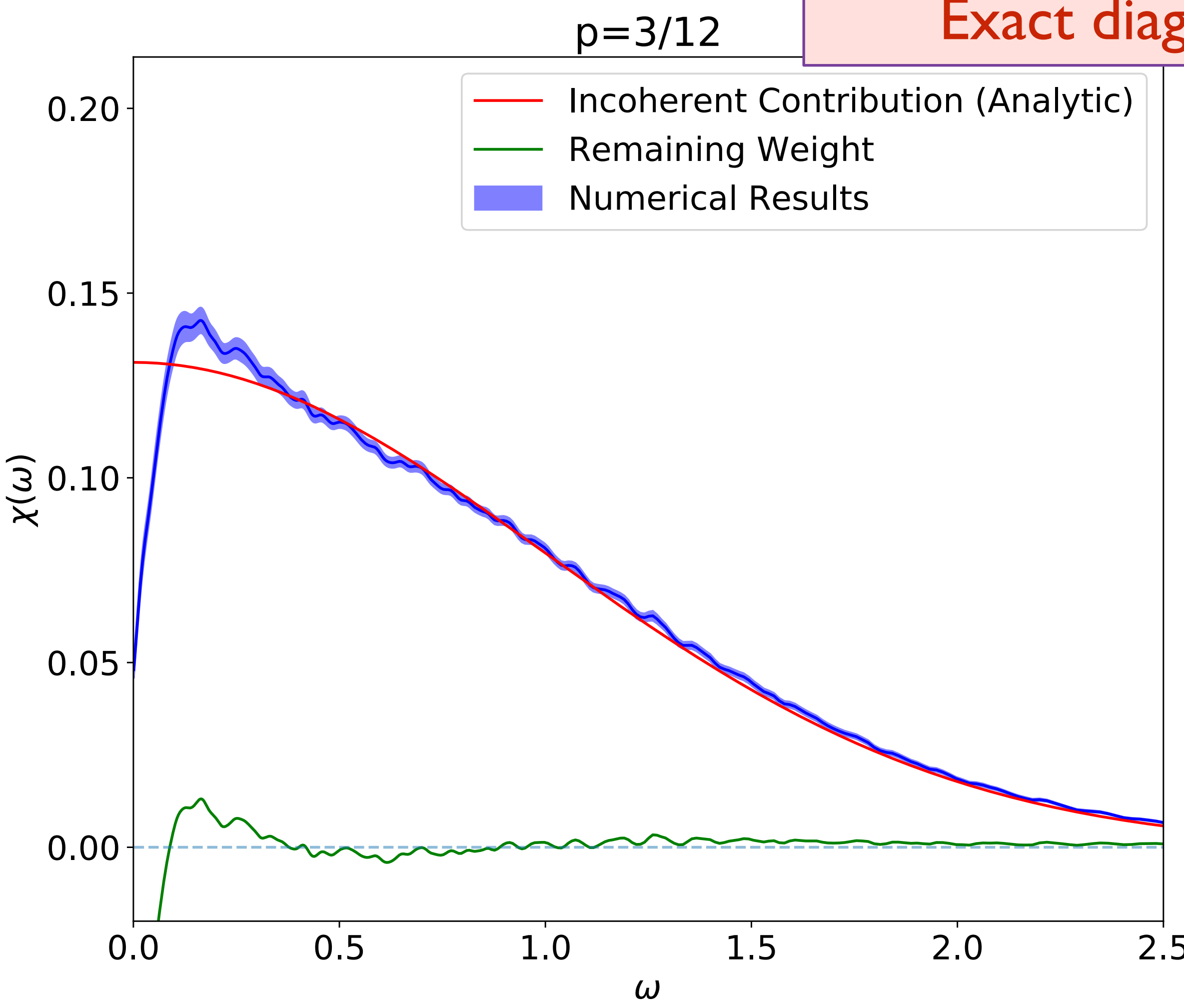

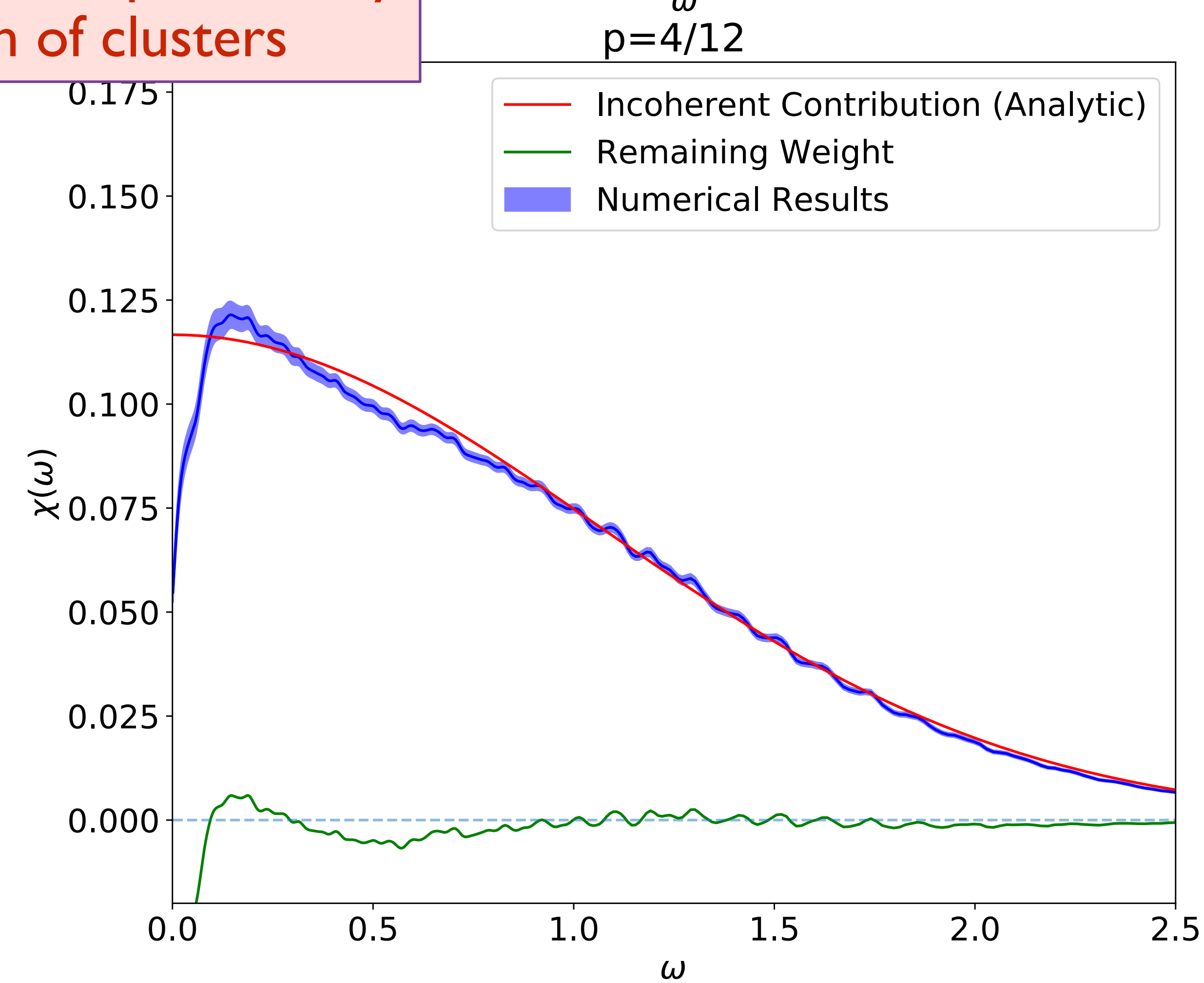

Random *t-J* model

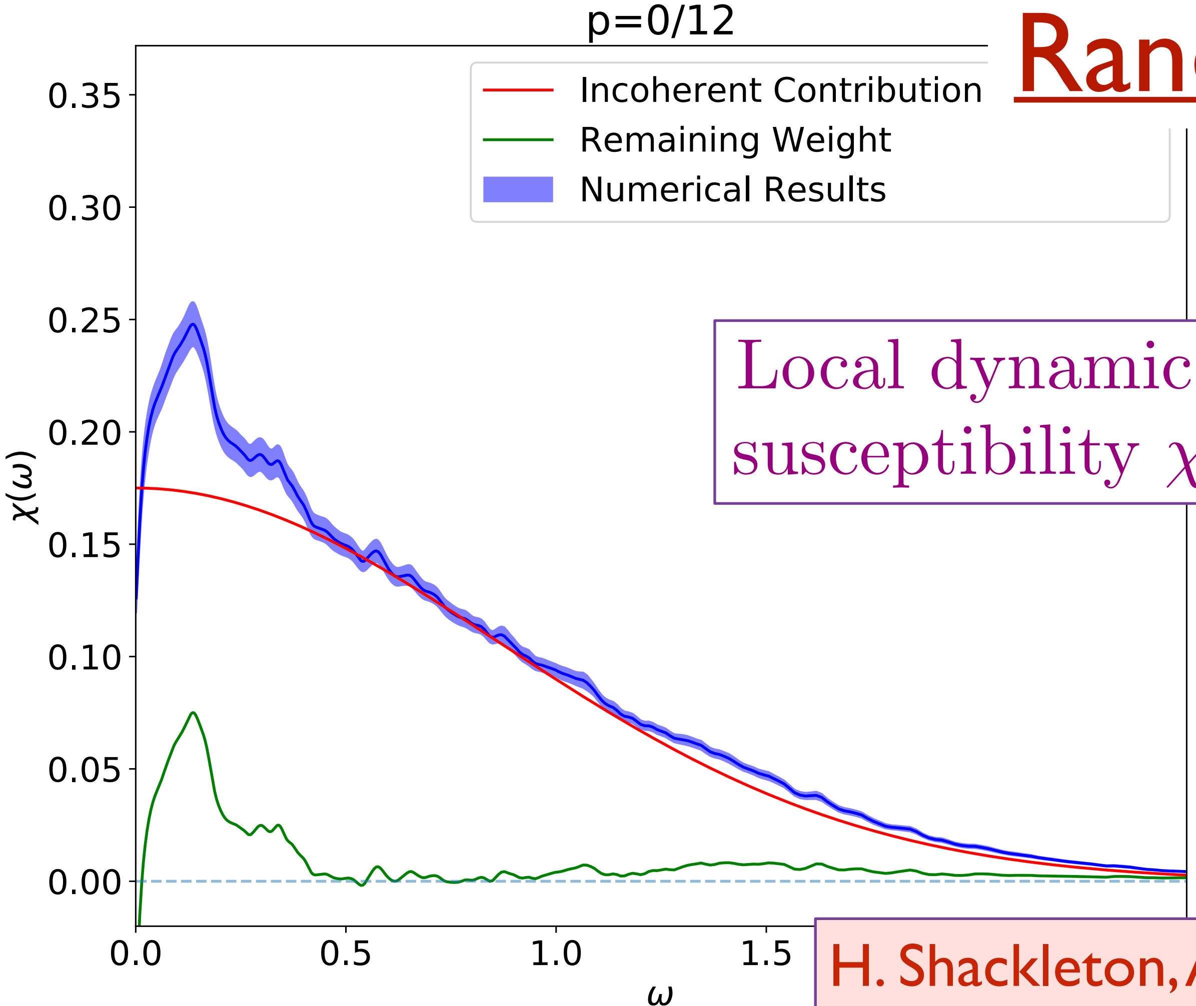

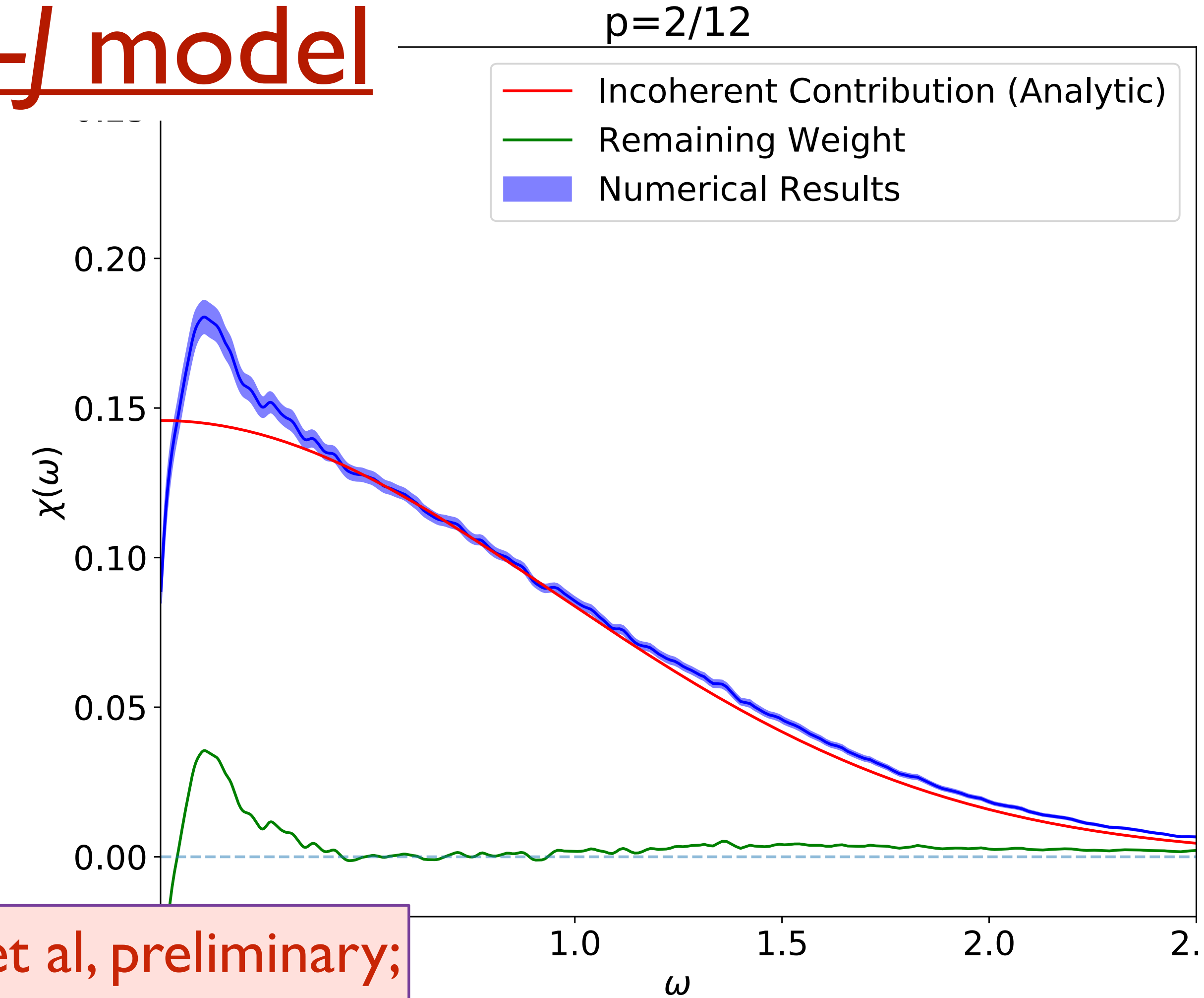

Local dynamic spin susceptibility $\chi''(\omega)$

H. Shackleton, A. Wietek et al, preliminary;
Exact diagonalization of clusters

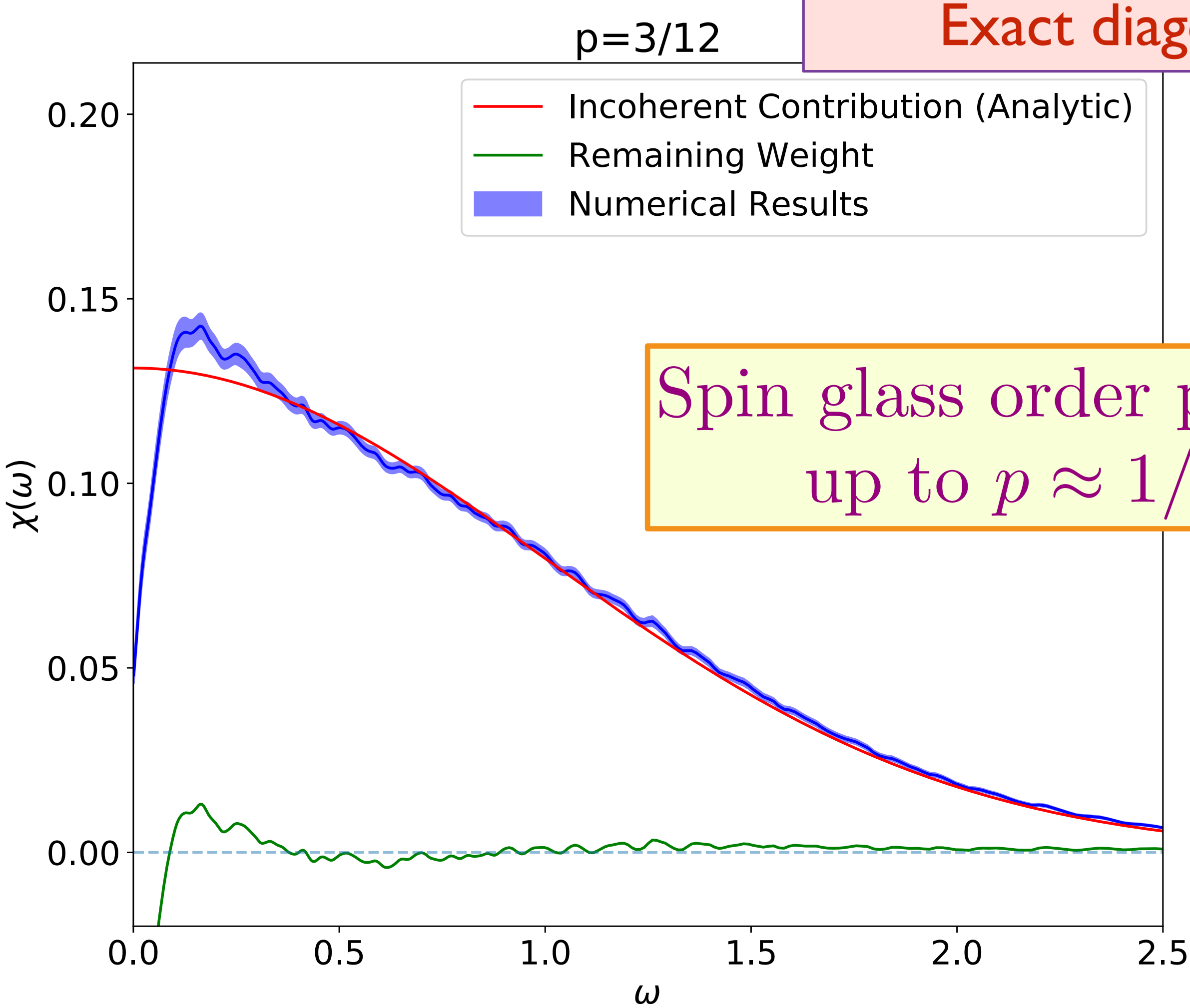

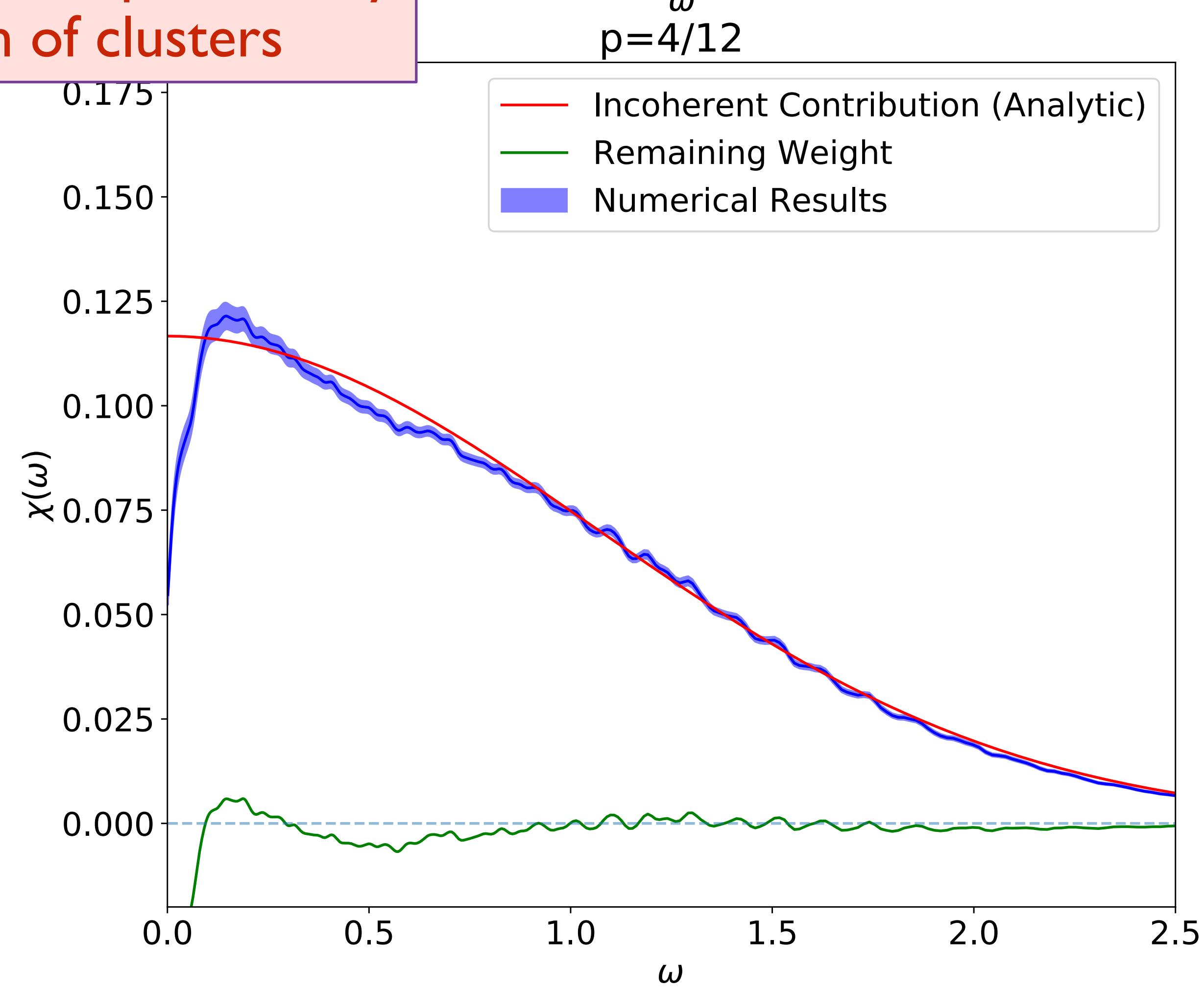

Spin glass order present up to $p \approx 1/3$.

Random t-J-U_H model

$$H = -\frac{1}{\sqrt{N}} \sum_{i,j=1}^{N} t_{ij}\, c_{i\alpha}^\dagger c_{j\alpha} + \frac{1}{\sqrt{N}} \sum_{i<j=1}^{N} J_{ij}\, \vec{S}_i \cdot \vec{S}_j + U_H \sum_{i=1}^{N} n_{i\uparrow} n_{i\downarrow}$$

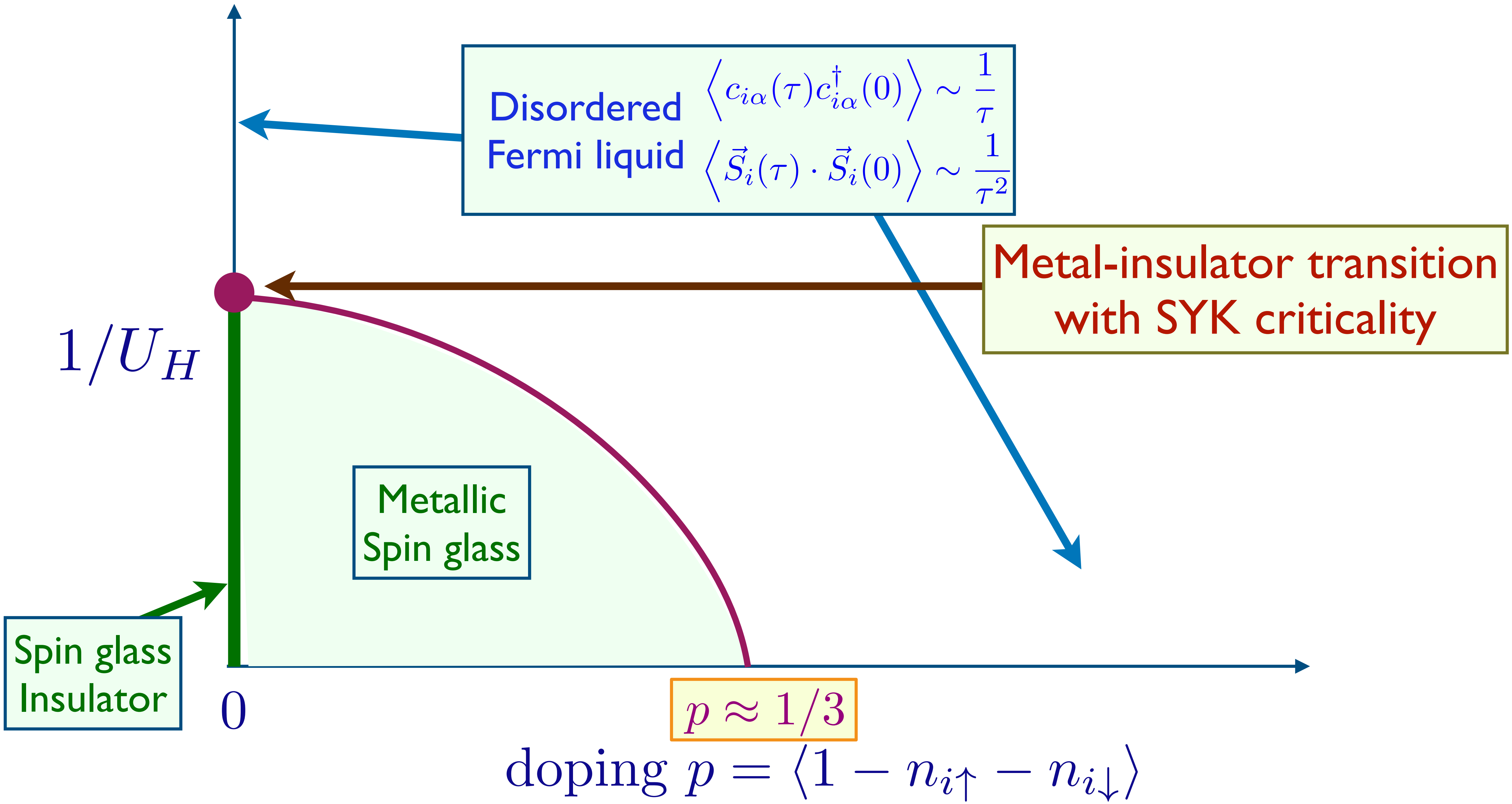

1. Non-random t-*J* model (metals)

   Ancilla qubits and ghost Fermi surfaces

2. All-to-all random Hubbard and *t-J* models

   Numerical results

3. Random *J* model (insulator)

   RG analysis and exact exponent

4. Random t-*J* model (metals)

   RG analysis and exact exponents

Random J model (insulator)

$$H = \frac{1}{\sqrt{N}} \sum_{i<j=1}^{N} J_{ij}\, \vec{S}_i \cdot \vec{S}_j$$

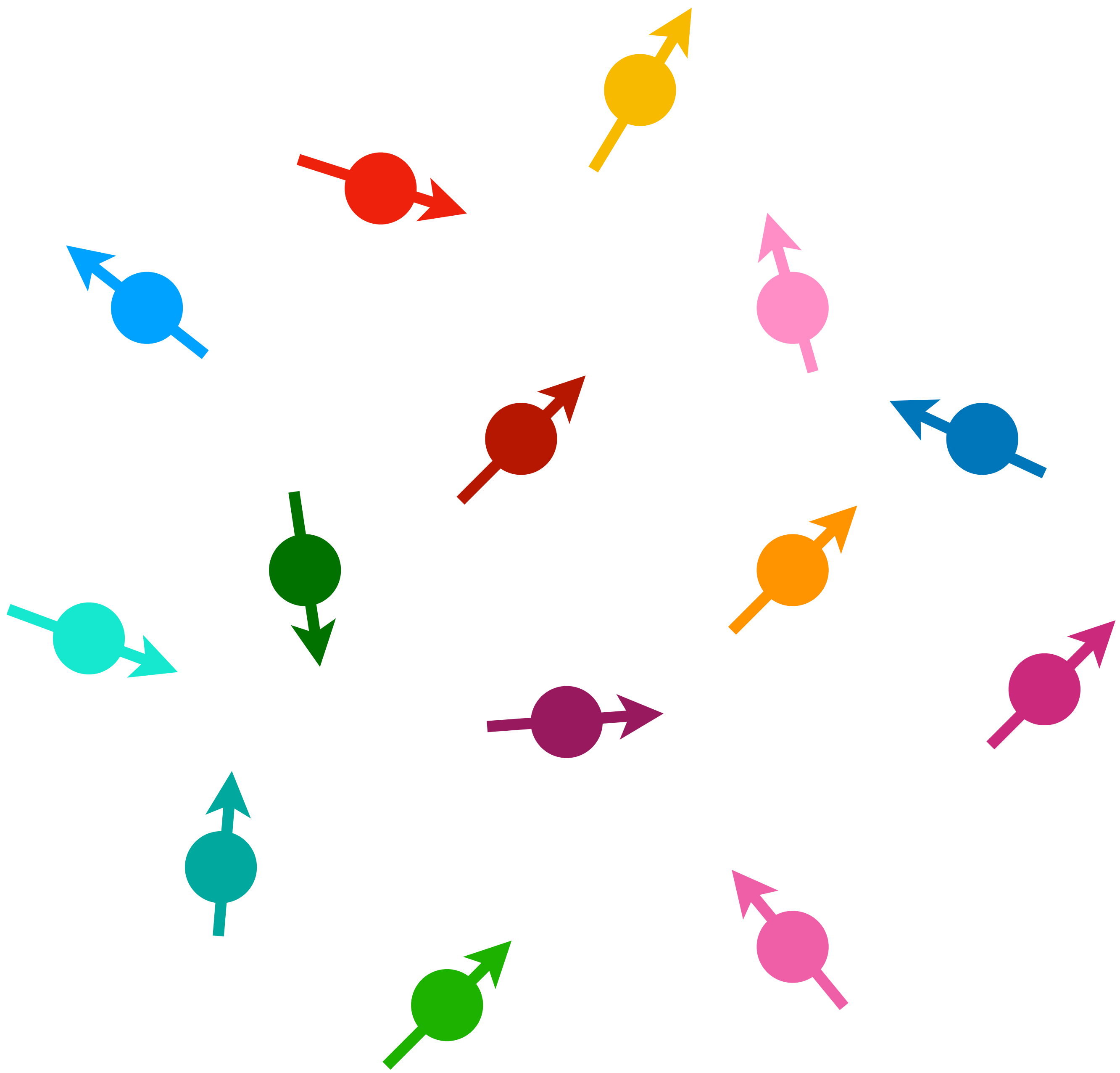

Random J model (insulator)

$$H = \frac{1}{\sqrt{N}} \sum_{i<j=1}^{N} J_{ij} \vec{S}_i \cdot \vec{S}_j$$

$$\alpha = \uparrow, \downarrow, \quad \vec{S}_i = \frac{1}{2} f_{i\alpha}^{\dagger} \vec{\sigma}_{\alpha\beta} f_{i\beta}, \quad \sum_{\alpha} f_{i\alpha}^{\dagger} f_{i\alpha} = 1$$

$$J_{ij} \text{ random}, \overline{J_{ij}} = 0, \overline{J_{ij}^2} = J^2$$

Random J model (insulator)

$$H = \frac{1}{\sqrt{N}} \sum_{i<j=1}^{N} J_{ij}\, \vec{S}_i \cdot \vec{S}_j$$

$$\alpha = \uparrow, \downarrow, \quad \vec{S}_i = \frac{1}{2} \mathfrak{b}^{\dagger}_{i\alpha} \vec{\sigma}_{\alpha\beta} \mathfrak{b}_{i\beta}, \quad \sum_{\alpha} \mathfrak{b}^{\dagger}_{i\alpha} \mathfrak{b}_{i\alpha} = 1$$

$$J_{ij} \text{ random}, \ \overline{J_{ij}} = 0, \ \overline{J^2_{ij}} = J^2$$

Random J model (insulator)

$$\mathcal{Z} = \int \mathcal{D}\vec{S}(\tau)\delta(\vec{S}^2 - 1)e^{-\mathcal{S}_B - \mathcal{S}_J}$$

$$\mathcal{S}_B = \frac{i}{2}\int_0^1 du \int d\tau \vec{S} \cdot \left(\frac{\partial \vec{S}}{\partial \tau} \times \frac{\partial \vec{S}}{\partial u} \right)$$

$$\mathcal{S}_J = -\frac{J^2}{2} \int d\tau d\tau' Q(\tau - \tau')\vec{S}(\tau) \cdot \vec{S}(\tau') \,.$$

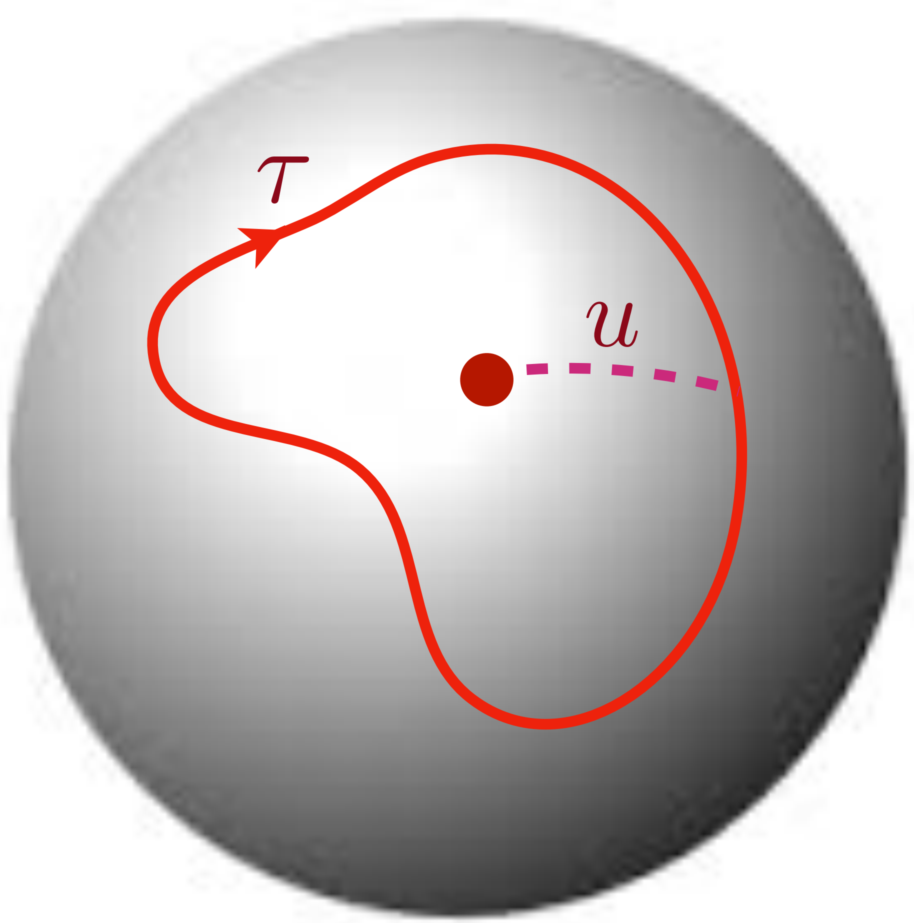

S. Sachdev and J. Ye, PRL **70**, 3339 (1993)

Random J model (insulator)

$$\mathcal{Z} = \int \mathcal{D}\vec{S}(\tau)\delta(\vec{S}^2 - 1)e^{-\mathcal{S}_B - \mathcal{S}_J}$$

$$\mathcal{S}_B = \frac{i}{2}\int_0^1 du \int d\tau \vec{S} \cdot \left(\frac{\partial \vec{S}}{\partial \tau} \times \frac{\partial \vec{S}}{\partial u} \right)$$

$$\mathcal{S}_J = -\frac{J^2}{2}\int d\tau d\tau' Q(\tau - \tau')\vec{S}(\tau) \cdot \vec{S}(\tau') \,.$$

From this action we compute

$$\overline{Q}(\tau - \tau') = \frac{1}{3}\left\langle \vec{S}(\tau) \cdot \vec{S}(\tau') \right\rangle_{\mathcal{Z}}$$

and then impose the self-consistency condition

$$\boxed{Q(\tau) = \overline{Q}(\tau).}$$

S. Sachdev and J. Ye, PRL **70**, 3339 (1993)

Random J model (insulator):RG

We assume a power-law decay

$$Q(\tau) \sim \frac{\gamma^2}{|\tau|^\alpha}\,.$$

Ignore the self-consistency condition for now. We decouple the $\vec{S}(\tau)\cdot\vec{S}(0)$ interaction by introducing a bosonic (ϕ_a, $a = 1\ldots3$) bath. Then the problem reduces to the Hamiltonian

$$H_{\rm imp} \;=\; \gamma S_a\,\phi_a(0) + \frac{1}{2}\int d^d x\left[\pi_a^2 + (\partial_x \phi_a)^2\right]$$

where π_a is canonically conjugate to the field ϕ_a, and $\phi_a(0) \equiv \phi_a(x=0)$. We identify $Q(\tau)$ with temporal correlator of $\phi_a(0)$, and then we need $\alpha = d-1$.

M. Vojta, C. Buragohain, and S. Sachdev, PRB **61**, 15152 (2000)
S. Sachdev, Physica C **357**, 78 (2001)

Random J model (insulator):RG

- The β-function of γ can by computed order-by-order in $\epsilon = 2 - \alpha$

$$\frac{d\gamma}{d\ell} = \epsilon\frac{\gamma}{2} - \gamma^3 .$$

- There is an attractive fixed point at $\gamma = \gamma^* = \mathcal{O}(\sqrt{\epsilon})$.

- Because of the quantized Berry phase (Wess-Zumino-Witten) term, the renormalization of the coupling γ is given only by the wavefunction renormalization. We can then prove that at this fixed point $\overline{Q}(\tau) \sim 1/|\tau|^{2-\alpha}$ to all orders in ϵ.

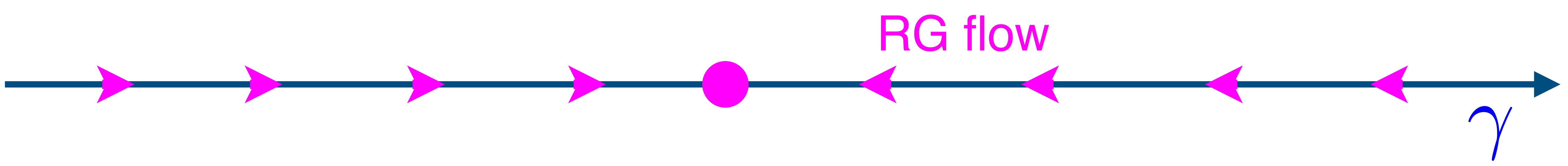

M. Vojta, C. Buragohain, and S. Sachdev, PRB **61**, 15152 (2000)
S. Sachdev, Physica C **357**, 78 (2001)

Random J model (insulator):RG

- The β-function of γ can by computed order-by-order in $\epsilon = 2 - \alpha$

$$\frac{d\gamma}{d\ell} = \epsilon \frac{\gamma}{2} - \gamma^3 \,.$$

- There is an attractive fixed point at $\gamma = \gamma^* = \mathcal{O}(\sqrt{\epsilon})$.

- Because of the quantized Berry phase (Wess-Zumino-Witten) term, the renormalization of the coupling γ is given only by the wavefunction renormalization. We can then prove that at this fixed point $\overline{Q}(\tau) \sim 1/|\tau|^{2-\alpha}$ to all orders in ϵ.

- The self-consistency condition therefore yields

$$\boxed{\left\langle \vec{S}(\tau) \cdot \vec{S}(0) \right\rangle \sim \frac{1}{|\tau|} \,.}$$

to all orders in ϵ.

M. Vojta, C. Buragohain, and S. Sachdev, PRB **61**, 15152 (2000)
S. Sachdev, Physica C **357**, 78 (2001)

1. Non-random t-*J* model (metals)

Ancilla qubits and ghost Fermi surfaces

2. All-to-all random Hubbard and *t-J* models

Numerical results

3. Random *J* model (insulator)

RG analysis and exact exponent

4. Random t-*J* model (metals)

RG analysis and exact exponents

Random *t-J* model $(U_H \to \infty)$

$$H = -\frac{1}{\sqrt{N}} \sum_{i,j=1}^{N} t_{ij}\, c_{i\alpha}^{\dagger} c_{j\alpha} + \frac{1}{\sqrt{N}} \sum_{i<j=1}^{N} J_{ij}\, \vec{S}_i \cdot \vec{S}_j$$

We consider the hole-doped case, with no double occupancy.

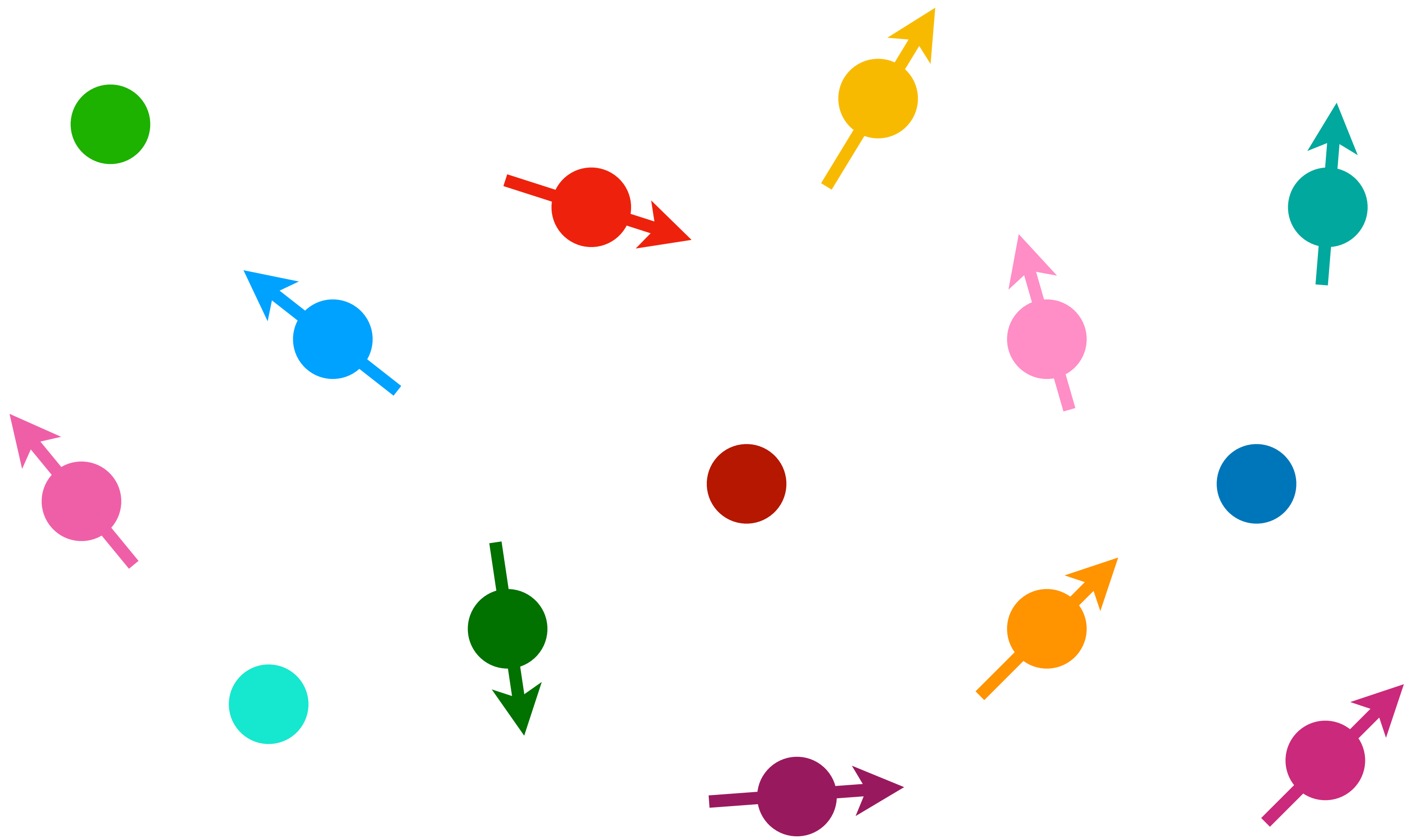

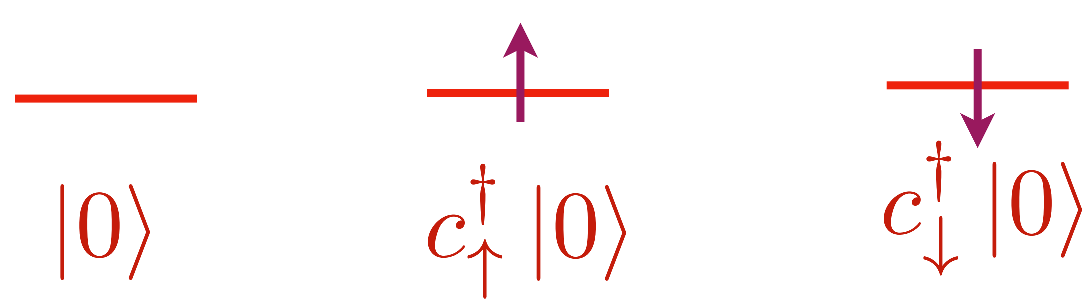

Random t-J model (metal)

$$H = -\frac{1}{\sqrt{N}} \sum_{i,j=1}^{N} t_{ij}\, c_{i\alpha}^{\dagger} c_{j\alpha} + \frac{1}{\sqrt{N}} \sum_{i<j=1}^{N} J_{ij}\, \vec{S}_i \cdot \vec{S}_j$$

Each site has 3 states which we map to the '*superspin*' space of a boson b (the holon) and a fermion f_α (the spinon):

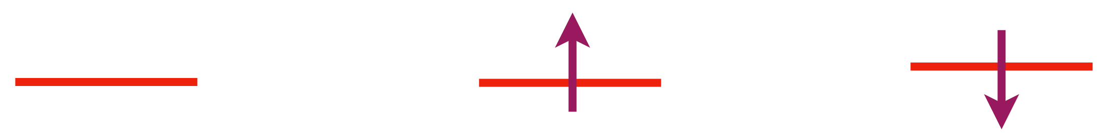

$$b^\dagger |v\rangle \qquad f_\uparrow^\dagger |v\rangle \qquad f_\downarrow^\dagger |v\rangle$$

$$\begin{aligned} c_\alpha &= f_\alpha b^\dagger \\ \vec{S} &= \frac{1}{2} f_\alpha^\dagger \sigma_{\alpha\beta} f_\beta \\ f_\alpha^\dagger f_\alpha + b^\dagger b &= 1 \end{aligned}$$

U(1) gauge invariance, $\quad b \to b e^{i\phi}\,, \quad f_\alpha \to f_\alpha e^{i\phi}$

The physical electron (c_α) and spin ($\vec{S}$) operators are rotations in this SU(1|2) superspin space.

Random t-J model (metal)

$$H = -\frac{1}{\sqrt{N}} \sum_{i,j=1}^{N} t_{ij}\, c_{i\alpha}^{\dagger} c_{j\alpha} + \frac{1}{\sqrt{N}} \sum_{i<j=1}^{N} J_{ij}\, \vec{S}_i \cdot \vec{S}_j$$

Each site has 3 states which we map to the '*superspin*' space of a fermion $\mathfrak{f}$ (the holon) and a boson $\mathfrak{b}_\alpha$ (the spinon):

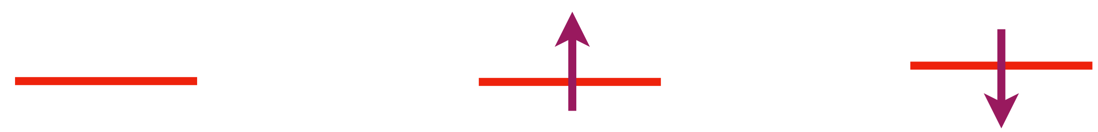

$\mathfrak{f}^\dagger \left| v \right\rangle$ $\qquad$ $\mathfrak{b}_\uparrow^\dagger \left| v \right\rangle$ $\qquad$ $\mathfrak{b}_\downarrow^\dagger \left| v \right\rangle$

$$
\begin{aligned}
c_\alpha &= \mathfrak{b}_\alpha \mathfrak{f}^\dagger \\
\vec{S} &= \frac{1}{2} \mathfrak{b}_\alpha^\dagger \sigma_{\alpha\beta} \mathfrak{b}_\beta \\
\mathfrak{b}_\alpha^\dagger \mathfrak{b}_\alpha + \mathfrak{f}^\dagger \mathfrak{f} &= 1
\end{aligned}
$$

U(1) gauge invariance, $\qquad \mathfrak{f} \to \mathfrak{f} e^{i\phi}, \quad \mathfrak{b}_\alpha \to \mathfrak{b}_\alpha e^{i\phi}$

The physical electron (c_α) and spin ($\vec{S}$) operators are rotations in this SU(2|1) superspin space.

Random t-J model (metal)

$$H = -\frac{1}{\sqrt{N}} \sum_{i,j=1}^{N} t_{ij}\, c^\dagger_{i\alpha} c_{j\alpha} + \frac{1}{\sqrt{N}} \sum_{i<j=1}^{N} J_{ij}\, \vec{S}_i \cdot \vec{S}_j$$

Each site has 3 states which we map to the '*superspin*' space of a fermion $\mathfrak{f}$ (the holon) and a boson $\mathfrak{b}_\alpha$ (the spinon):

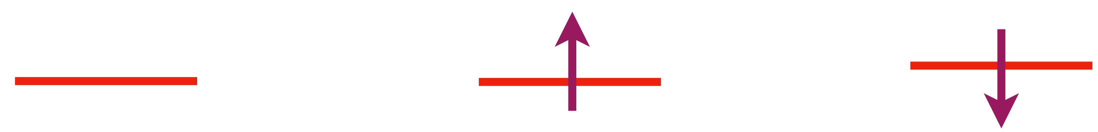

$\mathfrak{f}^\dagger \left| v \right\rangle$ $\qquad$ $\mathfrak{b}^\dagger_\uparrow \left| v \right\rangle$ $\qquad$ $\mathfrak{b}^\dagger_\downarrow \left| v \right\rangle$

$$\begin{aligned} c_\alpha &= \mathfrak{b}_\alpha \mathfrak{f}^\dagger \\ \vec{S} &= \frac{1}{2} \mathfrak{b}^\dagger_\alpha \sigma_{\alpha\beta} \mathfrak{b}_\beta \\ \mathfrak{b}^\dagger_\alpha \mathfrak{b}_\alpha + \mathfrak{f}^\dagger \mathfrak{f} &= 1 \\ \text{U(1) gauge invariance,} \quad & \mathfrak{f} \to \mathfrak{f} e^{i\phi}, \quad \mathfrak{b}_\alpha \to \mathfrak{b}_\alpha e^{i\phi} \end{aligned}$$

$\mathrm{SU}(1|2) \equiv \mathrm{SU}(2|1)$

The physical electron (c_α) and spin ($\vec{S}$) operators are rotations in this SU(2|1) superspin space.

Random t-J model (metal)

$$
\begin{aligned}
\mathcal{Z} &= \int \mathcal{D}\mathcal{P}(\tau) e^{-\mathcal{S}_B - \mathcal{S}_{tJ}} \\
\mathcal{S}_B &= i \int_0^1 du \int d\tau \, \mathrm{Tr}\left(\mathcal{P}\partial_\tau \mathcal{P} \partial_u \mathcal{P}\right) \\
\mathcal{S}_{tJ} &= \int d\tau d\tau' \, \mathrm{Tr}\left(\mathcal{P}(\tau)\mathcal{Q}(\tau-\tau')\mathcal{P}(\tau')\right) \\
&\qquad + \int d\tau \mathrm{Tr}\left(s_0 \, \mathcal{P}(\tau)\right) .
\end{aligned}
$$

Path integral over a superspin $\mathcal{P}(\tau)$ with a self-consistent self-interaction $\mathcal{Q}(\tau)$ and a 'Zeeman superfield' s_0.

D. Joshi, Chenyuan Li, G. Tarnopolsky, A. Georges, S. Sachdev, PRX **10**, 021033 (2020)

Random t-*J* model (metal):RG

- The RG analysis is very similar to that for the J model, except that the SU(2) spin is replaced by a SU(1|2) $\cong$ SU(2|1) superspin.

D. Joshi, Chenyuan Li, G. Tarnopolsky, A. Georges, S. Sachdev, PRX **10**, 021033 (2020)

Random t-J model (metal):RG

- The RG analysis is very similar to that for the J model, except that the SU(2) spin is replaced by a SU(1|2) $\cong$ SU(2|1) superspin.

- One crucial difference is that there is now a 'Zeeman' field s_0 in superspin space which breaks the degeneracy between spinon and holon states. This becomes the single relevant perturbation at a critical fixed point where $s_0 = 0$ at leading order *i.e.* the 3 states on each site are nearly degenerate at the critical point.

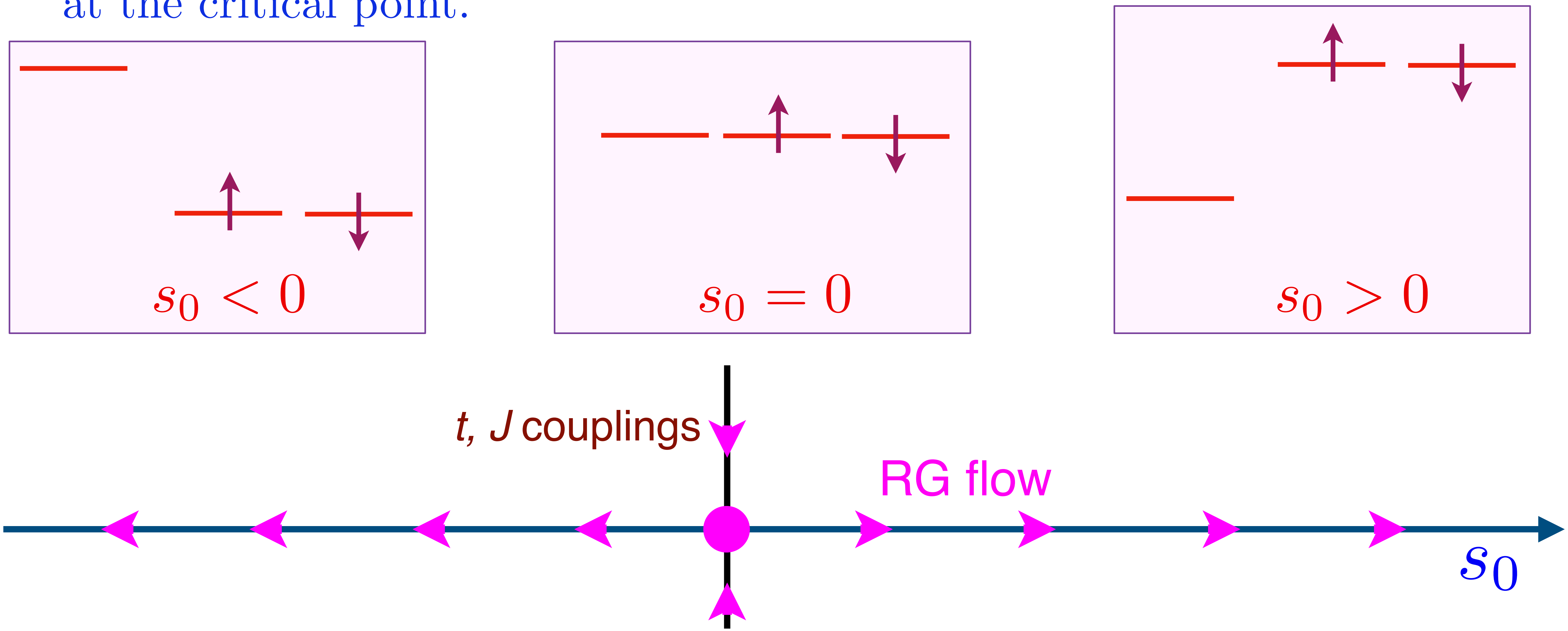

D. Joshi, Chenyuan Li, G. Tarnopolsky, A. Georges, S. Sachdev, PRX **10**, 021033 (2020)

Random t-J model (metal):RG

- The RG analysis is very similar to that for the J model, except that the SU(2) spin is replaced by a SU(1|2) $\cong$ SU(2|1) superspin.

- One crucial difference is that there is now a 'Zeeman' field s_0 in superspin space which breaks the degeneracy between spinon and holon states. This becomes the single relevant perturbation at a critical fixed point where $s_0 = 0$ at leading order *i.e.* the 3 states on each site are nearly degenerate at the critical point.

- The Wess-Zumino-Witten term in superspace now ensures the exact exponents at the fixed point

$$\left\langle \vec{S}(\tau) \cdot \vec{S}(0) \right\rangle \sim \frac{1}{|\tau|} \quad , \quad \left\langle c_\alpha(\tau) c_\alpha^\dagger(0) \right\rangle \sim \frac{1}{\tau} \, .$$

D. Joshi, Chenyuan Li, G. Tarnopolsky, A. Georges, S. Sachdev, PRX **10**, 021033 (2020)

Random t-J model (metal):RG

- The RG analysis is very similar to that for the J model, except that the SU(2) spin is replaced by a SU(1|2) $\cong$ SU(2|1) superspin.

- One crucial difference is that there is now a 'Zeeman' field s_0 in superspin space which breaks the degeneracy between spinon and holon states. This becomes the single relevant perturbation at a critical fixed point where $s_0 = 0$ at leading order *i.e.* the 3 states on each site are nearly degenerate at the critical point.

- The Wess-Zumino-Witten term in superspace now ensures the exact exponents at the fixed point

Square of spinon correlator

$$\left\langle \vec{S}(\tau) \cdot \vec{S}(0) \right\rangle \sim \frac{1}{|\tau|} \quad , \quad \left\langle c_\alpha(\tau) c_\alpha^\dagger(0) \right\rangle \sim \frac{1}{\tau} .$$

Product of spinon and holon correlators

- These exponents do not have a quasiparticle interpretation. However, they can be understood (in a large M limit of a model with SU(M) symmetry) by *fractionalization* of the electron into a spinon and holon, each of which decay as $1/\sqrt{\tau}$.

D. Joshi, Chenyuan Li, G. Tarnopolsky, A. Georges, S. Sachdev, PRX **10**, 021033 (2020)

t-J phase diagram: RG using *either* SU(2|1) or SU(1|2)

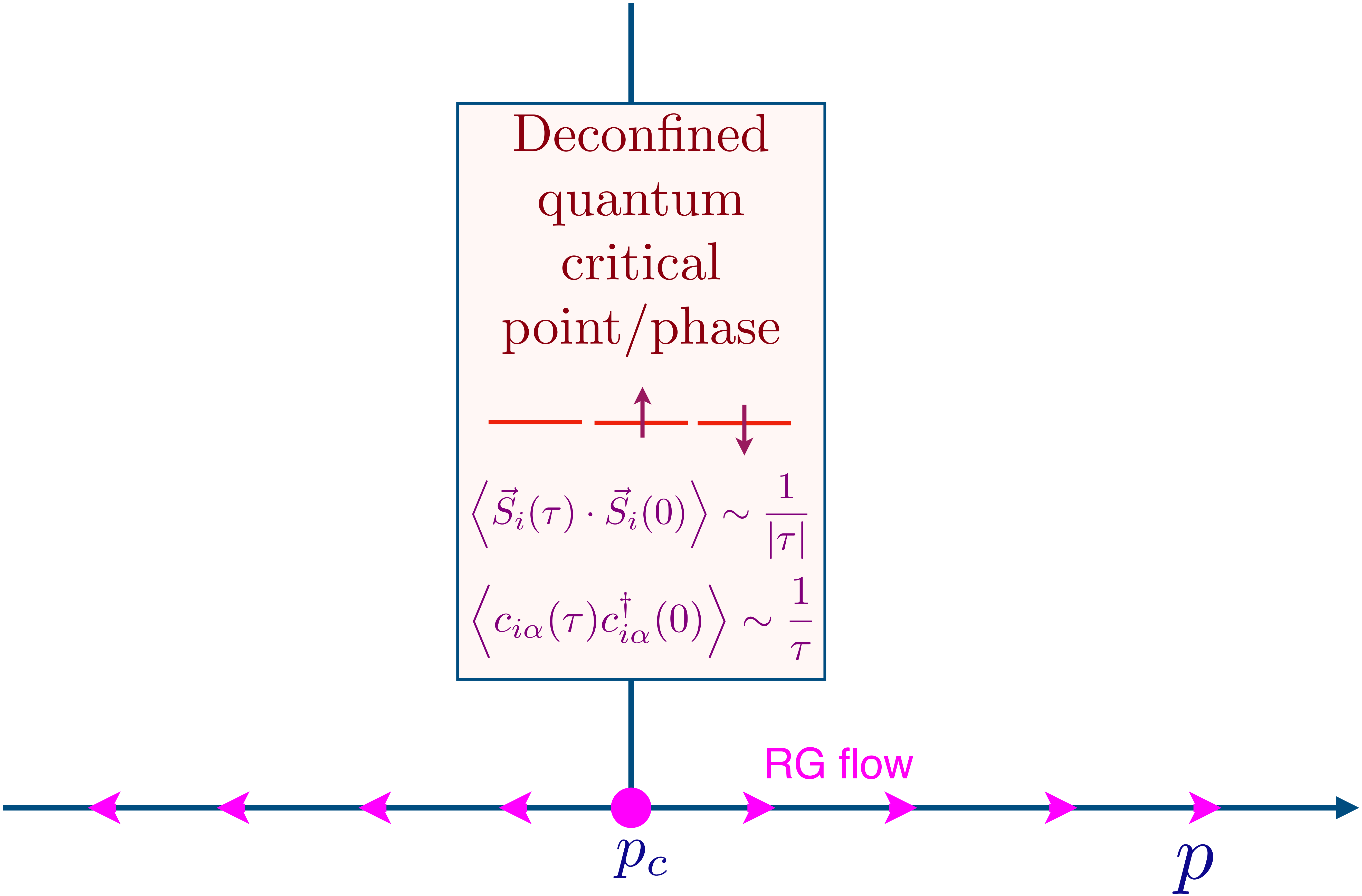

D. Joshi, Chenyuan Li, G. Tarnopolsky, A. Georges, S. Sachdev, PRX **10**, 021033 (2020)

t-J phase diagram: RG using *either* SU(2|1) or SU(1|2)

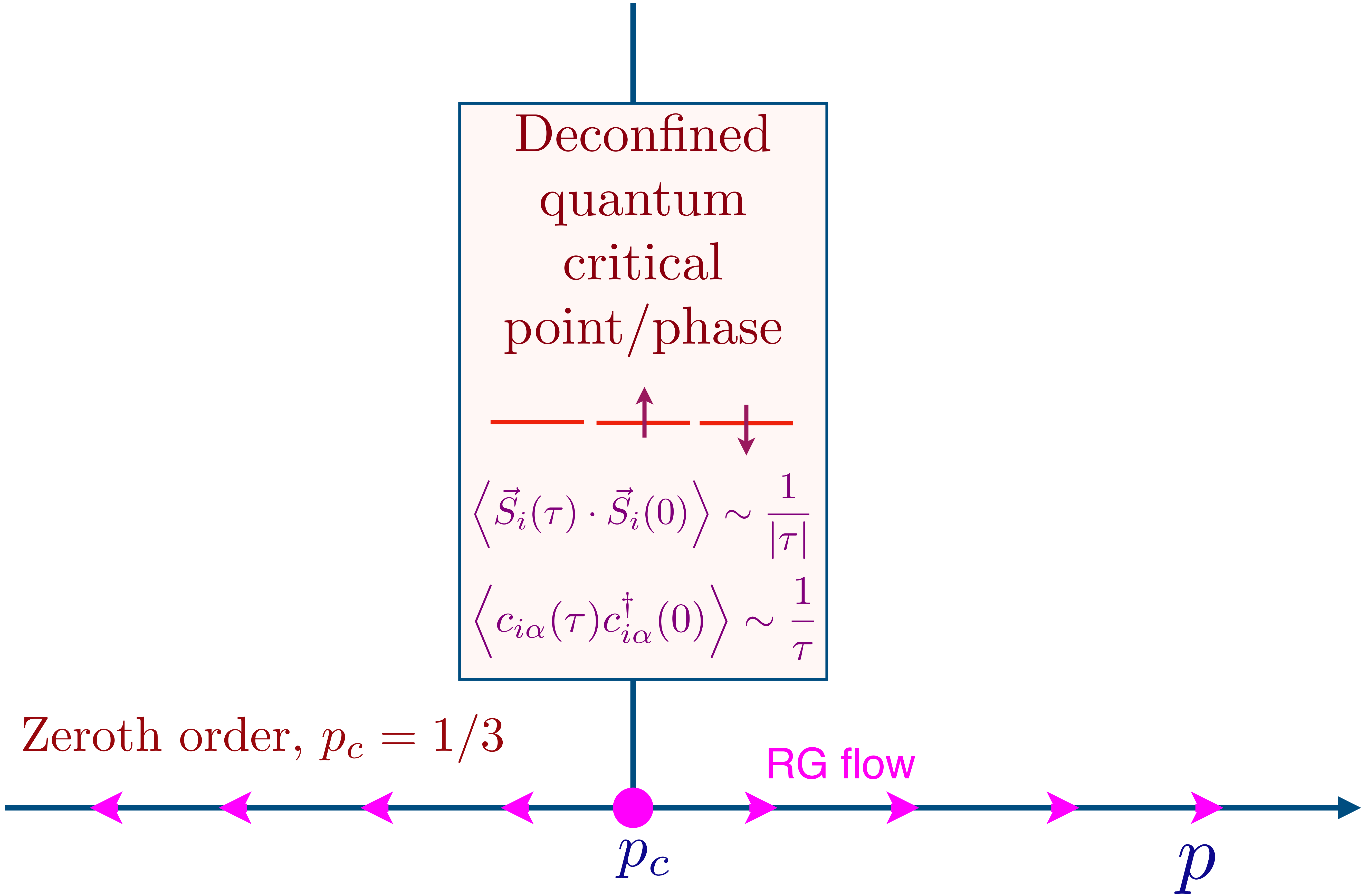

D. Joshi, Chenyuan Li, G. Tarnopolsky, A. Georges, S. Sachdev, PRX **10**, 021033 (2020)

t-J phase diagram: RG using *either* SU(2|1) or SU(1|2)

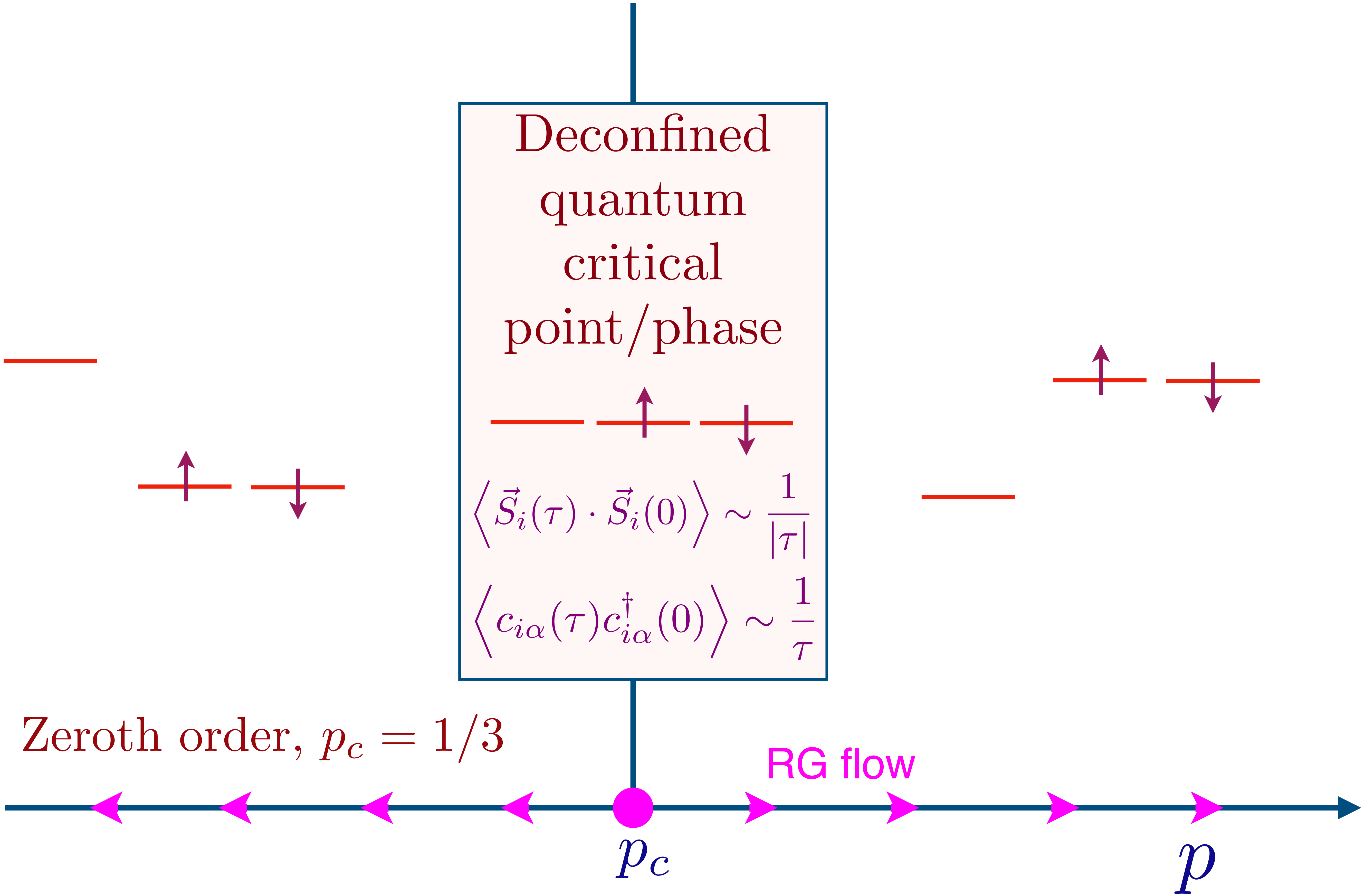

D. Joshi, Chenyuan Li, G. Tarnopolsky, A. Georges, S. Sachdev, PRX **10**, 021033 (2020)

t-J phase diagram: RG using *either* SU(2|1) or SU(1|2)

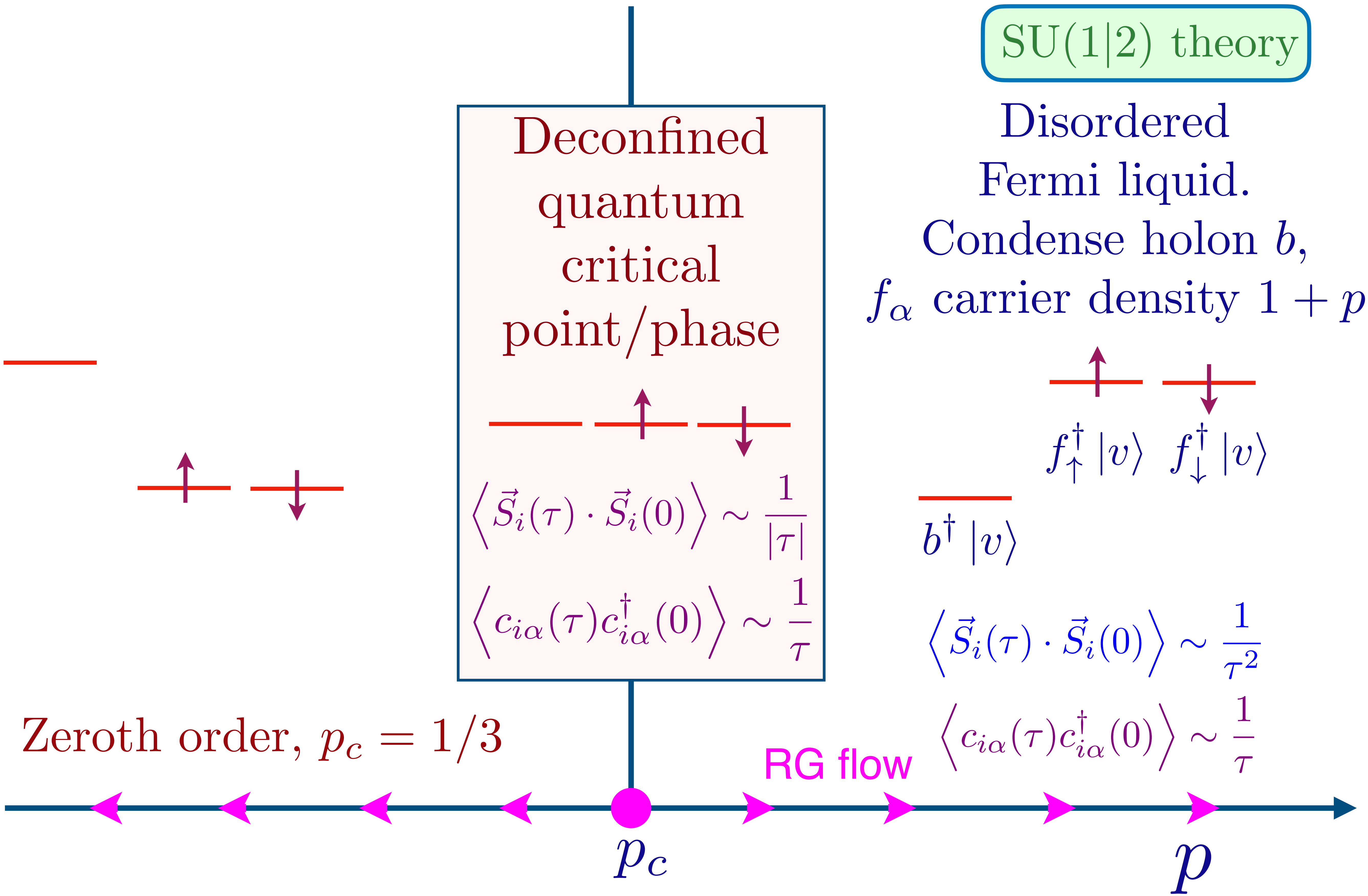

D. Joshi, Chenyuan Li, G. Tarnopolsky, A. Georges, S. Sachdev, PRX **10**, 021033 (2020)

t-J phase diagram: RG using *either* SU(2|1) or SU(1|2)

SU(2|1) theory

Metallic spin glass.
Condense spinon $\mathfrak{b}_\alpha$, $\mathfrak{f}$ carrier density p

$\mathfrak{f}^\dagger |v\rangle$

$\mathfrak{b}_\uparrow^\dagger |v\rangle$ $\mathfrak{b}_\downarrow^\dagger |v\rangle$

$$\left\langle \vec{S}_i(\tau) \cdot \vec{S}_i(0) \right\rangle \sim \text{constant}$$

$$\left\langle c_{i\alpha}(\tau) c_{i\alpha}^\dagger(0) \right\rangle \sim \frac{1}{\tau}$$

Deconfined quantum critical point/phase

$$\left\langle \vec{S}_i(\tau) \cdot \vec{S}_i(0) \right\rangle \sim \frac{1}{|\tau|}$$

$$\left\langle c_{i\alpha}(\tau) c_{i\alpha}^\dagger(0) \right\rangle \sim \frac{1}{\tau}$$

SU(1|2) theory

Disordered Fermi liquid.
Condense holon b, f_α carrier density $1 + p$

$f_\uparrow^\dagger |v\rangle$ $f_\downarrow^\dagger |v\rangle$

$b^\dagger |v\rangle$

$$\left\langle \vec{S}_i(\tau) \cdot \vec{S}_i(0) \right\rangle \sim \frac{1}{\tau^2}$$

$$\left\langle c_{i\alpha}(\tau) c_{i\alpha}^\dagger(0) \right\rangle \sim \frac{1}{\tau}$$

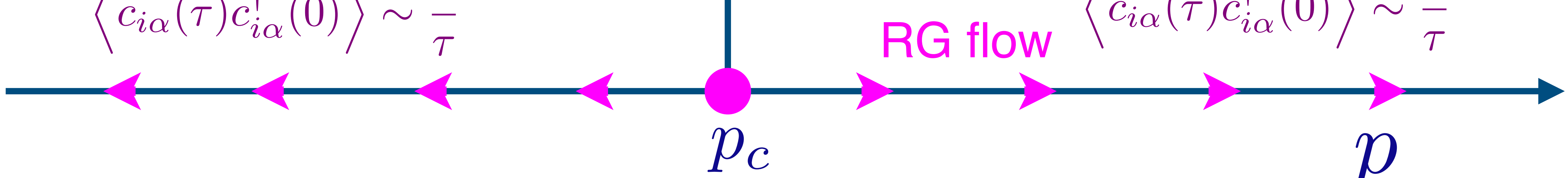

D. Joshi, Chenyuan Li, G. Tarnopolsky, A. Georges, S. Sachdev, PRX **10**, 021033 (2020)

Random t-J-U_H model

$$H = -\frac{1}{\sqrt{N}} \sum_{i,j=1}^{N} t_{ij}\, c_{i\alpha}^{\dagger} c_{j\alpha} + \frac{1}{\sqrt{N}} \sum_{i<j=1}^{N} J_{ij}\, \vec{S}_i \cdot \vec{S}_j + U_H \sum_{i=1}^{N} n_{i\uparrow} n_{i\downarrow}$$

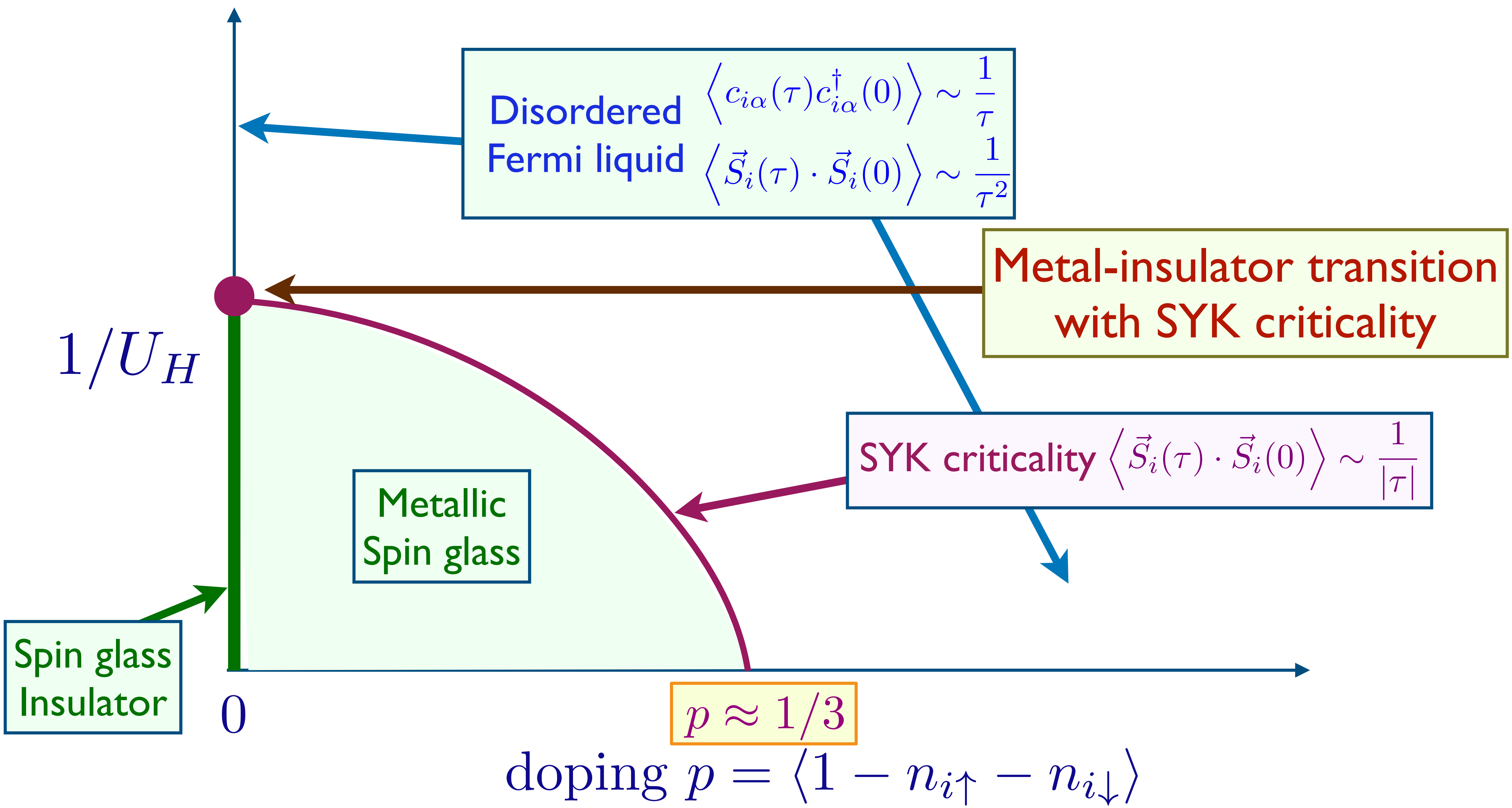

At the critical point/phase of the t-J model, the Fermi liquid-like behavior of the electron Green's function

$$\left\langle c_{i\alpha}(\tau) c_{i\alpha}^{\dagger}(0) \right\rangle \sim \frac{1}{\tau}$$

leads to a non-zero *residual resitivity*, $\rho(0) \neq 0$.

However, the critical state is *not* a Fermi liquid, as indicated by the slow decay of the spin correlations

$$\left\langle \vec{S}_i(\tau) \cdot \vec{S}_i(0) \right\rangle \sim \frac{1}{|\tau|}$$

Moreover, in a Fermi liquid, we expect $\rho(T) - \rho(0) \sim T^2$, which also does not hold here.

Time reparameterization soft mode

An important correction to the SL(2,R) invariant critical Green's function arises from the time reparameterization soft mode, and this takes the form

$$\left\langle c_{i\alpha}(\tau) c^\dagger_{i\alpha}(0) \right\rangle \sim \frac{\pi T}{\sin(\pi T \tau)} \left(1 + \alpha_G \frac{T}{J} \Phi_{\text{non-conformal}}(T\tau) \right)$$

where $\Phi_{\text{non-conformal}}(T\tau)$ is a computable (in the large M limit) scaling function, and α_G is universally proportional to the co-efficient α_S of the Schwarizan action for the time reparameterization mode.

J. Maldacena and D. Stanford, PRD **94**, 106002 (2016)
A. Kitaev and J. Suh, JHEP 183 (2018)
Haoyu Guo, Yingfei Guo, S. Sachdev, Annals of Physics **418**, 168202 (2020)

Time reparameterization soft mode

Computing the resistivity from this Green's function via the Kubo formula, we find

$$\rho(T) = \rho(0)\left(1 + 8\alpha_G \frac{T}{J} + \dots\right)$$

Haoyu Guo, Yingfei Guo, S. Sachdev, Annals of Physics **418**, 168202 (2020)

- The t-J model with random and all-to-all hopping and exchange displays a phase diagram which captures many of the key characteristics of the cuprate phase diagram.

- It has an optimal doping metal-metal deconfined transition with SYK criticality.

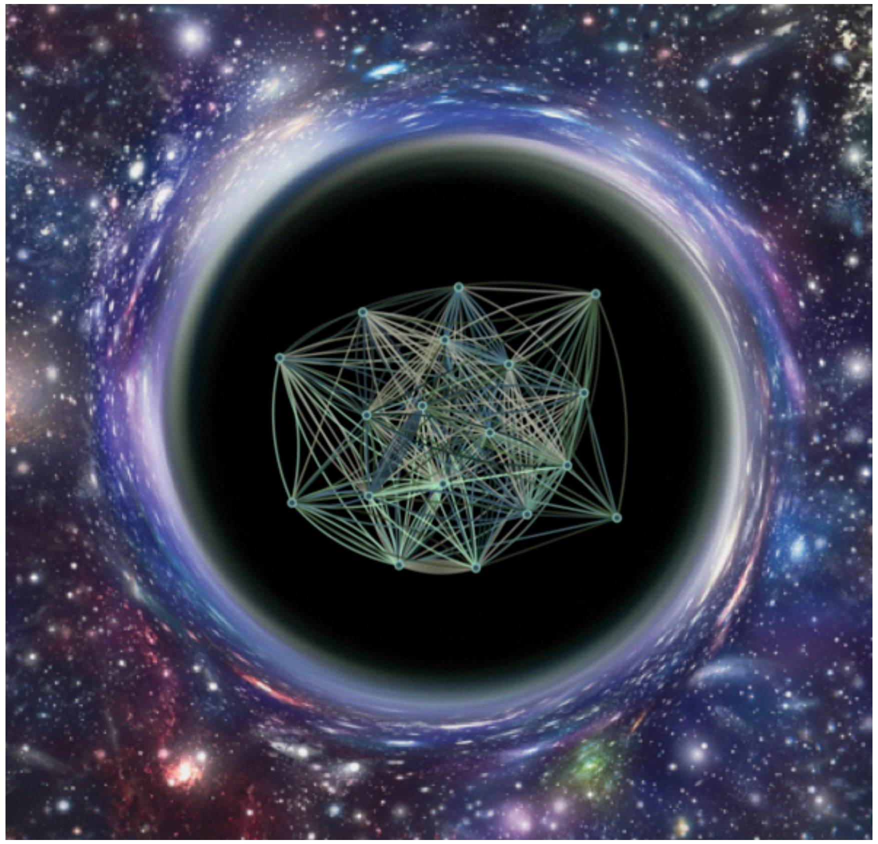

- Critical electron Green's function $G_c(\tau) \sim 1/\tau$ and local spin correlator $Q(\tau) \sim 1/|\tau|$.

- Can be interpreted in terms of fractionalization with spinon and holon correlators $\sim 1/\sqrt{\tau}$ (deconfined criticality).

- Linear-in-T resistivity down to $T = 0$ at the critical point from the time reparameterization soft mode (but there could be other singular modes).

- Carrier density p for $p < p_c$, and $1 + p$ for $p > p_c$.

Metal-metal transitions in a ***one-band*** model

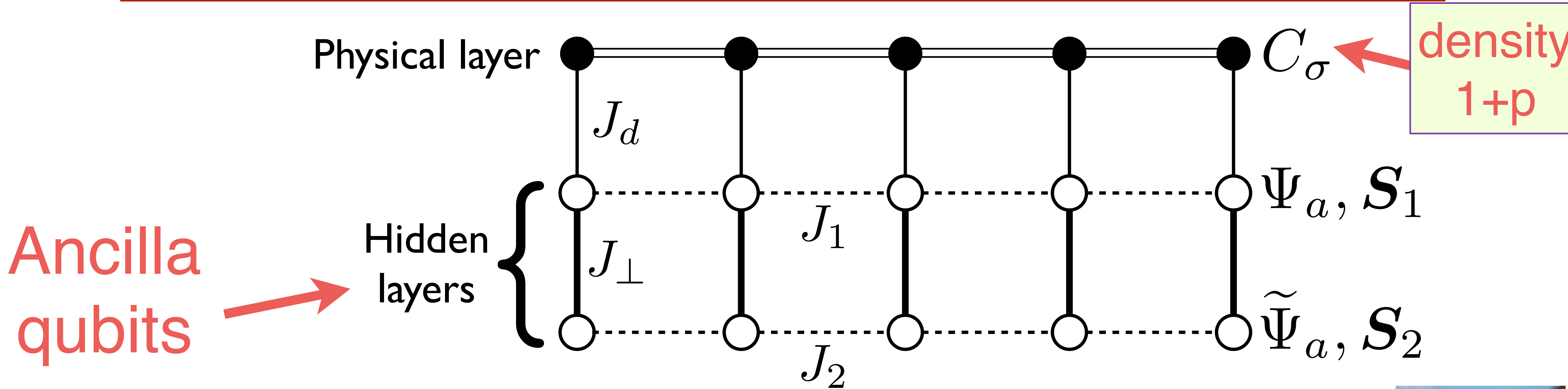

$(U(1) \times U(1))/Z_2$ gauge theory of a ghost Fermi surface and a 'hybridization-Higgs' boson which condenses on the 'Small Fermi surface' side.

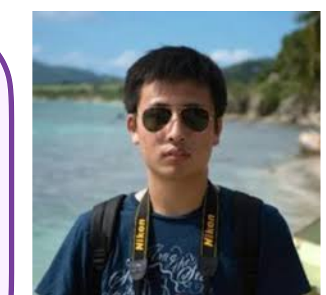

Yahui Zhang

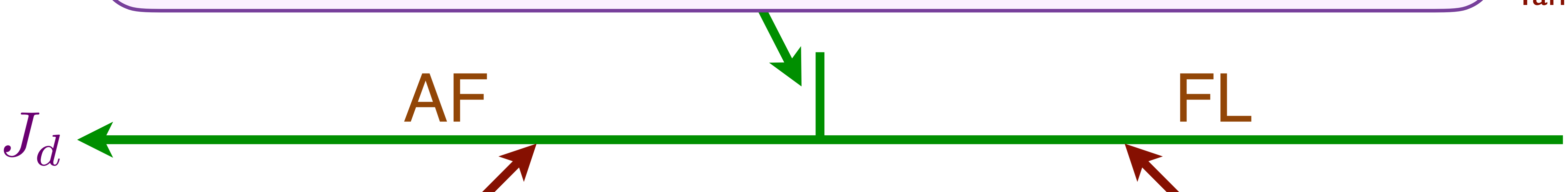

Small Fermi surface of size p

$$|\Phi\rangle = \left[\text{Projection onto rung singlets of } \Psi, \widetilde{\Psi}\right] \bowtie |\text{Slater determinant of } (C, \Psi)\rangle \otimes \left|\text{Slater determinant of } \widetilde{\Psi}\right\rangle$$

Large Fermi surface of size $1 + p$

$$|\Phi\rangle = \left|\text{Rung singlets of } \Psi, \widetilde{\Psi}\right\rangle \otimes |\text{Slater determinant of } C\rangle$$

Ya-Hui Zhang, S. Sachdev, PRR **2**, 023172 (2020); arXiv:2006.01140.